fabrizioantonioli2@gmail.com
fabrizio.antonioli@igag.cnr.it

Consiglio Nazionale delle Ricerche

IGAG
Istituto di Geologia Ambientale e Geoingegneria


Carmelo
Monaco
Paolo
Orrù
Stefano
Furlani
Alessandro
Fontana
Kurt
Lambeck
Paolo
Stocchi
Giorgio
Spada
Carla
Braitenberg


Marcello Mannino
Luigi Ferranti
Gabriella Mangano
Gianmaria Sannino
Kurt Lambeck
Francesco Latino Chiocci
Fabrizio Antonioli
Simonepietro Canese
Mariarita Palombo
Laura Bonfiglio
Raimondo Catalano
Valeria Lopresti
Maurizio Gasparo
Stefano Furlani
Renato Tonielli

Eleonora de Sabata

Paolo Orrù ed
Emanuela Solinas

Egidio Trainito

Gianfranco Scicchitano
e
Luigi Ferranti

Surveys and publications with marine archaeologists:

- Sebastiano Tusa Sopr. of Trapani
- Flavio Enei, Museum of Pirgy
- Marinella Pasquinucci, University of Pisa
- Jonathan Benjamin, University of Newcastle
- Heud Galili University of Haifa, Israel
- Timothy Gambin, University of Malta
- Vladimir Kovacic, Museum of Porec
- Silvia Ducci, Sopr. Archeologica della Toscana
- Alessandro Porqueddu, Archaeologist
- Rubens Doriano, Sopr. Archeologica Olbia

Irena Radic
University of Zadar

Elena F. Castagnino
University of Catania

Flavio Enei
Museo di Pirgy

Emanuela Solinas
Museo di Cagliari, Italy

Alessandra Benini
University of Calabria, Italy

Rita Auriemma
University of Lecce, Italy

Sebastiano Tusa presso la grotta del Tuono, Marettimo

Presente, perchè
sale il mare? E’ una risalita naturale o riscaldamento climatico dovuto all’uomo?

Passato
quali indicatori ci raccontano dove stava il mare, 2000, 20.000, 200.000, 2 milioni di anni fa?

Presente
dati strumentali mareografi satellite;

Futuro
previsioni IPCC fino al 2100-2300

Milankovitch matematico Sloveno che a inizio secolo intuì che le variazioni del clima erano dovute alle variazioni dell’asse terrestre. Tutte le sue teorie sono state confermate.

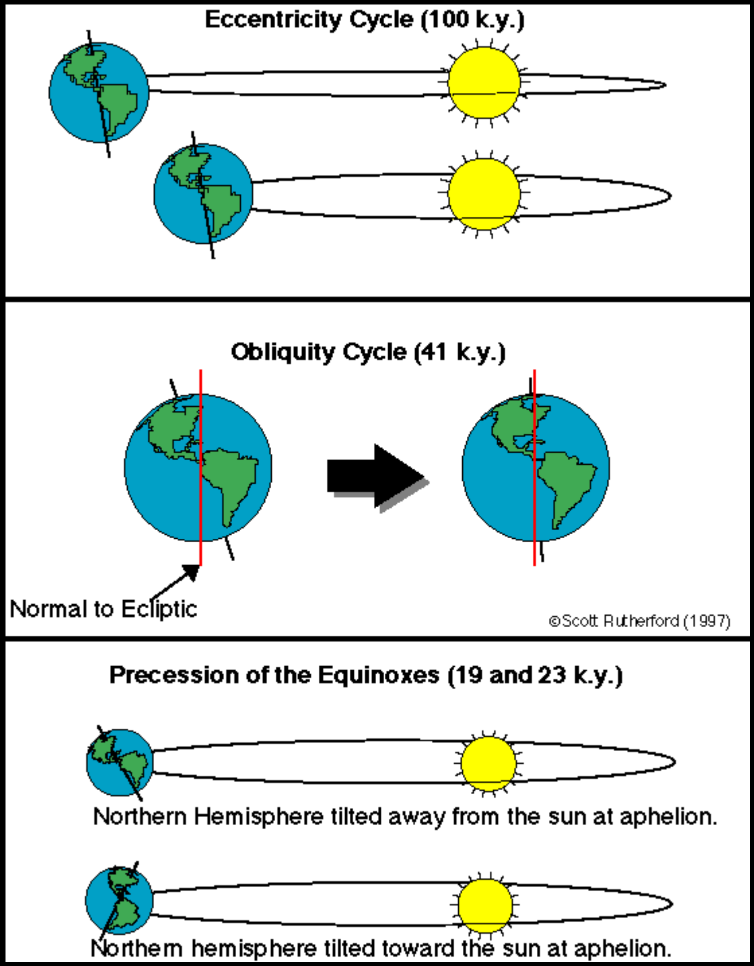

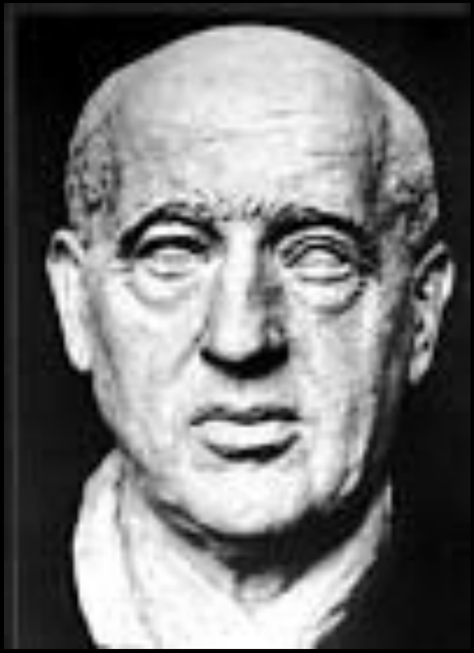

Variazioni del livello del mare da 450 mila anni fa al presente, da SPECMAP, Martinson et al., 1991et al. 2001

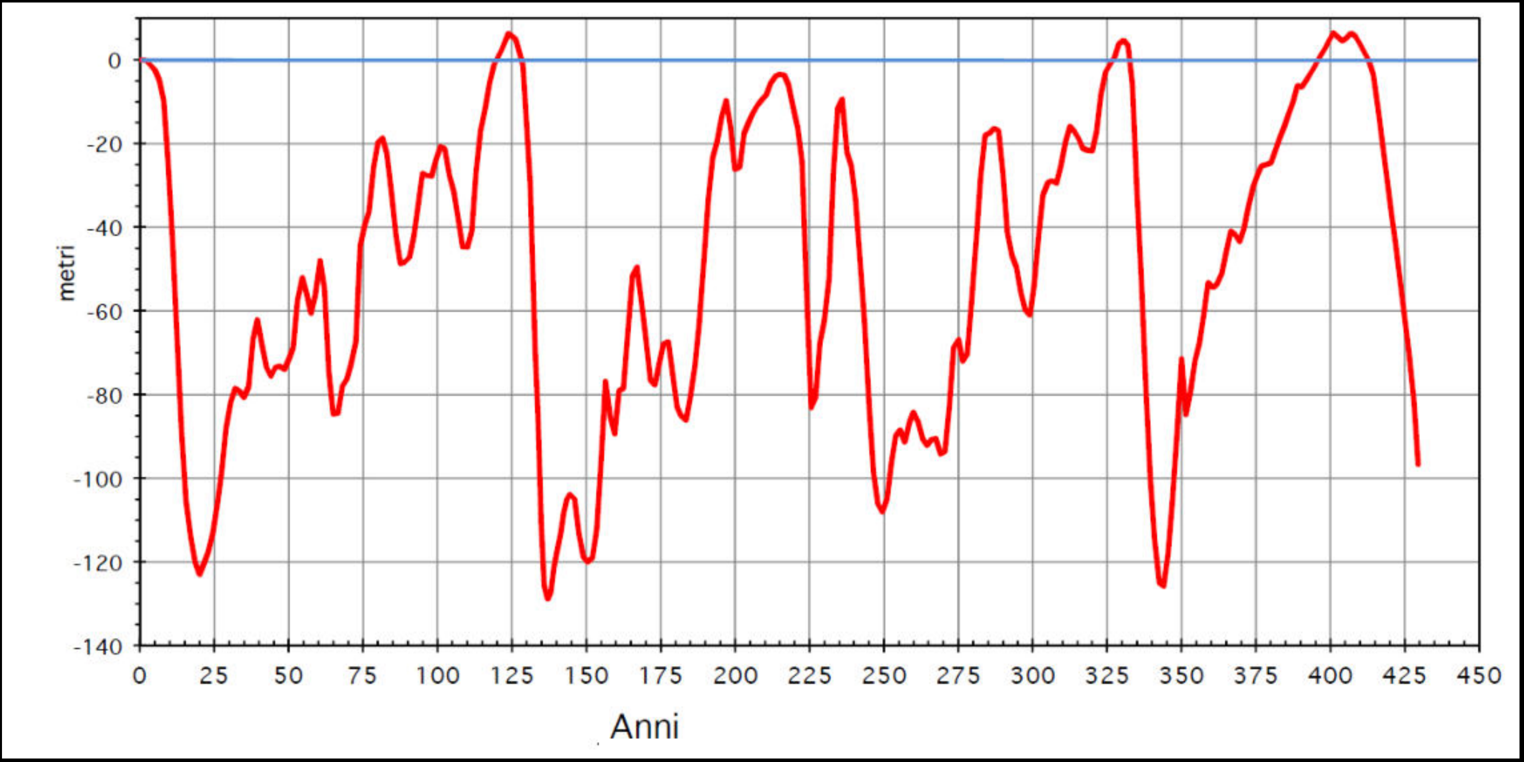

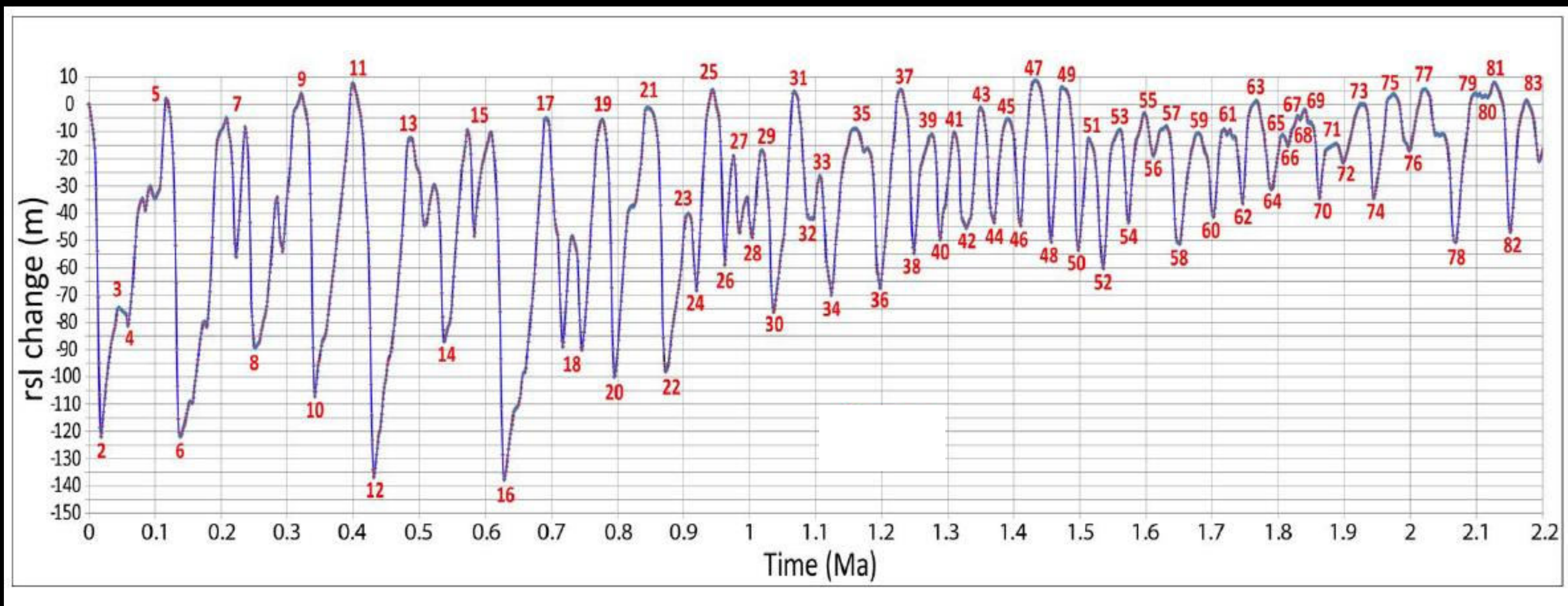

rsl change (m)
Time (Ma)

Ocean Drilling Program (ODP), carote sui fondi

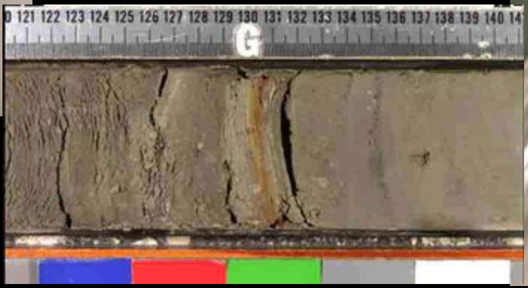

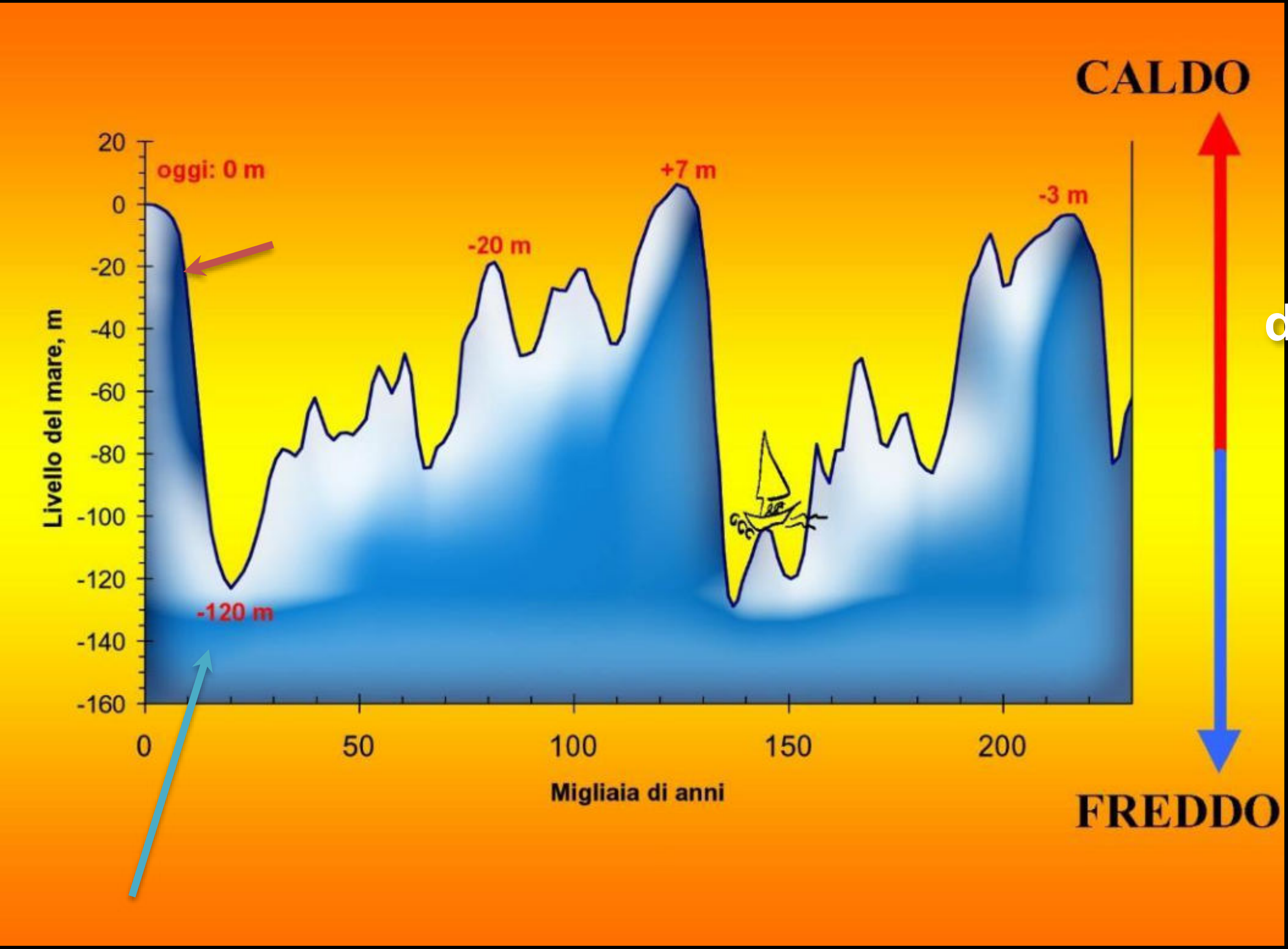

Le variazioni eustatiche durante gli ultimi 250.000 anni

Carote di ghiaccio, Antartide

Carote di ghiaccio, Antartide

Marzo 2020
415 ppm CO_2

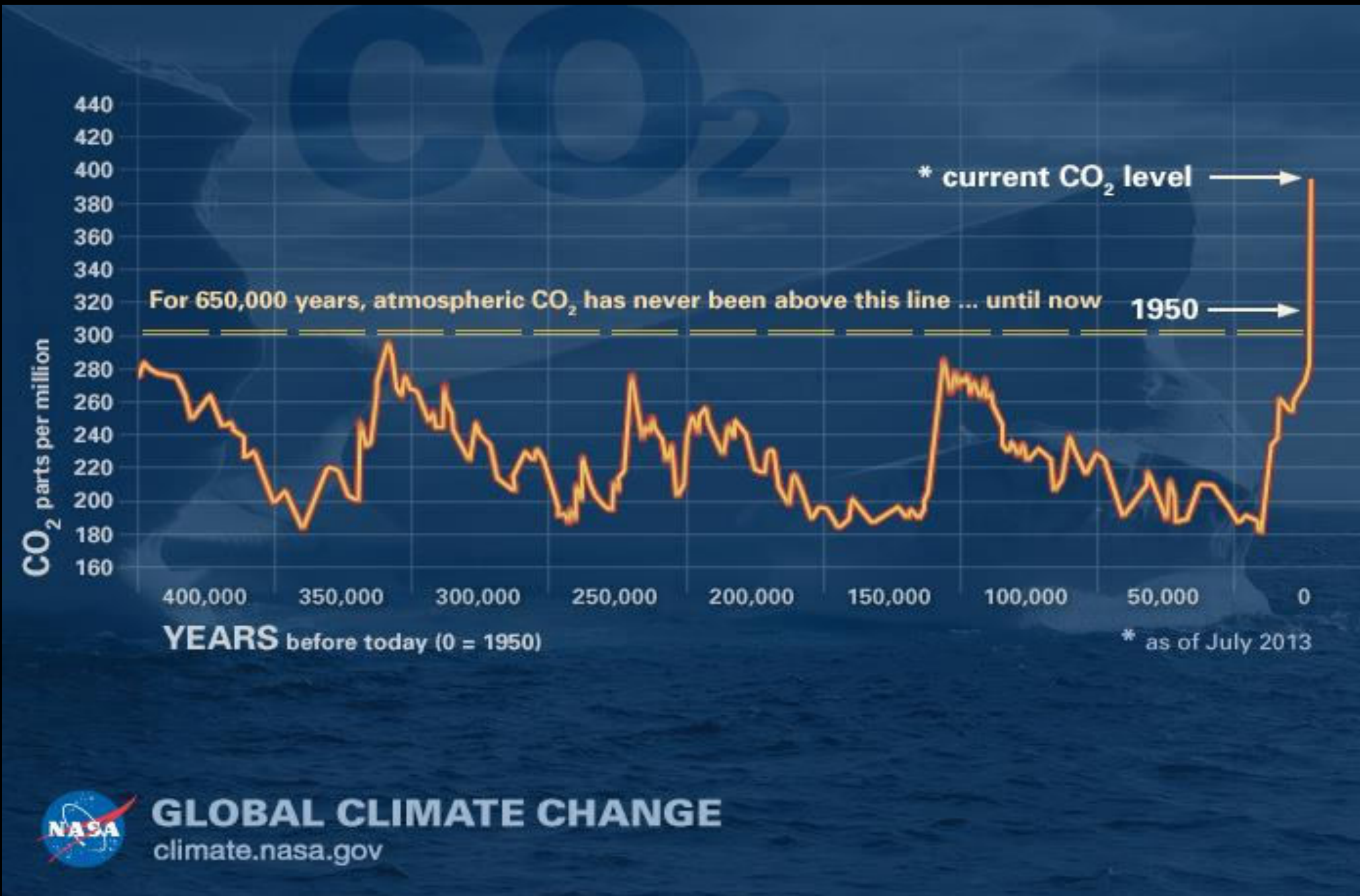

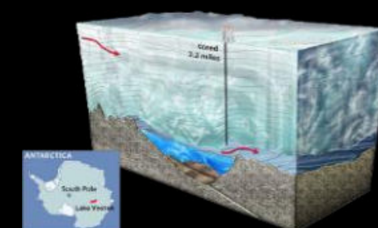


Sardegna, Golfo di Orosei
Solco di battente fossile, 125.000 anni fa: + 8 m
290 parti per milione di CO2
Solco di battente attuale :
424 parti per milione di CO2


CO2
* current CO2 level
For 650,000 years, atmospheric CO2 has never been above this line ... until now
1950
CO2 parts per million
440
420
400
380
360
340
320
300
280
260
240
220
200
180
160
400,000
350,000
300,000
250,000
200,000
150,000
100,000
50,000
0
YEARS before today (0 = 1950)
* as of July 2013
GLOBAL CLIMATE CHANGE
climate.nasa.gov


WMO
UNEP
ipcc
INTERGOVERNMENTAL PANEL ON climate change
Working Group I (WG 1) - The Physcal Science Basis
IPCC Workshop on Sea Level Rise
and Ice Sheet Instabilities
21-24 June 2010
Kuala Lumpur, Malaysia

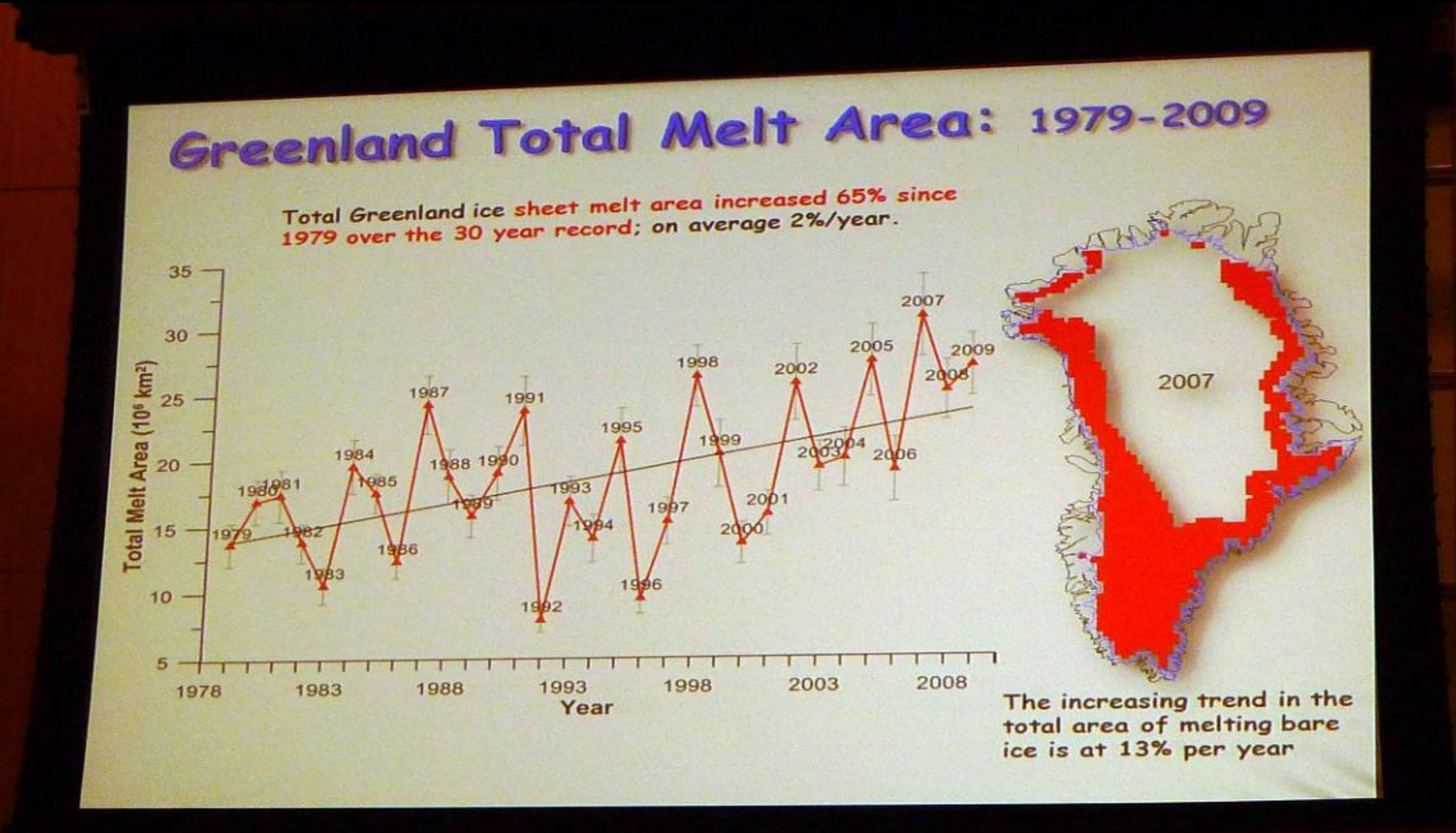
Greenland Total Melt Area: 1979-2009
Total Greenland ice sheet melt area increased 65% since 1979 over the 30 year record; on average 2%/year.
Total Melt Area (10⁶ km²)
Year
2007
The increasing trend in the total area of melting bare ice is at 13% per year

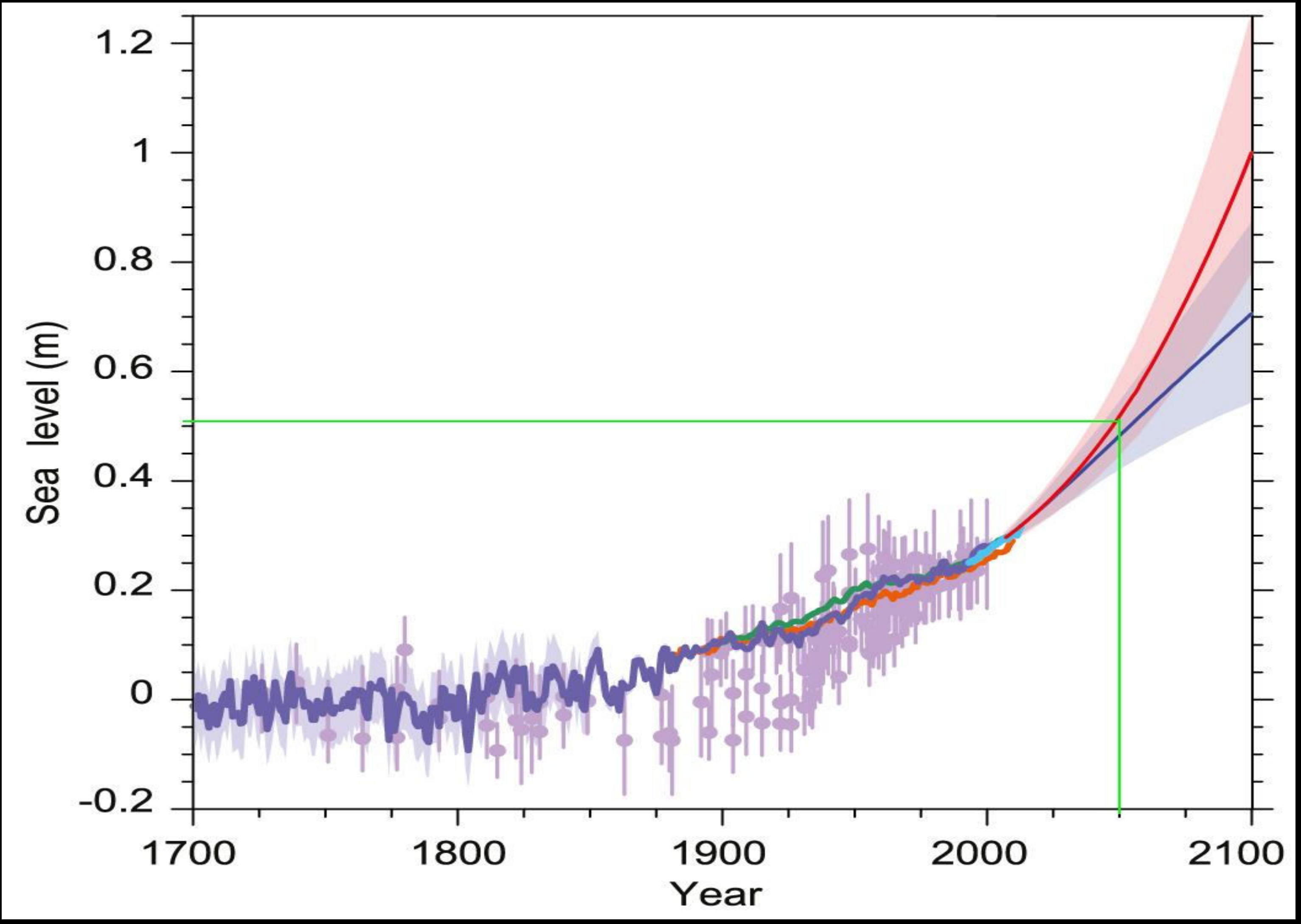

1.2
1
0.8
0.6
0.4
0.2
0
-0.2
Sea level (m)
1700
1800
1900
2000
2100
Year

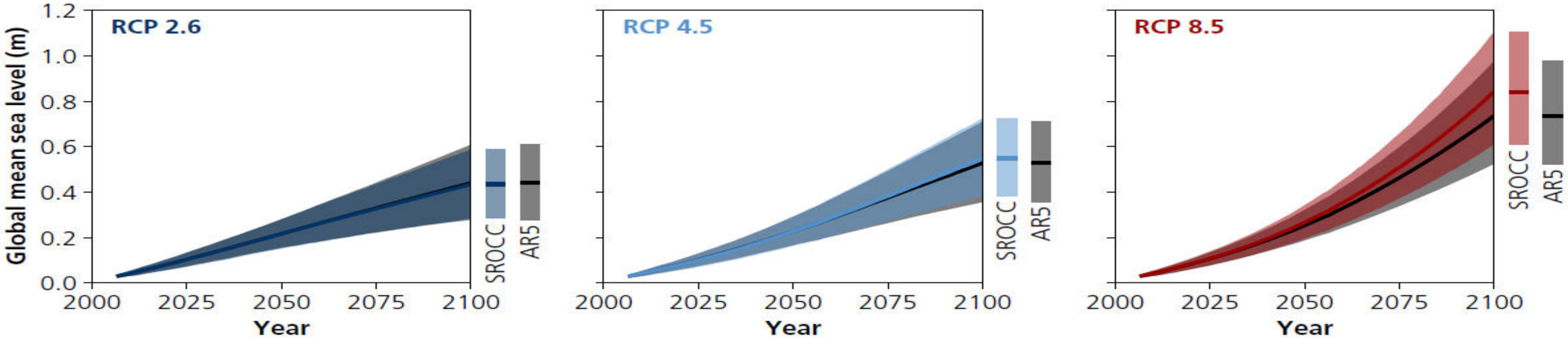

Figure 4.9: Time series of GMSL for RCP2.6, RCP4.5 and RCP8.5 as used in this report and, for reference the AR5 results (Church et al., 2013). Results are based on AR5 results for all components except the Antarctic contribution. Results for the Antarctic contribution in 2081–2100 are provided in Table 4.4. The shaded region should be considered as the *likely range*.

Le variazioni relative del livello del mare

costituiscono la sommatoria di:

Eustatismo (Scioglim. Ghiacci + dilatazione termica) **+ isostasia + tettonica**

Scioglimento dei ghiacci e dilatazione termica

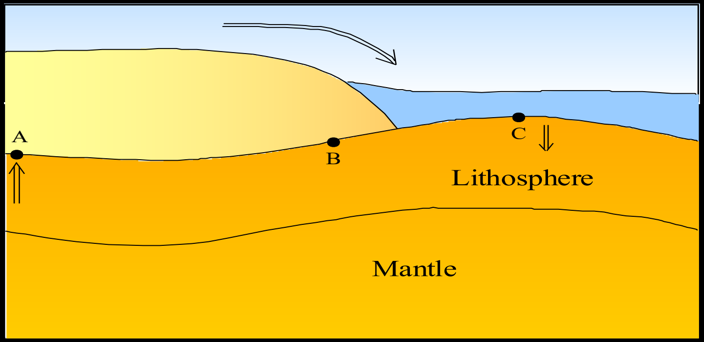

Isostasia

Tettonica e compattazione

Recent changes of the Antarctic ice sheet

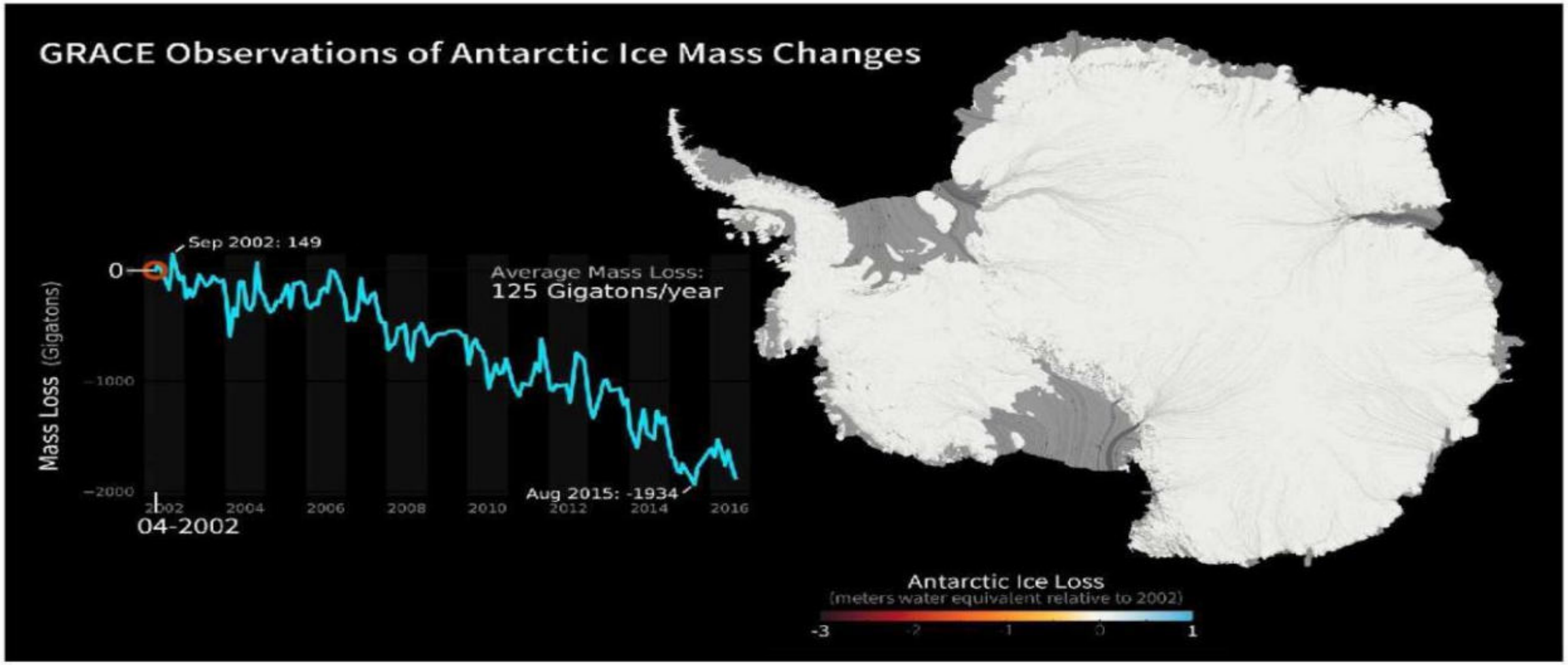

Ice Thickness

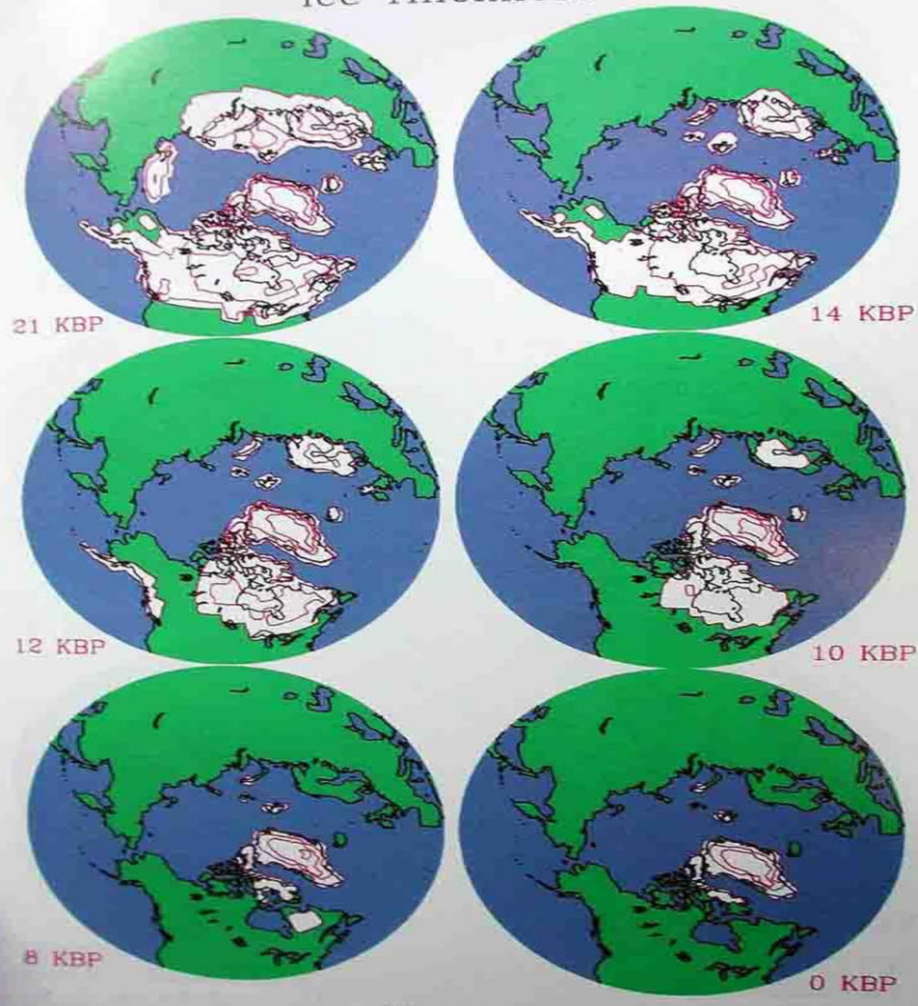

Figure 4.3

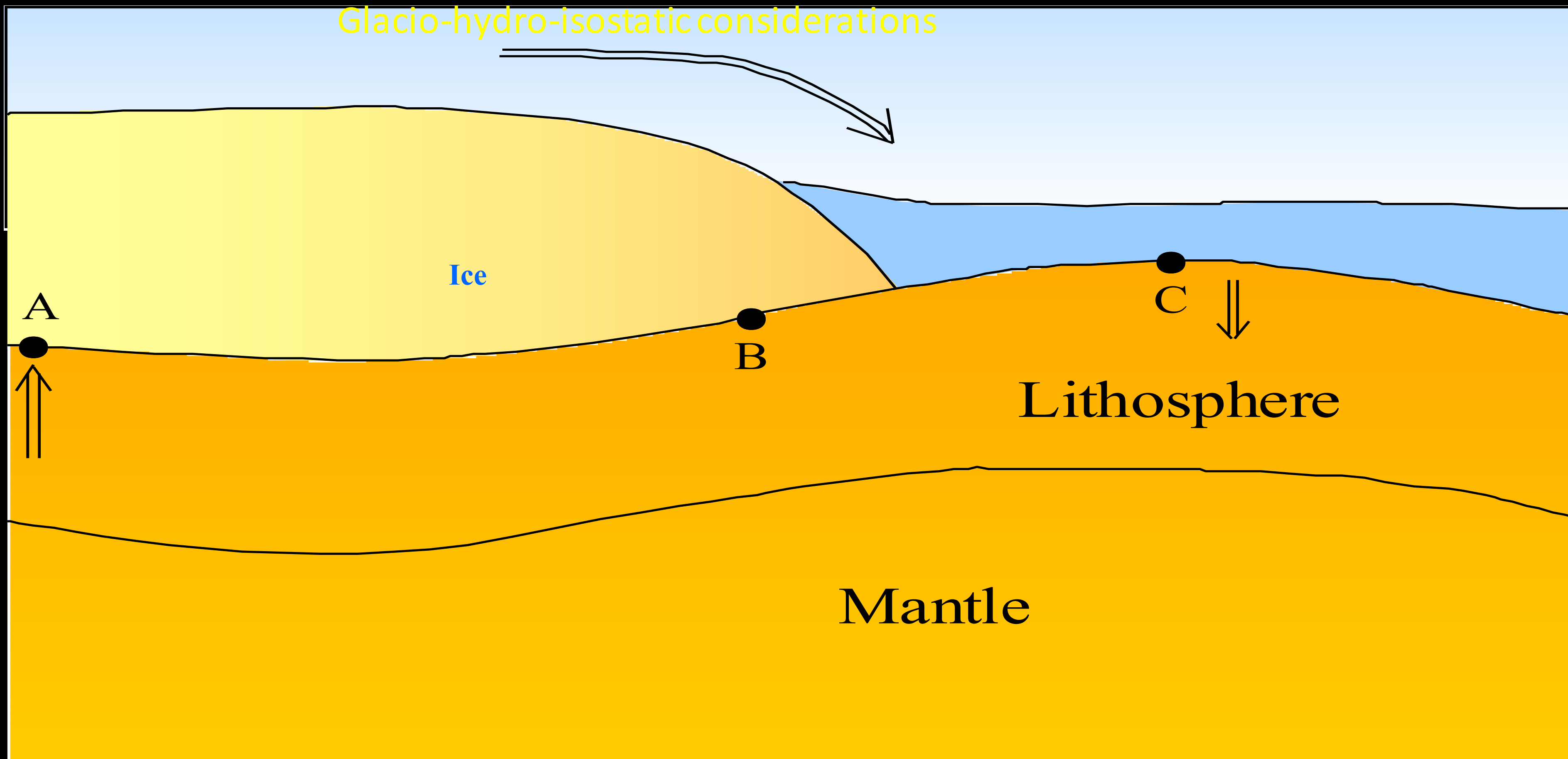
Glacio-hydro-isostatic considerations
Ice
A
B
C
Lithosphere
Mantle

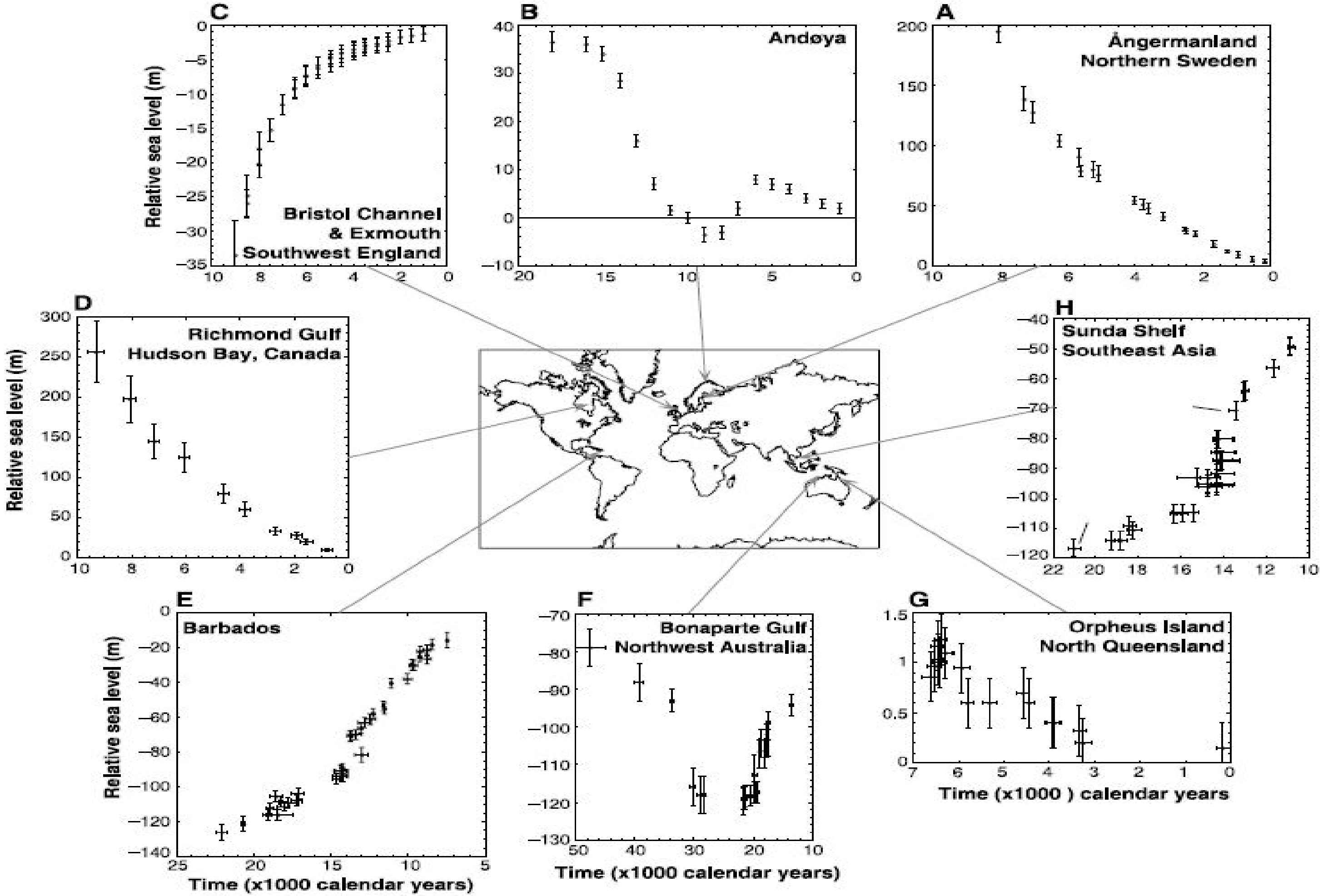
C
Bristol Channel
& Exmouth
Southwest England
B
Andøya
A
Ångermanland
Northern Sweden
D
Richmond Gulf
Hudson Bay, Canada
H
Sunda Shelf
Southeast Asia
E
Barbados
F
Bonaparte Gulf
Northwest Australia
G
Orpheus Island
North Queensland
Relative sea level (m)
Time (x1000 calendar years)
Time (x1000) calendar years

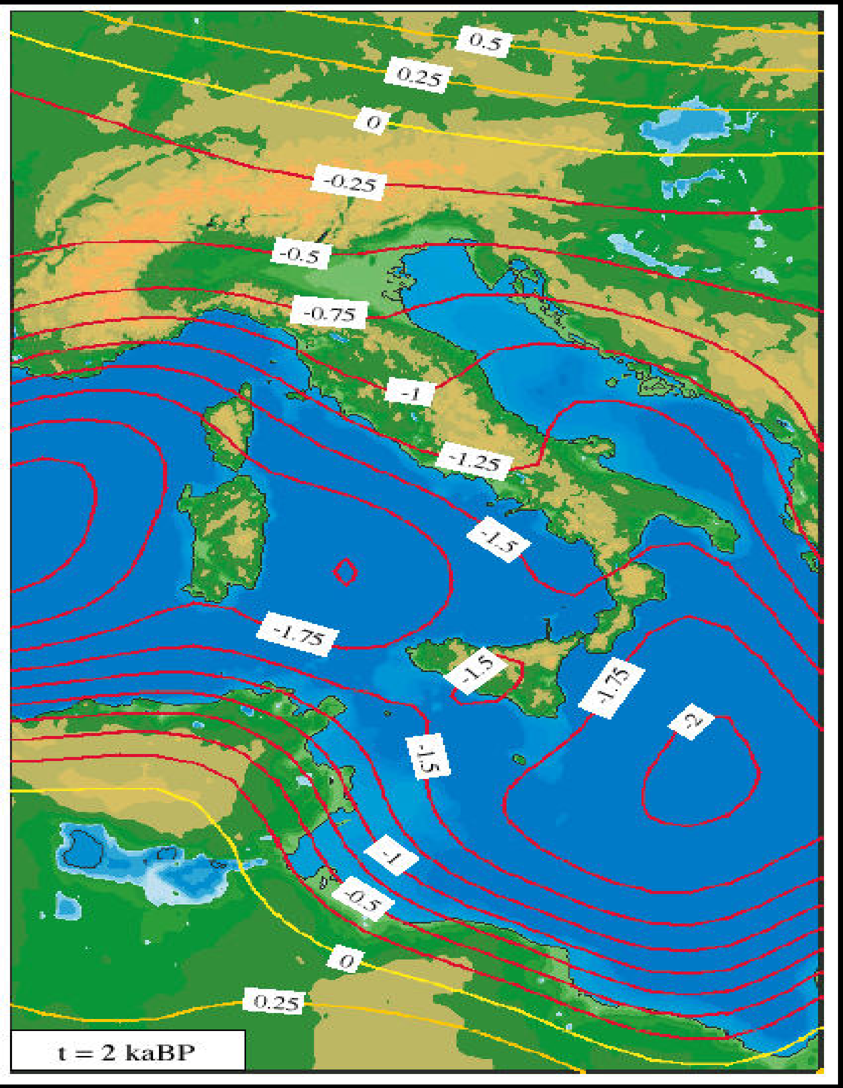
0.5
0.25
0
-0.25
-0.5
-0.75
-1
-1.25
-1.5
-1.75
-1.5
-1.75
-2
-1.5
-1
-0.5
0
0.25
t = 2 kaBP

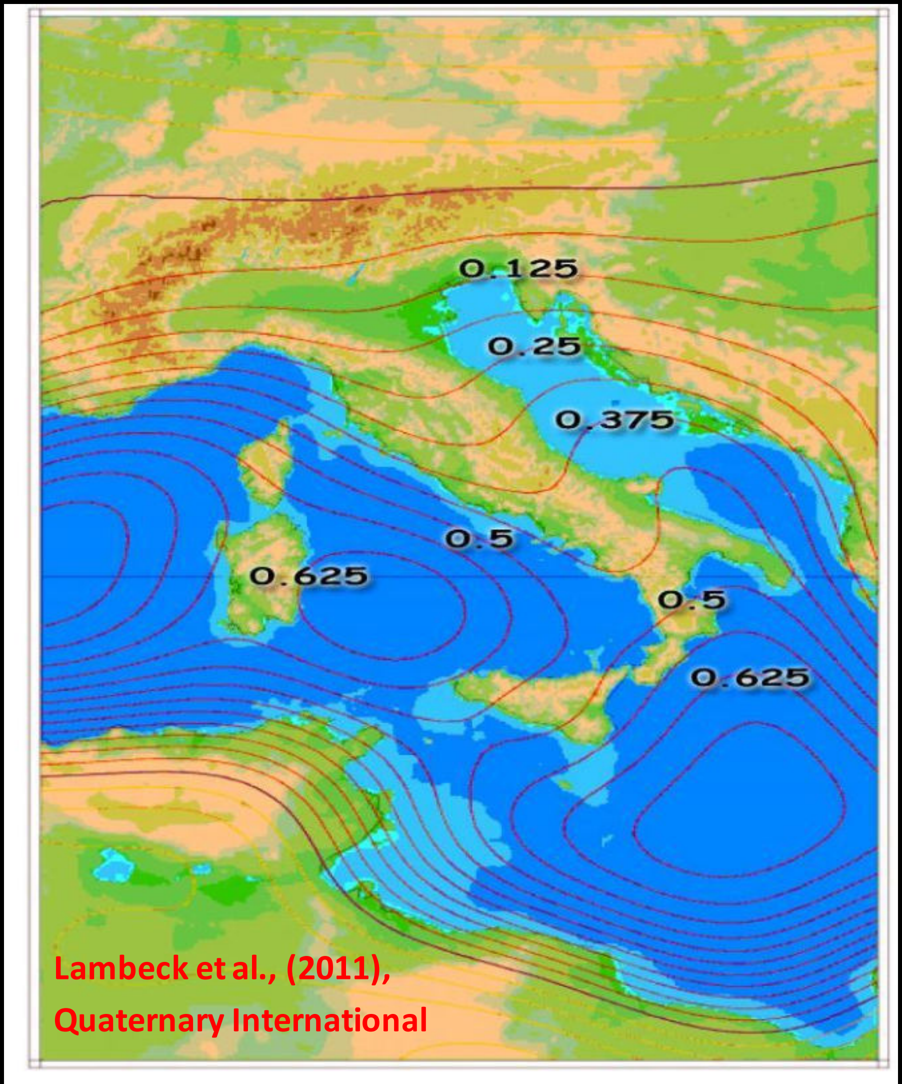
0.125
0.25
0.375
0.5
0.625
0.5
0.625
Lambeck et al., (2011),
Quaternary International

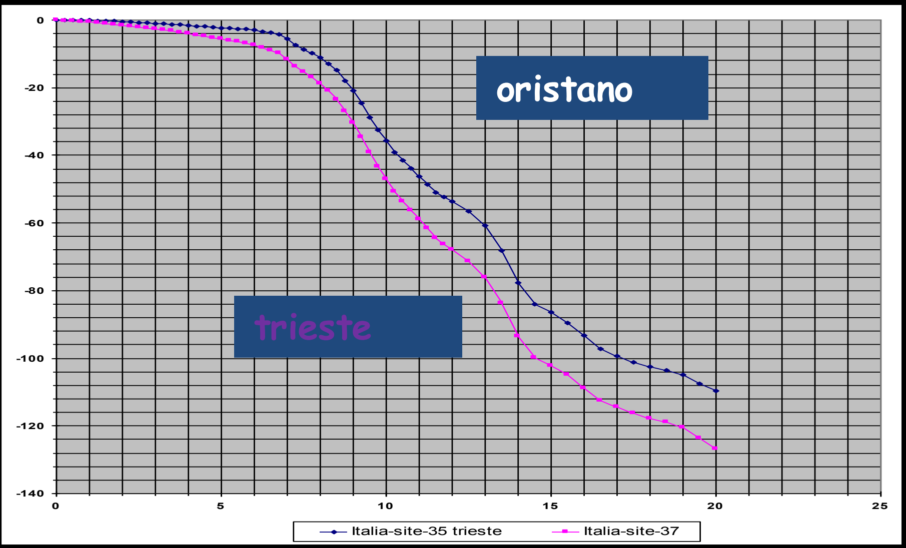

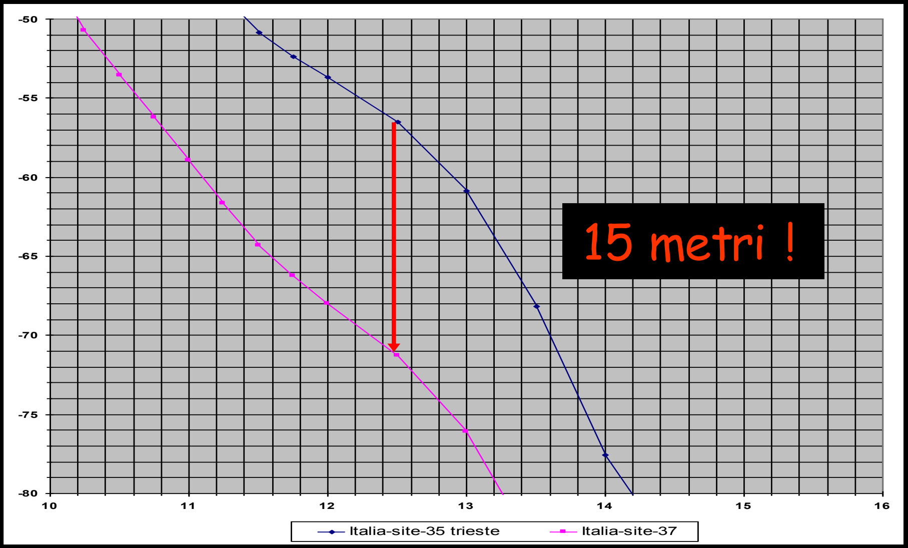

Curve di risalita di livello del mare predette dal modello di Lambeck et al., 2011. E possibile osservare, le enormi differenze dovute solamente all'isostasia (GIA) tra l'area costiera di Trieste (minimi valori di riaggiustamento isostatico e Oristano (massimi valori di isostasia per l'Italia

Indicatori s.l.

Geomorfologici

Terrazzi solchi

Sedimentologici

Speleotemi…

Biologici

Fossili (lagunari) Vermetidi

Archeologici

Piscine, moli…

…

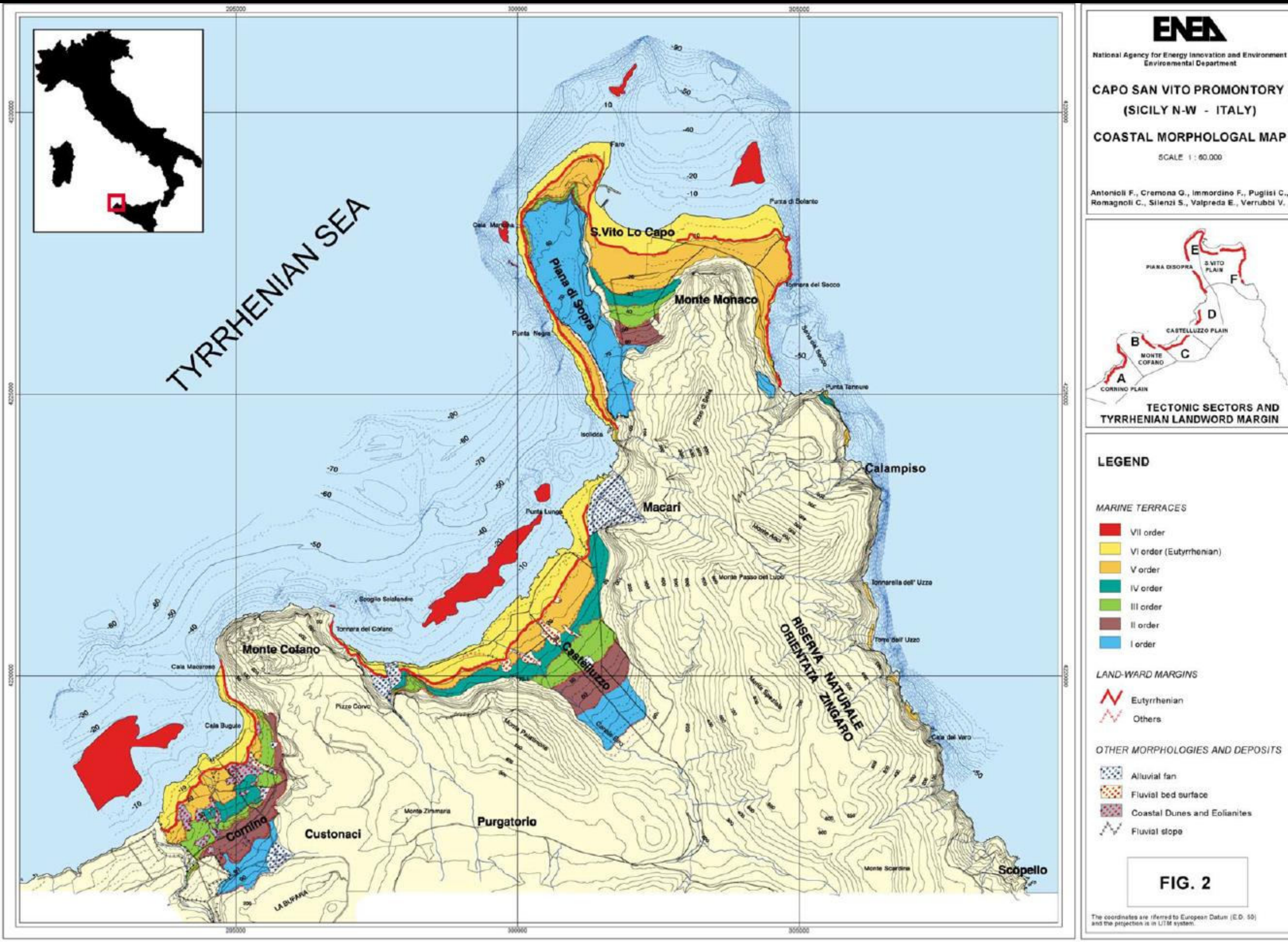

TYRRHENIAN SEA
S.Vito Lo Capo
Piana di Sopra
Monte Monaco
Punta di Solanto
Tonnara del Secco
Punta Tonnara
Cala Mancina
Punta Negra
Faro
Isolidda
Calampiso
Macari
Punta Lunga
Scoglio Solafanèr
Tonnara del Cofano
Monte Cofano
Cala Macarone
Cala Bugule
Pizzo Corvo
Castelluzzo
Monte Passo del Lupo
Tonnarella dell' Uzzo
Torre dell' Uzzo
RISERVA NATURALE ORIENTATA ZINGARO
Cala del Varo
Cornino
Custonaci
Monte Zimmaria
Purgatorio
LA BUFARA
Monte Scardina
Scopello
ENEA
National Agency for Energy Innovation and Environment
Environmental Department
CAPO SAN VITO PROMONTORY
(SICILY N-W - ITALY)
COASTAL MORPHOLOGAL MAP
SCALE 1 : 60.000
Antonioli F., Cremona G., Immordino F., Puglisi C., Romagnoli C., Silenzi S., Valpreda E., Verrubbi V.
PIANA DISOPRA
S.VITO PLAIN
CASTELLUZZO PLAIN
MONTE COFANO
CORNINO PLAIN
A
B
C
D
E
F
TECTONIC SECTORS AND TYRRHENIAN LANDWORD MARGIN
LEGEND
MARINE TERRACES
VII order
VI order (Eutyrrhenian)
V order
IV order
III order
II order
I order
LAND-WARD MARGINS
Eutyrrhenian
Others
OTHER MORPHOLOGIES AND DEPOSITS
Alluvial fan
Fluvial bed surface
Coastal Dunes and Eolianites
Fluvial slope
The coordinates are riferred to European Datum (E.D. 50) and the projection is in UTM system.

FIG. 2

Margine interno di un terrazzo marino risalente a circa 125.000 anni fa

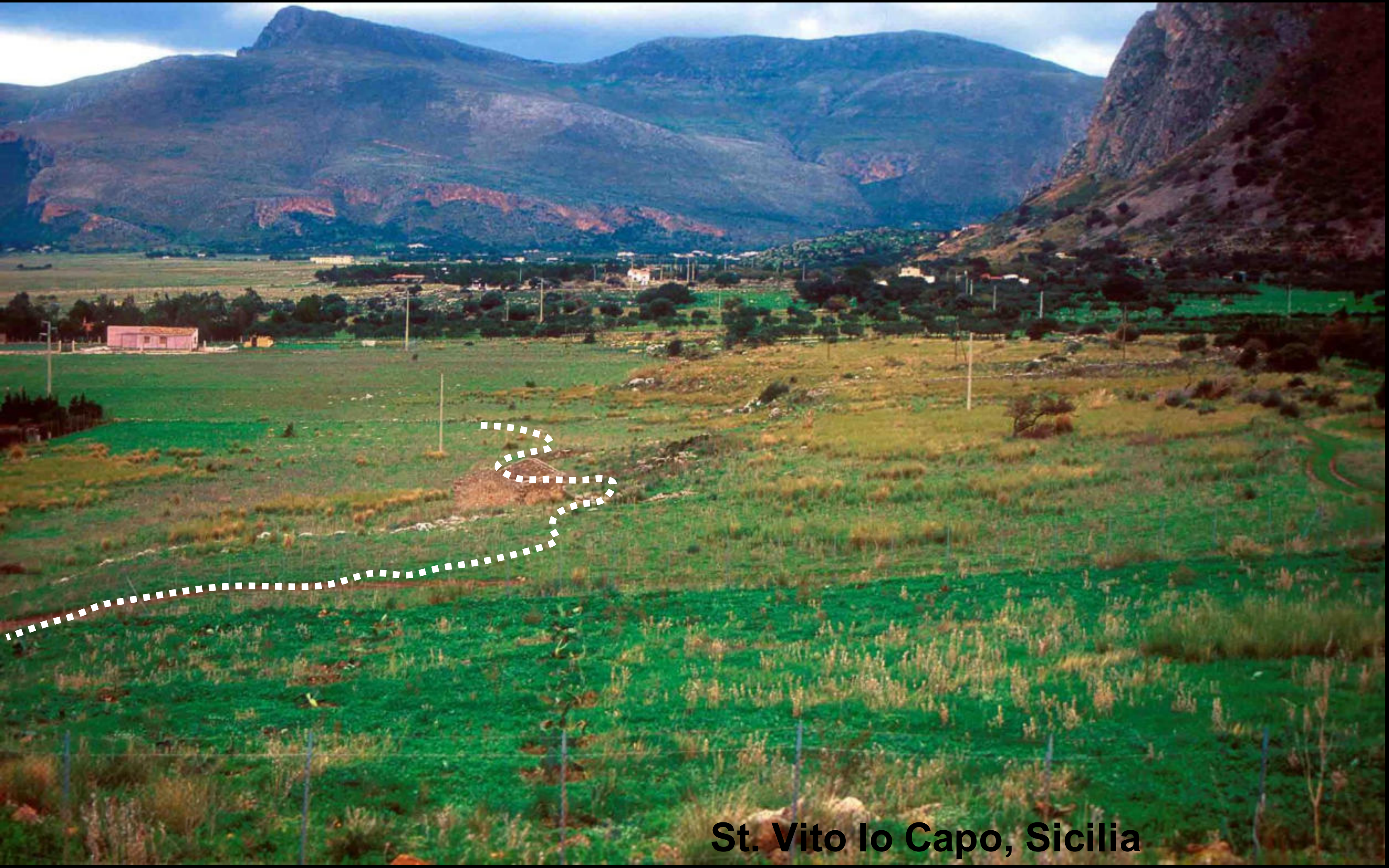

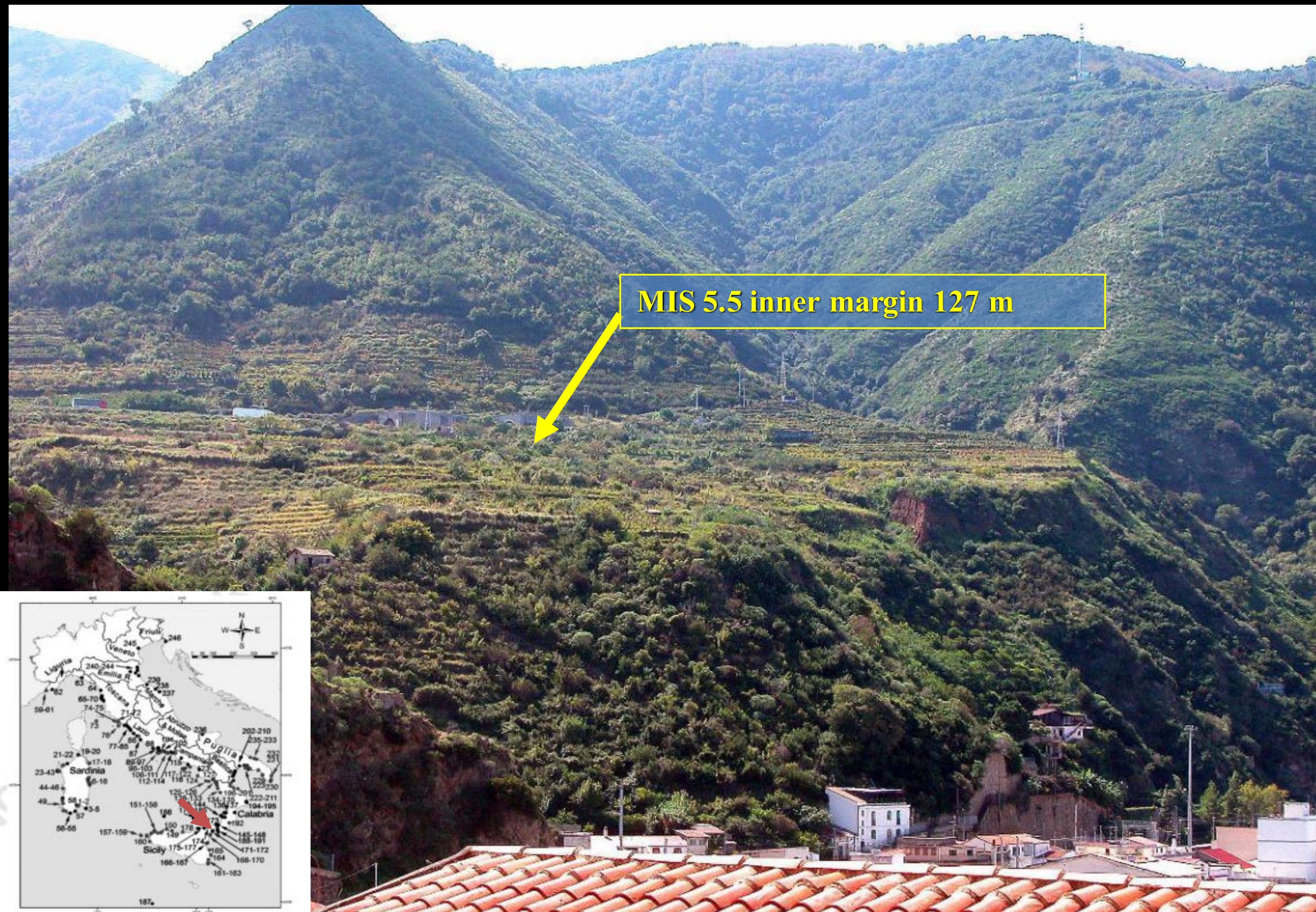
MIS 5.5 inner margin 127 m
Liguria
Veneto
Friuli
Sardinia
Puglia
Calabria
Sicily

water MDPI

Article

MIS 5.5 highstand, and future sea level flooding at 2100 and 2300 in tectonically stable areas of central Mediterranean sea: Sardinia and the Pontina Plain (southern Latium), Italy

Giacomo Deiana[1,2*], Fabrizio Antonioli[3], Lorenzo Moretti[4], Paolo E. Orrù[1,2], Giovanni Randazzo[5], Valeria Lo Presti[3]

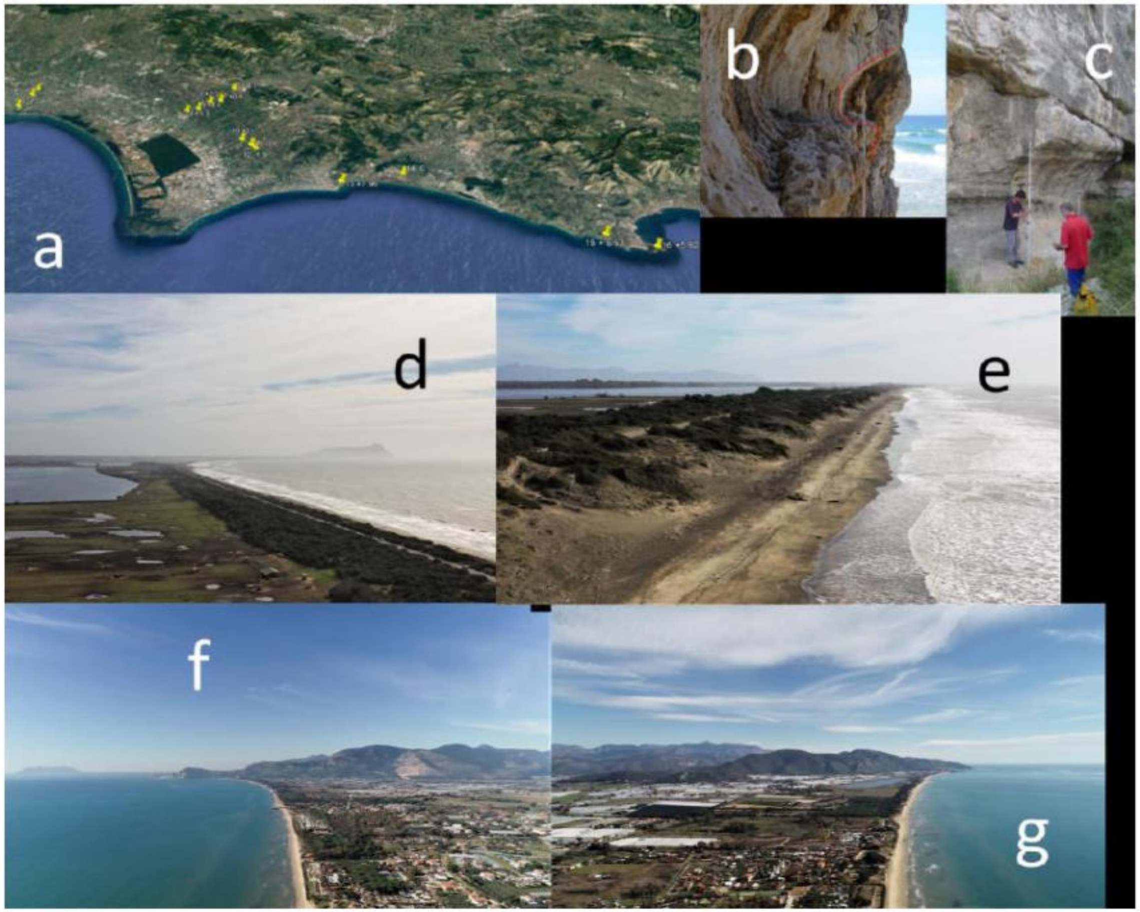

Figure 13. a, Google earth image of the Pontina and Fondi Plain with the carbonatic promontory of Terracina, Sperlonga on which are carved the fossil tidal notches (b and c) aged MIS 5.5 the yellow arrow indicate samples number and altitude (see Table 3) Pianura Pontina e di Fondi. d, the coastal area of northern Pontina Plain (on background he limestone Circeo Promontory); e, the coastal area of northern Pontina Plain (on background he limestone Terracina promontory. f, the coastal area of Fondi Plain (on background the limestone Terracina Promontory; g same point but a southern view, with Sperlonga promontory.

Figure 14. a: *Cerastoderma edulis* sampled in a section outcropping in the channel of this figure in **e**. **b** *Tapes decussatus* from the outcrop on the reclamation drainage c channel; **c** and **e** the channel d the Mussolini channel during the excavation in 30s; **f** *the outcrop Nassa mutabilis Tapes decussatus, Cerastoderma edulis;* **f** a fossiliferous level very rich of lagoon fauna. See also Table 3 site 7.1.

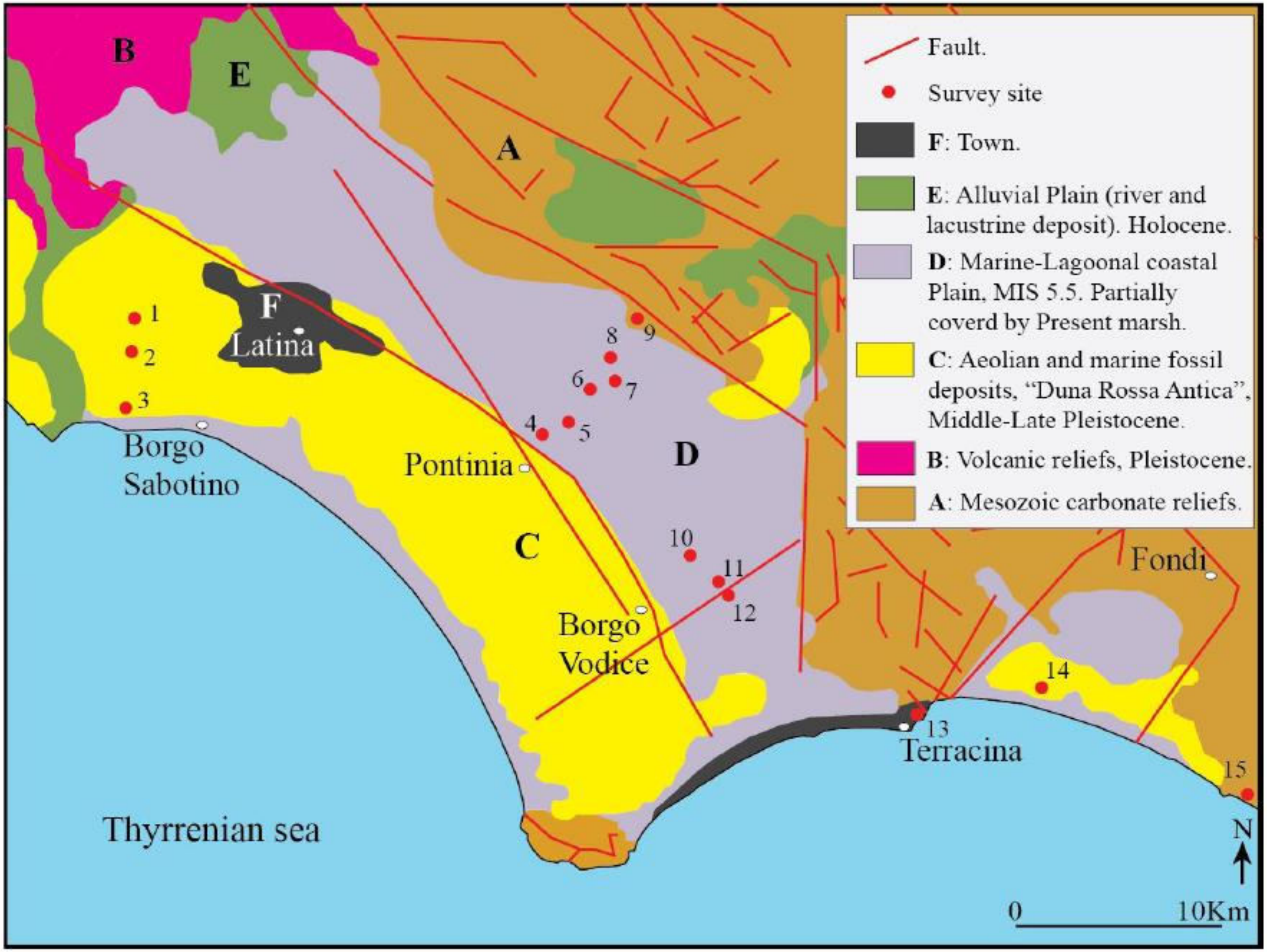

Figure 12. - Main geological outcrocps of the Pontina Plain, this map is a compilation of: i) Italian Geological Survey sheet numbers 170, 158 and 159; ii) Map of the soil [51], iii) sinkhole map of Regione Lazio http://www.regione.lazio.it/binary/rl_main/tbl_documenti/AMB_PBL_Carta_Sinkholes_Lazio_2011.pdf. The red dots refer to the sites described in Table 3.

2	Canale Mussolini	41.4483 12.8107	**5.1 ± 0.1**	Fossil beach containing *Persistrombus latus*	Senegalese Fauna Aminoacid	[37,40,43]
3	Nuclear power plant Borgo Sabotino	41.4231 12.8053	**-4.3 +5 ± 0.5**	Fossil beach containing *Persistrombus latus*	Senegalese Fauna	[43]
4	Pontinia 1	41.4129 13.0449	**+5.3 ± 0.5**	Lagoonal facies with *Cerastoderma s.p.*	Geomorphological correlation	[17,46]
5	Pontinia 2	41.4172 13.0600	**+4.4 ± 0.5**	Lagoonal facies with *Cerastoderma*	Geomorphological correlation	[17,46]
6	Pontinia 3	41.4323 13.0721	**+2.3 ± 0.5**	Lagoonal facies with *Cerastoderma s.p.*	Geomorphological correlation	[17,46]
7	Pontinia 4	41.4355 13.0864	**+0.8 ± 0.5**	Lagoonal facies with *Cerastoderma s.p.*	Geomorphological correlation	[17,46]
7.1	Check in field	41.434771 13.062667	**-1± 0.5**	Cerastoderma e Tapes, travertino con incrostazioni	Geomorphological correlation	This paper
7.2	Check in field	41.3757510 13.1281060	**-2± 0.5**	Lagoonal facies with *Cerastoderma s.p.*	Geomorphological correlation	This paper
7.3	Check in field	41.363875 13.140631	**-3± 0.5**	Lagoonal facies with *Cerastoderma edulis, Tapes decussatus, Nassa mutabilis*	Geomorphological correlation	This paper
8	Pontinia 5	41.4424 13.0751	**-0.5 ± 0.5**	Lagoonal facies with Cerastoderma	Geomorphological correlation	[17,46]
9	Mezzaluna core	41 27 47 13 06 01	**-14.30 -11.41 ± 0.5**	Venus and Cerastoderma	Pollen Analysis, U\Th and aminoacid	[45]
10	Borgo Vodige 1	41.3571 13.1317	**1 ± 0.5**	Lagoonal facies with Cerastoderma	Aminoacid	[17,46]
11	Borgo Vodige 2	41.3497 13.1293	**-0.6 ± 0.5**	Lagoonal facies with Cerastoderma	Aminoacid	[17,46]
12	Borgo Vodige 3	41.350 13.117	**-1.80 ± 0.5**	Lagoonal facies with Cerastoderma	Aminoacid	[17,46]
13	Terracina	41.288 13.260	**7.96 ± 0.1**	Tidal notch	Geomorphological correlation at 5 km from aged MIS 5.5 deposit	[7]
14	Fondi APT4	41.0065 13.331	**-6 \ -24**	Marsh with Cerastoderma Aminozone E	Aminoacid	[44]



Quaternary Science Reviews 119 (2015) 66–84

Contents lists available at ScienceDirect

Quaternary Science Reviews

journal homepage: www.elsevier.com/locate/quascirev

Tidal notches in Mediterranean Sea: a comprehensive analysis

Fabrizio Antonioli [a], Valeria Lo Presti [b, a, *], Alessio Rovere [c, d], Luigi Ferranti [e], Marco Anzidei [f], Stefano Furlani [g], Giuseppe Mastronuzzi [h], Paolo E. Orru [i], Giovanni Scicchitano [j], Gianmaria Sannino [a], Cecilia R. Spampinato [k], Rossella Pagliarulo [l], Giacomo Deiana [i], Eleonora de Sabata [m], Paolo Sansò [n], Matteo Vacchi [o], Antonio Vecchio [f]

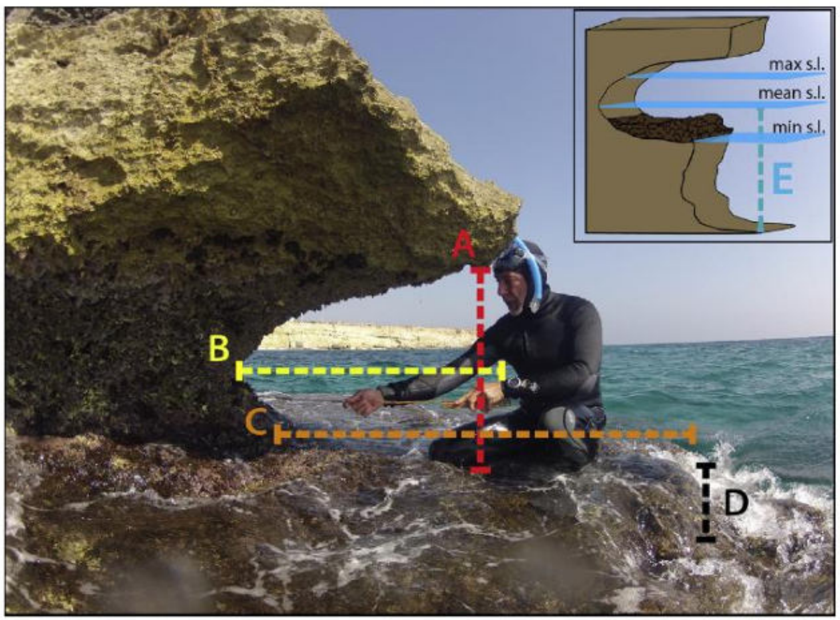

Fig. 3. Morphometric measures: A) Average notch width, B) Notch depth, C) Bottom depth (reef when present), D) reef and step (if present) thickness, E) Depth of cliff toe at mean sea level.

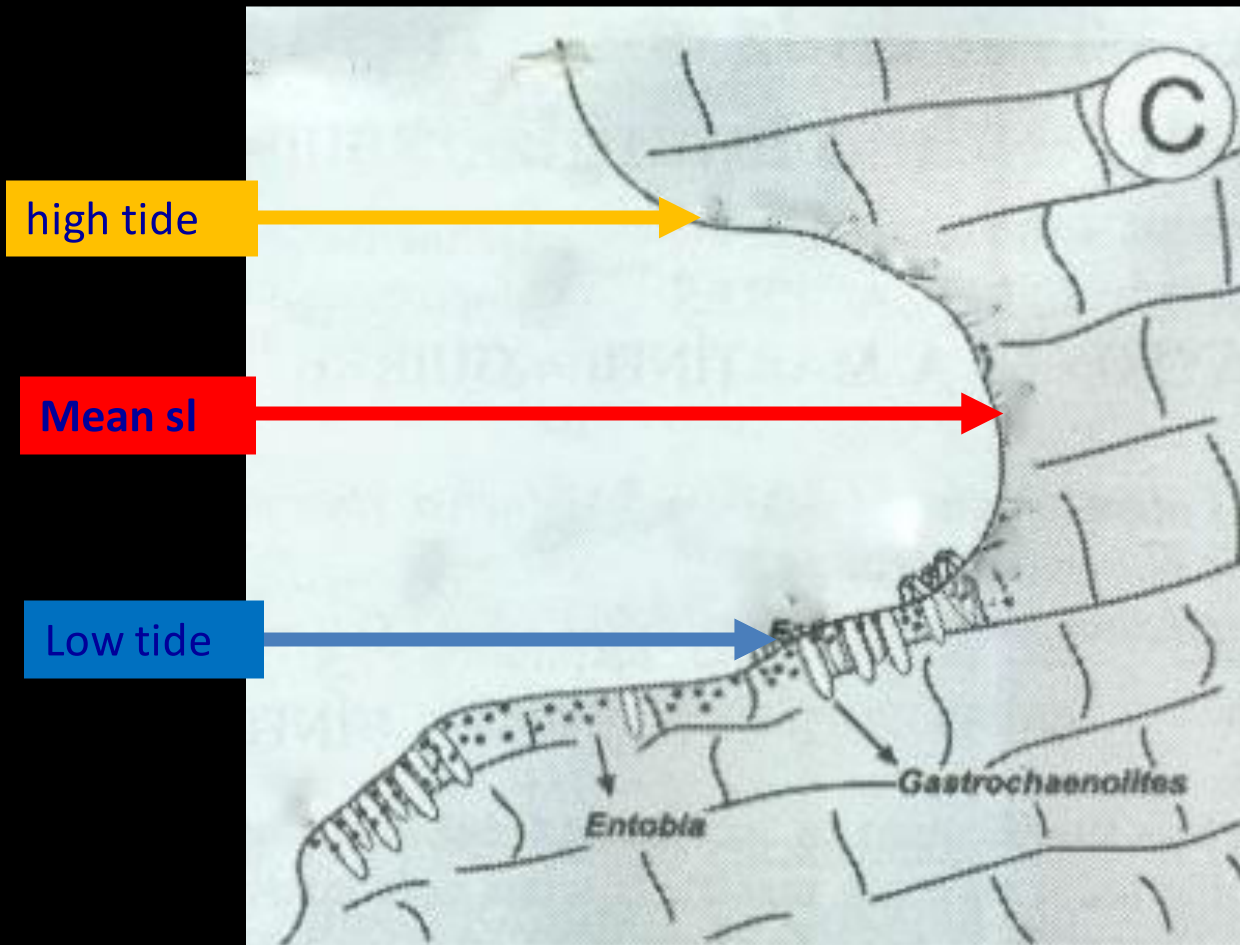

high tide
Mean sl
Low tide
C
Entobia
Gastrochaenolites

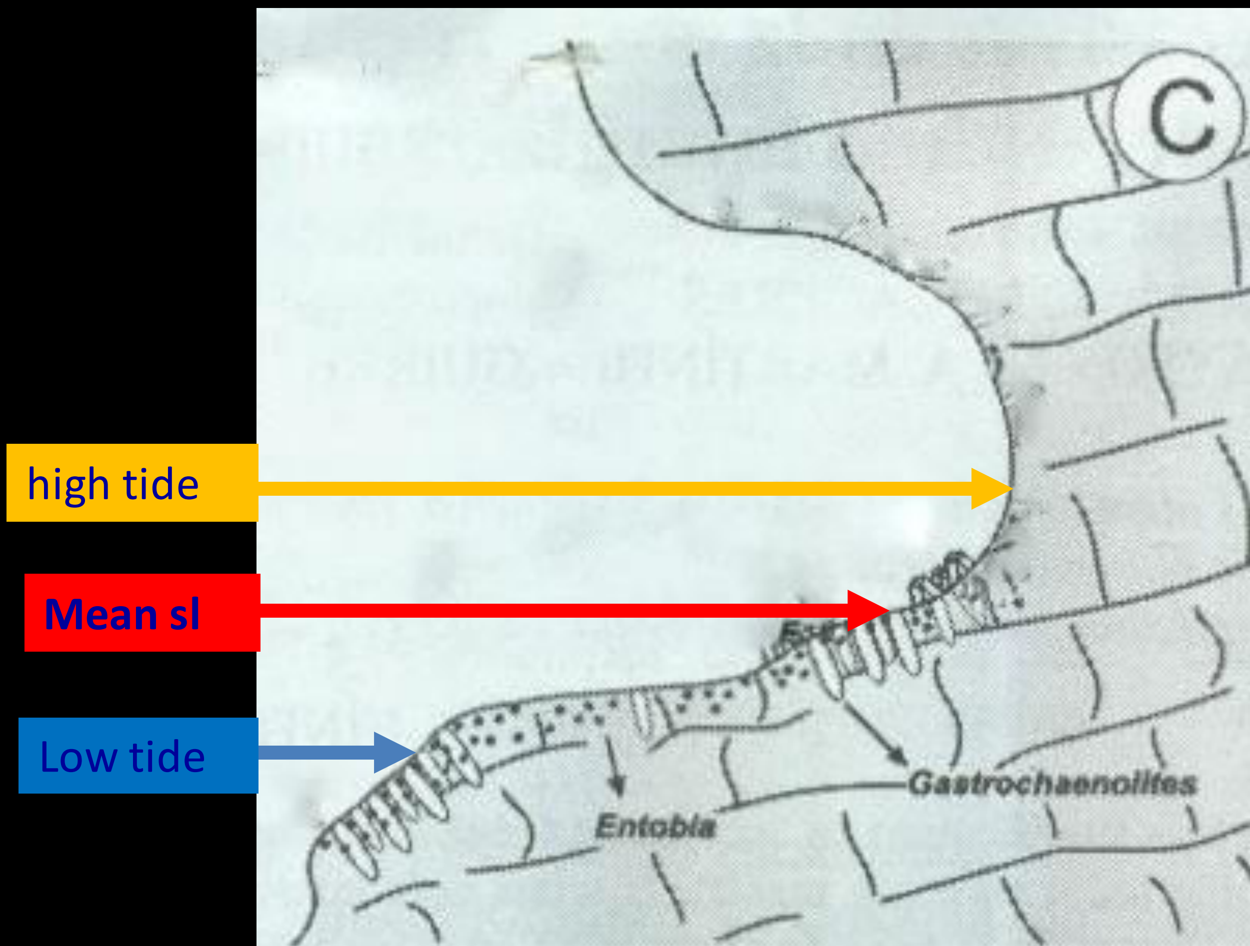
high tide
Mean sl
Low tide
C
Gastrochaenolites
Entobia

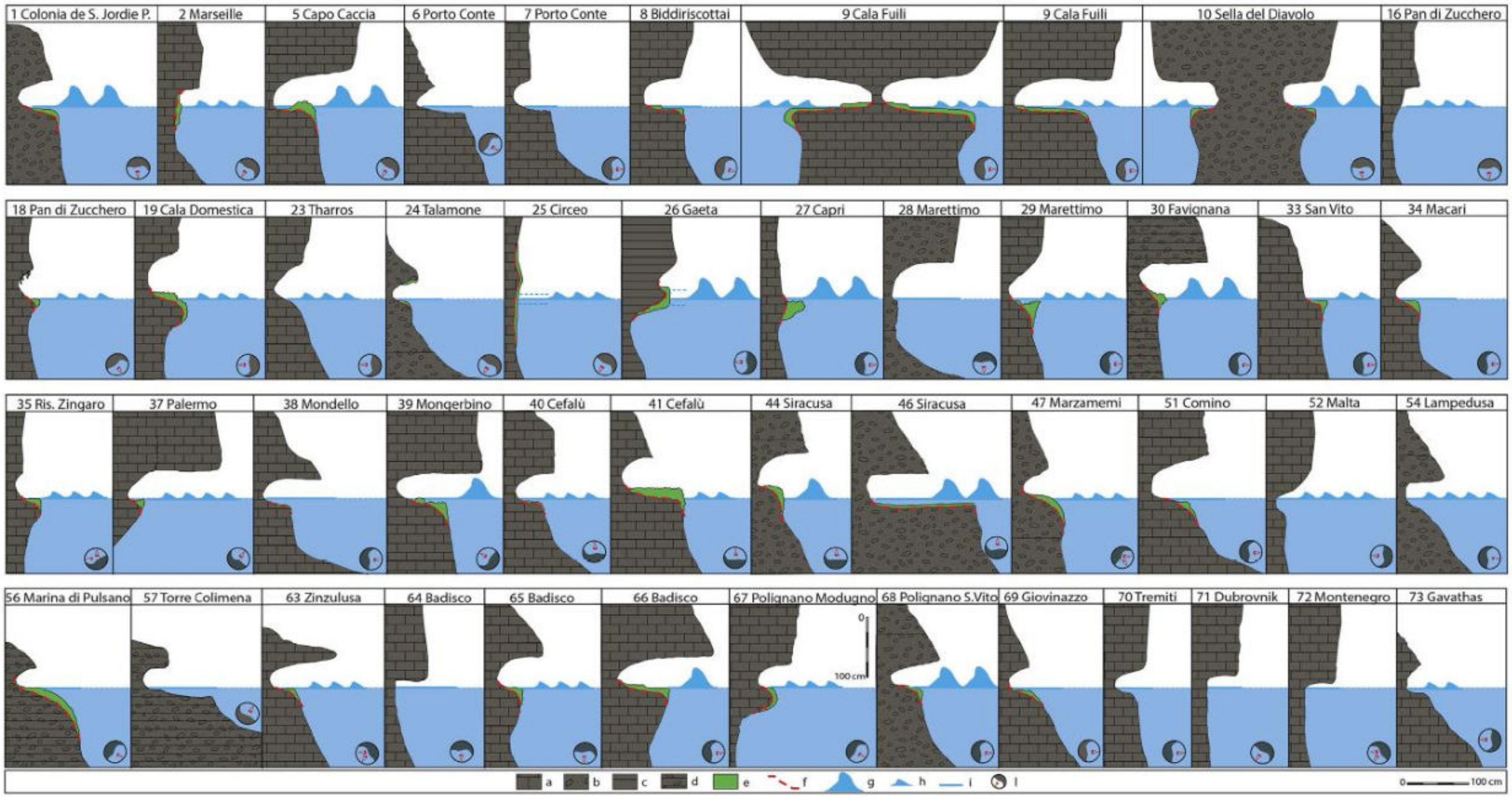

Fig. 6. Representative sections of most significant tidal notches studied. a) limestone, b) sandstone and very erosive limestone, c) stratified limestone, d) stratified sandstone and very erosive limestone, e) reef, f) supposed limit between rock and reef. Fetch and kind of sea energy: g) very exposed, h) exposed, i) sheltered. l) geographical exposure (see Table 2).

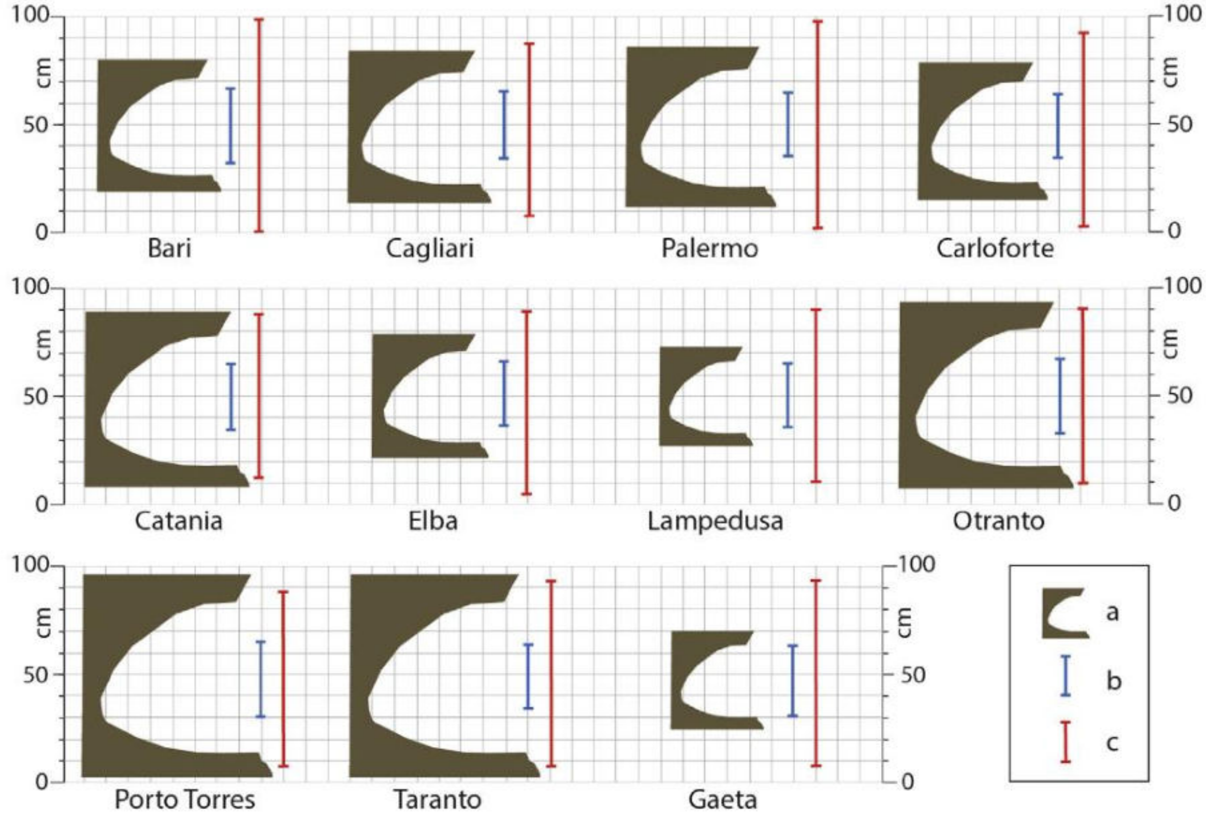

Fig. 7. Relationship between notch width (a), mean tide values (b) and extreme (max−min) tide values (c) in locations where notches have been measured near a tide station.

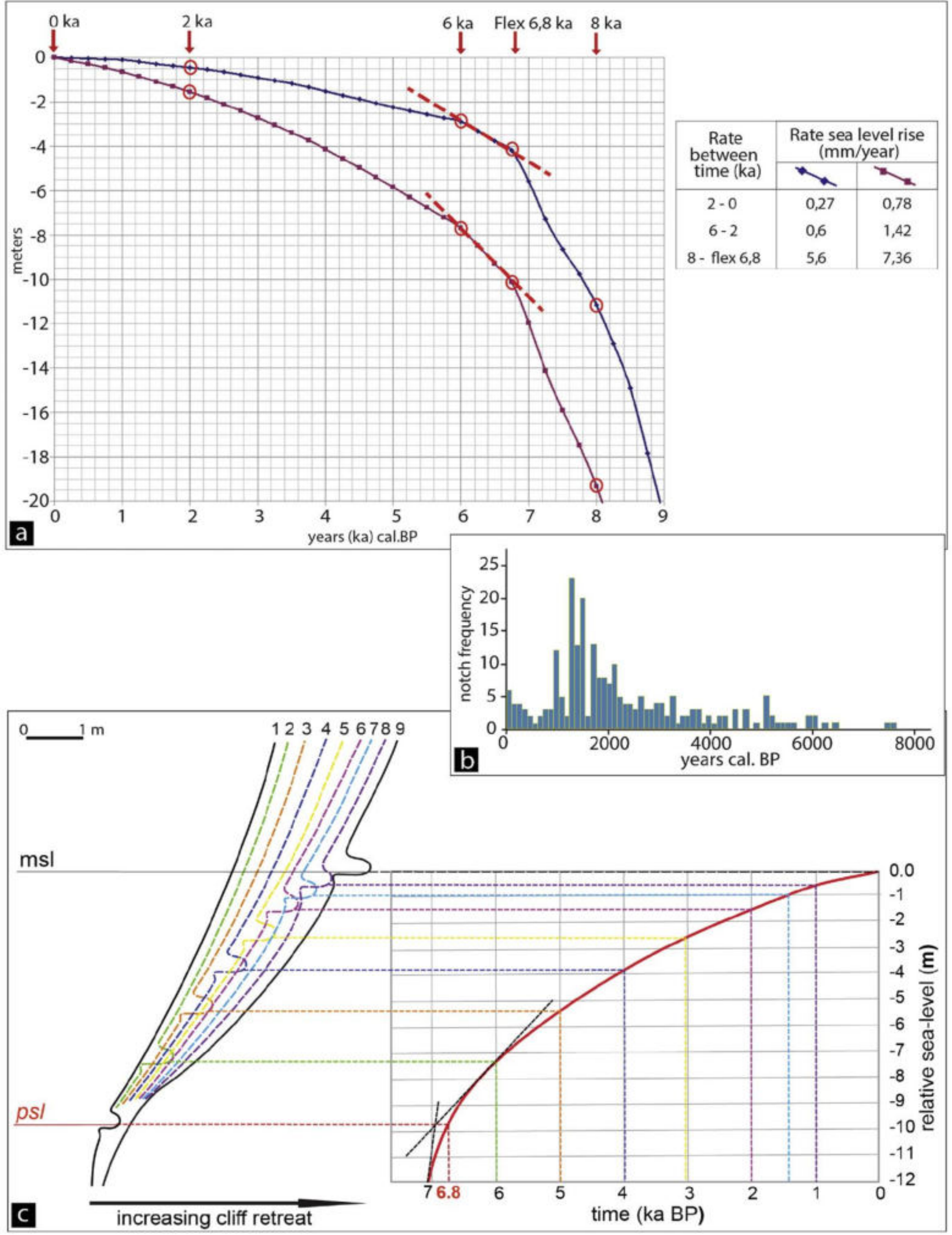

Fig. 10. a) Sea level rise rates from 8 ka cal BP to the Present using the predicted sea level rise curves (Lambeck model, 2011) with maximum (Cagliari, purple line) and minimum (Trieste, blue line) isostatic subsidence values. The inflection at 6.8 ka marks the change of rise. **b)** Frequency of notches formation from 8 ka to 0 ka (modified from Boulton and Stewart, 2015). **c)** Model of tidal notches formation from 6.8 ka to the present. (For interpretation of the references to colour in this figure legend, the reader is referred to the web version of this article.)

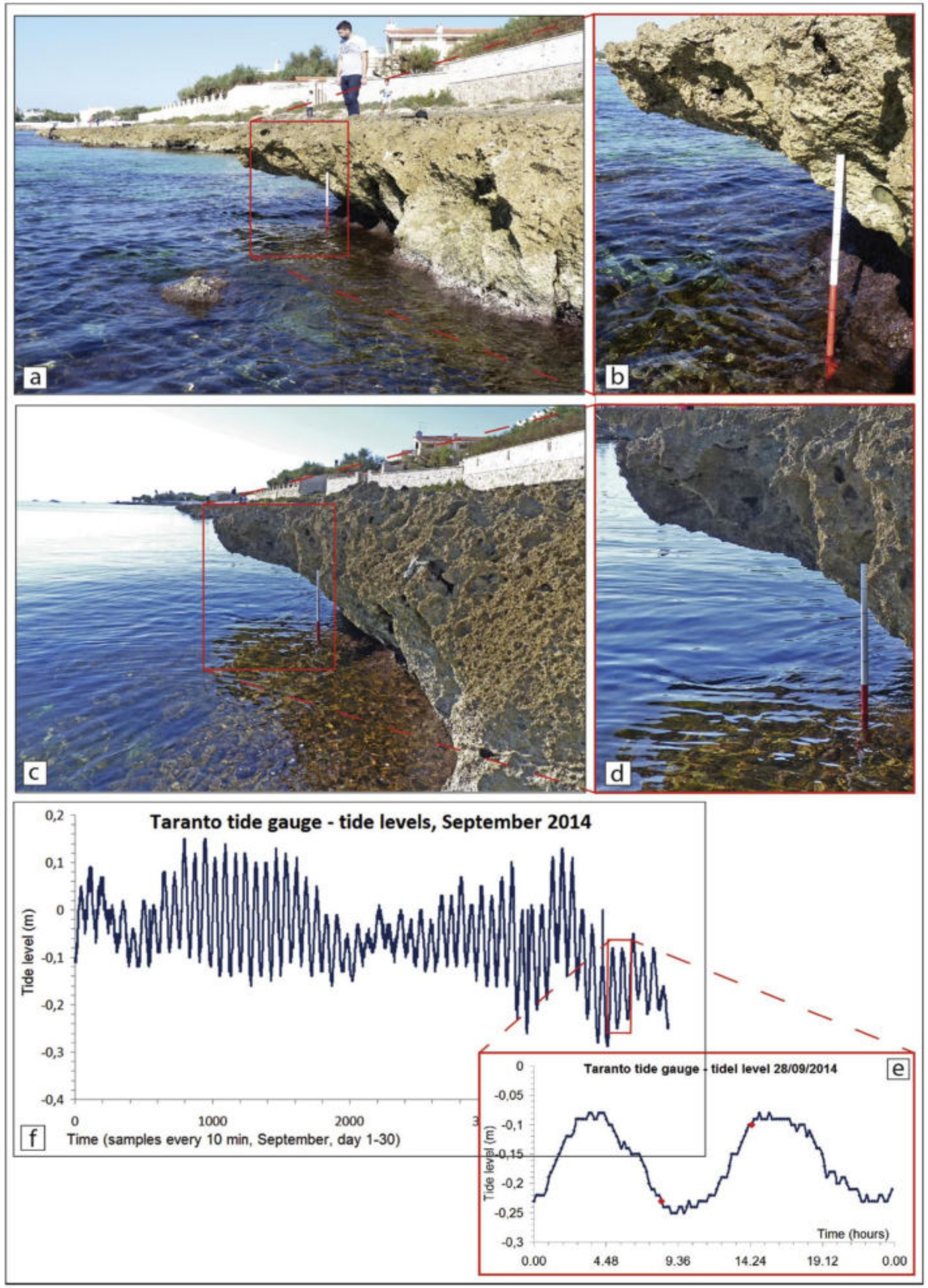

Fig. 12. Tidal range measured on the Taranto – San Vito notch (site 68 Table 1 and S1. Measured on 09/28/2014 at 10.00 am (a,b), and 16.30 pm (c,d). Observations are in agreement with the instrumental data collected at the nearest tide gauge located at Taranto. Plots show the daily tide during the observations (e) while in f) are the tides for one month cycle of September. The red arrow indicate the time of the notch measures (a,b,c,d). (For interpretation of the references to colour in this figure legend, the reader is referred to the web version of this article.)

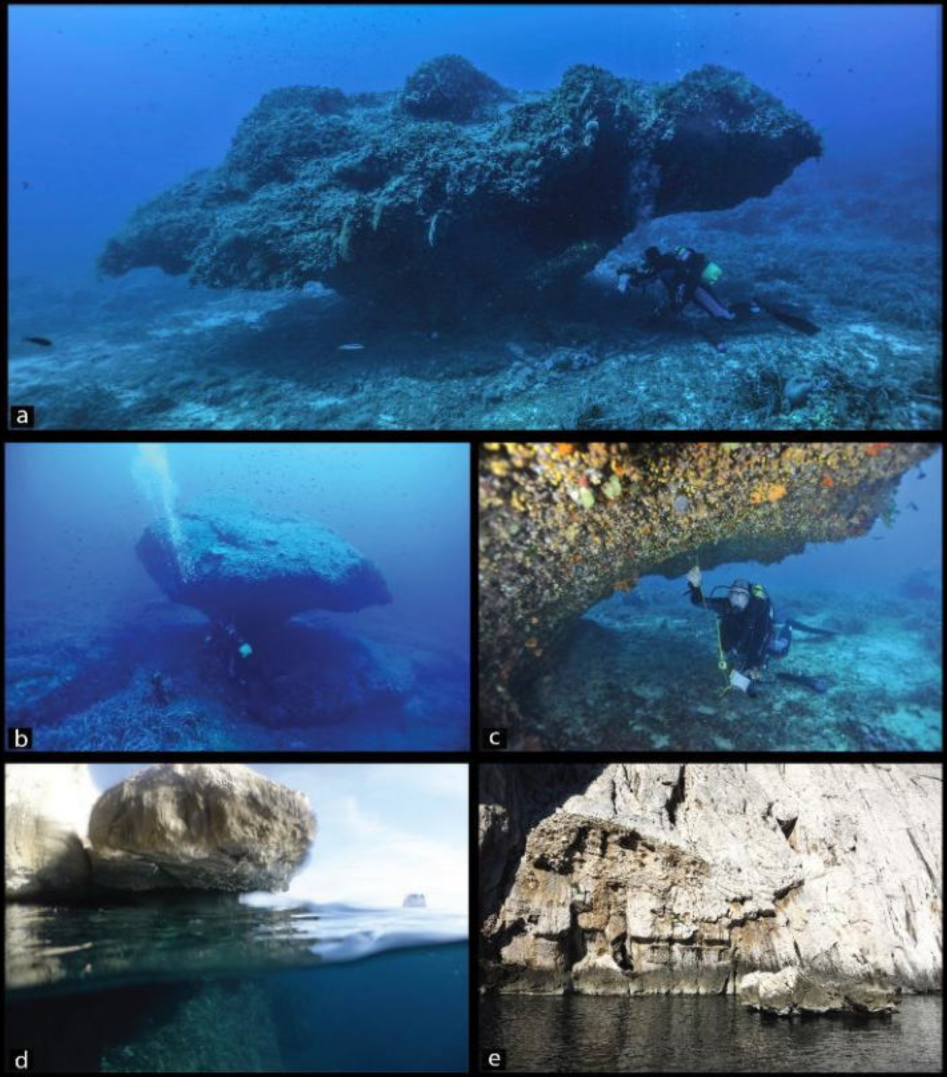
a
b
c
d
e

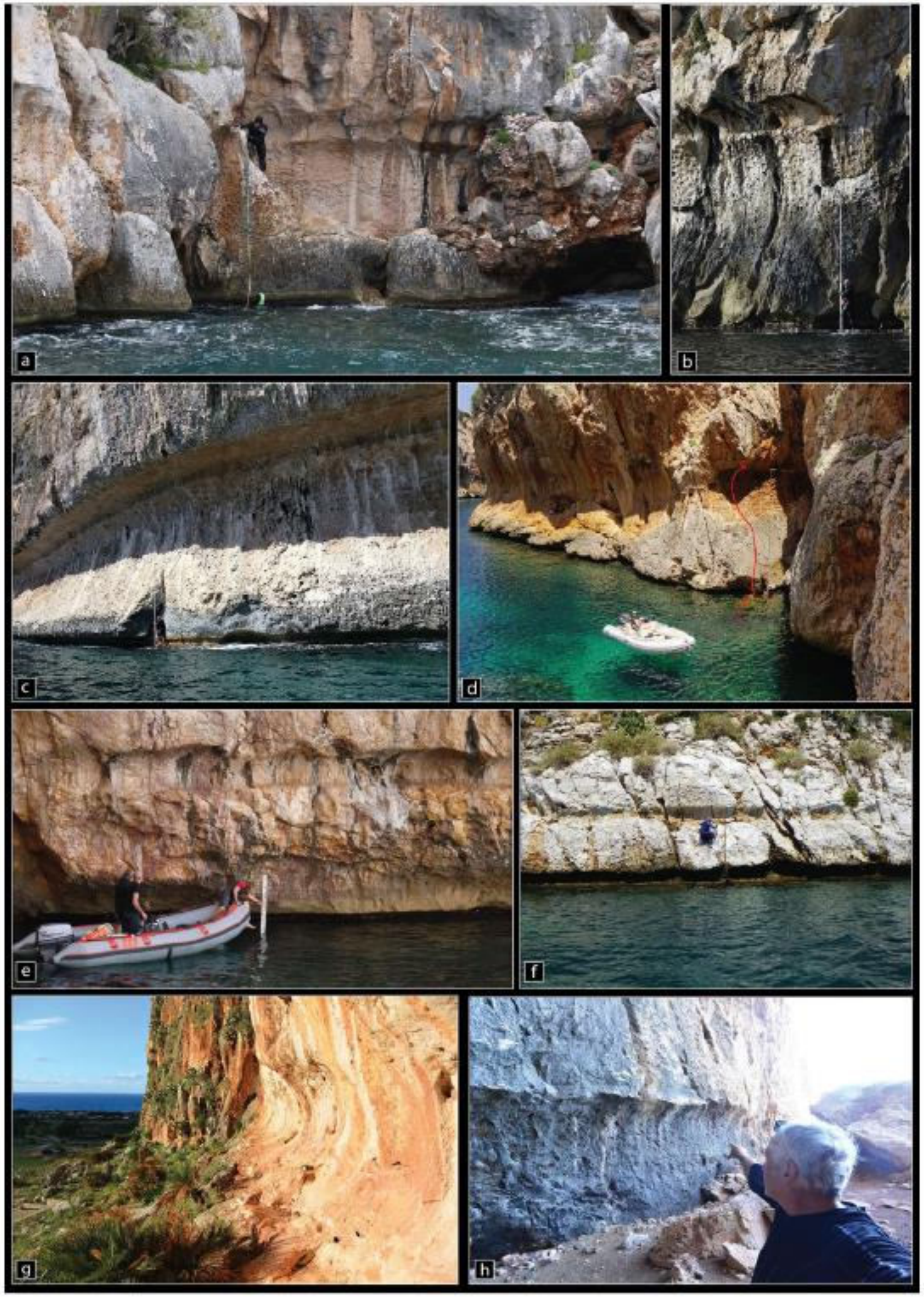
a
b
c
d
e
f
g
h

Earth-Science Reviews 185 (2018) 600–623

Contents lists available at ScienceDirect

Earth-Science Reviews

journal homepage: www.elsevier.com/locate/earscirev

Morphometry and elevation of the last interglacial tidal notches in tectonically stable coasts of the Mediterranean Sea

Antonioli F.[a], Ferranti L.[b], Stocchi P.[c], Deiana G.[d], Lo Presti V.[a], Furlani S.[e], Marino C.[b], Orru P.[d], Scicchitano G.[f], Trainito E.[g], Anzidei M.[h], Bonamini M.[i], Sansò P.[j], Mastronuzzi G.[k]

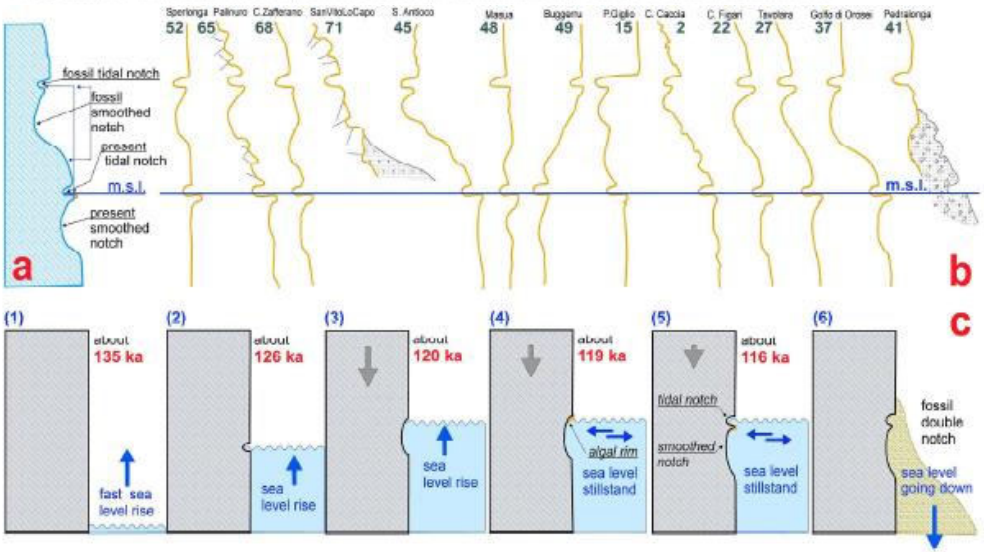

Fig. 2. a) MIS 5.5 and PTN notches morphological sketch. b) Tidal and smoothed notch as is possible to observe today in some sections we studied. c) Evolution of the tidal and smoothed notch during MIS 5.5, the final coverage of fans or aeolianites deposits preserves the notches from the dissolution.

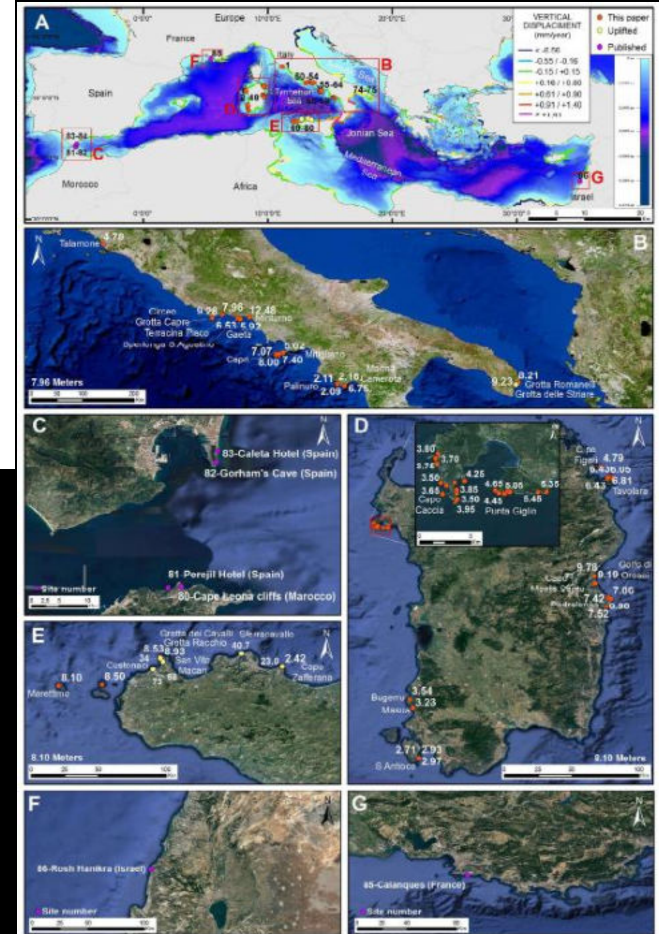

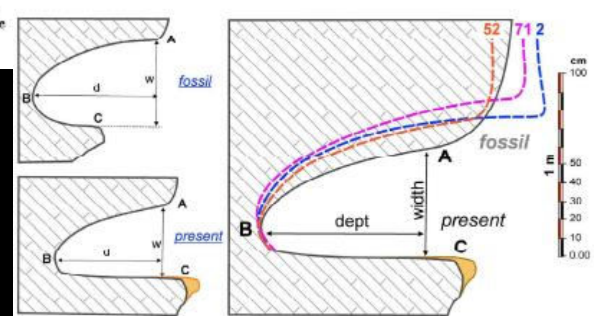

Fig. 3. Sections of fossil and present tidal notch morphology. The letters refer to the width (w), depth (d) and the base of the notch (c). On the right an overlap between the present and the fossil tidal notch (for the sites 52, 71 and 2 of Table 1) morphology highlights the marine and subaerial erosion that slightly modified the original morphology, but preserves a similar width.

Earth-Science Reviews 185 (2018) 600–623

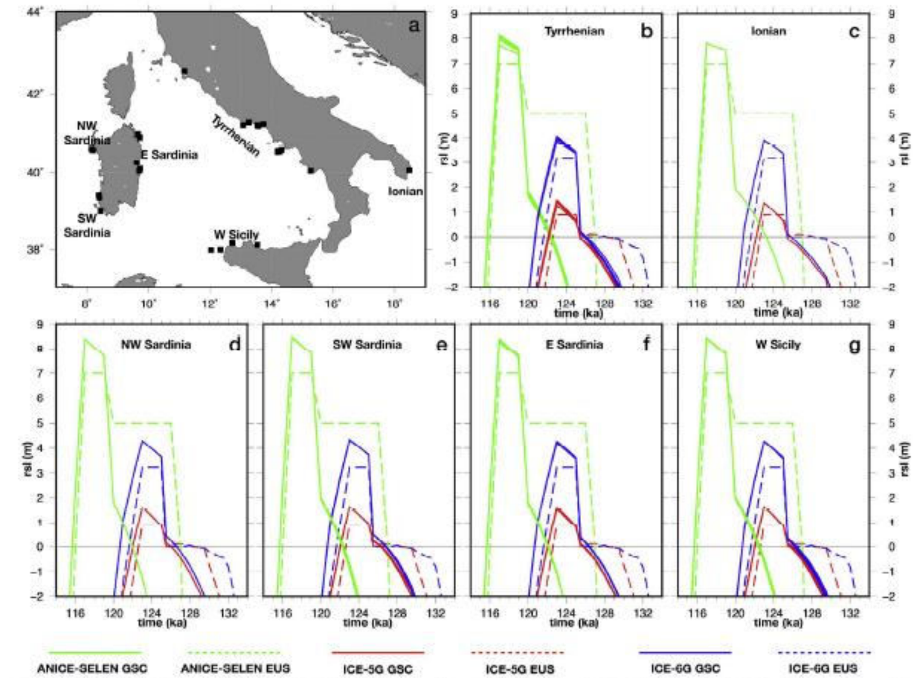

Fig. 6. Predicted MIS 5.5 RSL curves at sites along the Italian coastlines according to ICE-5G (red curves), ICE-6G (blue curves) and ANICE-SELEN (green curves) ice-sheet models. The dashed curves represent the eustatic trend, while the solid curves represent the GIA-induced RSL changes. The RSL curves are computed at each investigated site and are plotted cumulatively for different sub-regions. (For interpretation of the references to colour in this figure legend, the reader is referred to the web version of this article.)

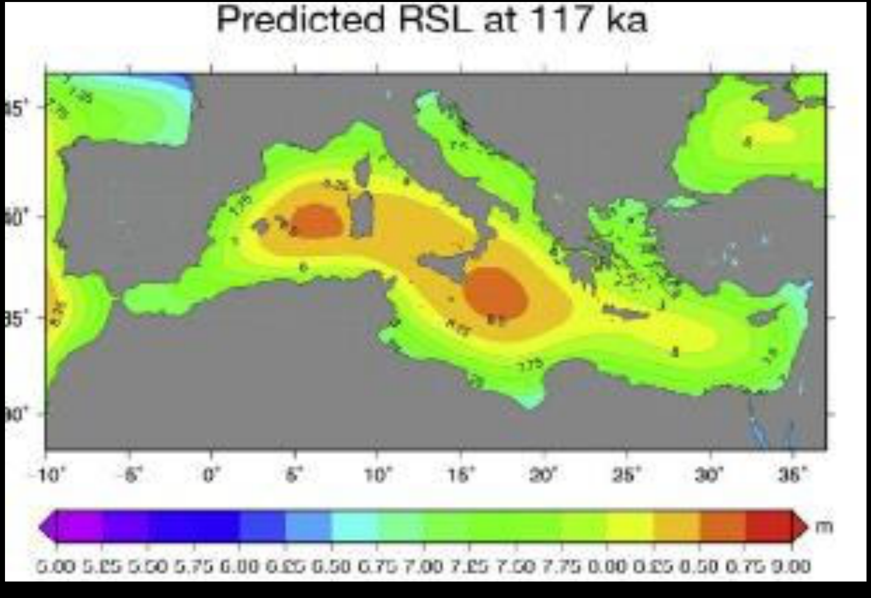

Fori di *Litophaga* fossili a Marettimo, si osservano fino a 7.30 metri. Ad 8 metri è presente un solco di battente fossile

San Vito lo Capo, Sicily, scogliere a Vermetidi (Dendropoma petreum), un gasteropode coloniale che vive a livello del mare, e risulta utilissimo quando trovato fossile. Qui sotto la sezione di un frammento di reef, i Vermetidi oggi fossili, campionati e datati nella parte inferiore, hanno fornito una data di circa 600 anni a -30 centimetri, Antonioli et al., 1991, Marine Geology. Alcune note aree della Sicilia vengono naturalmente ripascite per la distruzione da parte di tempeste, di questi gasteropodi coloniali che forniscono preziosissimo materiale sabbioso sulla costa.


N
R
R
R
R
R
2/3
R
R
1
R
R
R
R
R
Data SIO, NOAA, U.S. Navy, NGA, GEBCO
Google earth
3
2
1

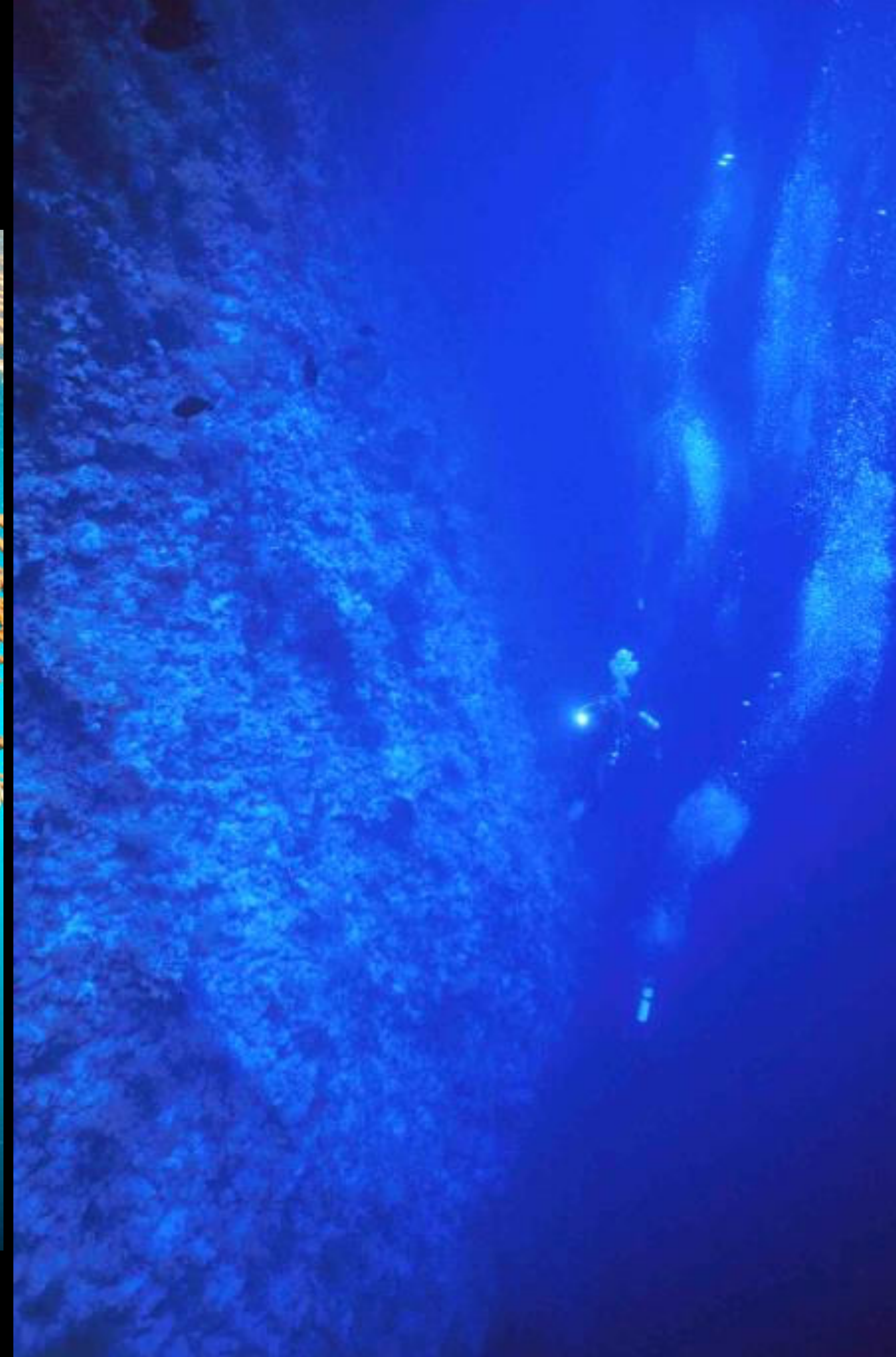

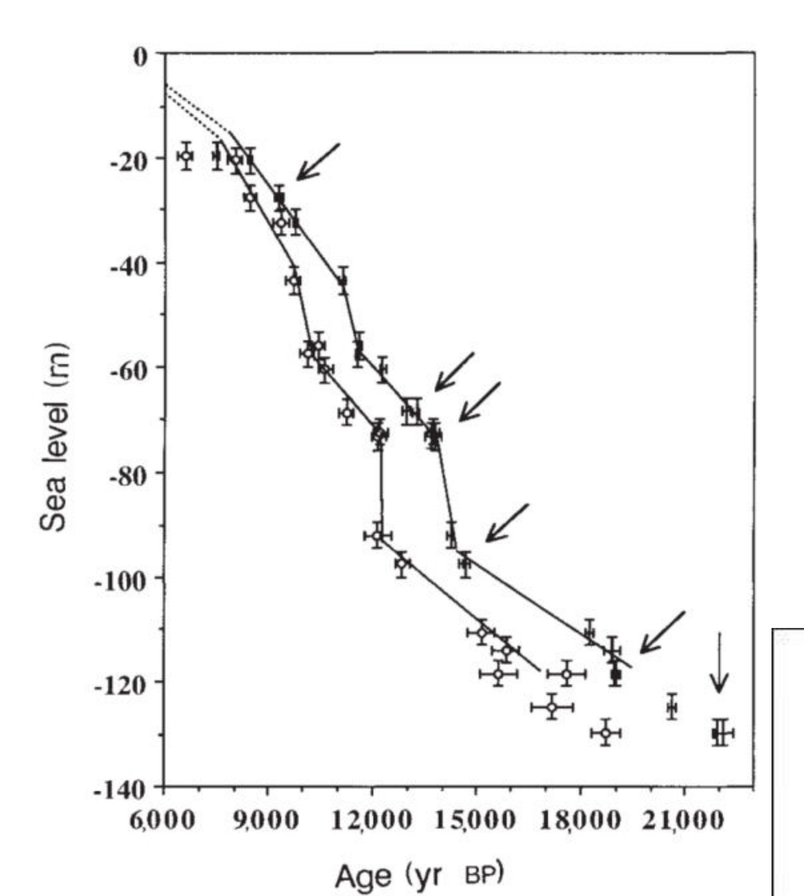

0
-20
-40
-60
-80
-100
-120
-140
Sea level (m)
6,000
9,000
12,000
15,000
18,000
21,000
Age (yr BP)

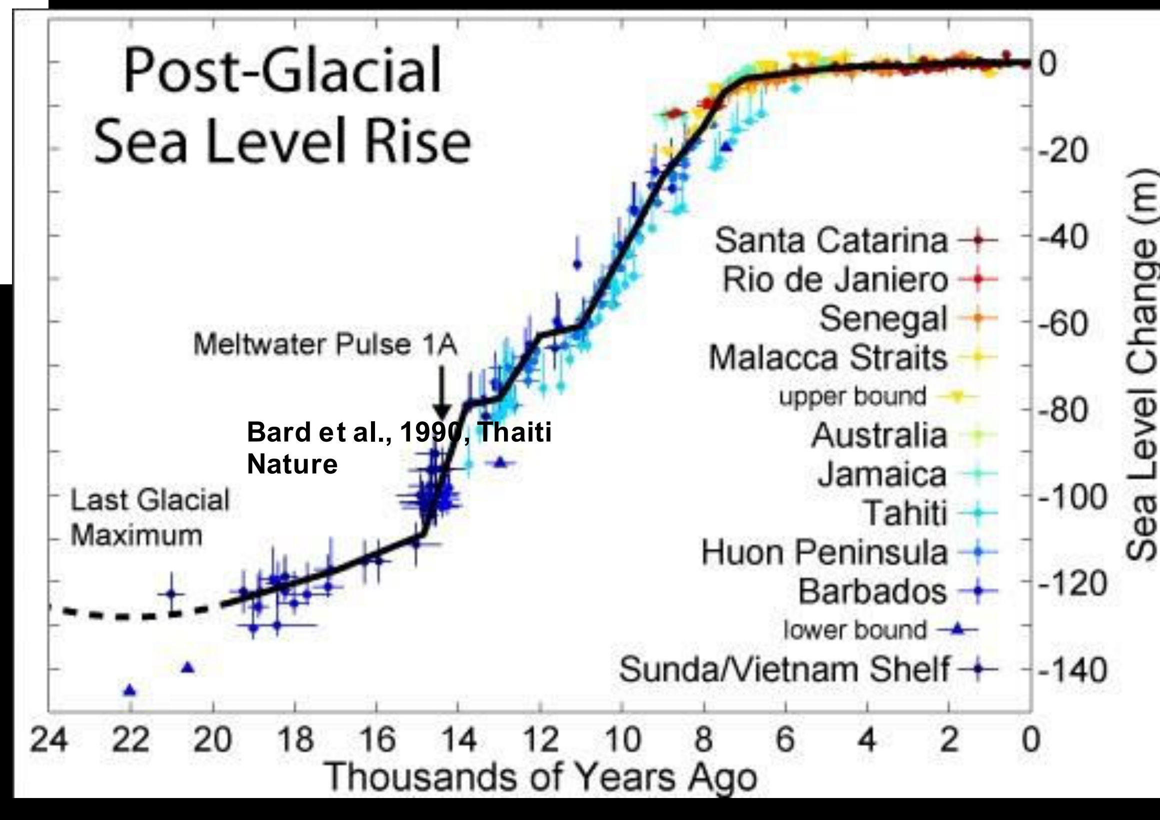

Post-Glacial
Sea Level Rise
Meltwater Pulse 1A
Bard et al., 1990, Thaiti
Nature
Last Glacial
Maximum
Santa Catarina
Rio de Janiero
Senegal
Malacca Straits
upper bound
Australia
Jamaica
Tahiti
Huon Peninsula
Barbados
lower bound
Sunda/Vietnam Shelf
0
-20
-40
-60
-80
-100
-120
-140
Sea Level Change (m)
24
22
20
18
16
14
12
10
8
6
4
2
0
Thousands of Years Ago

Thanks to: Giorgio Caramanna,

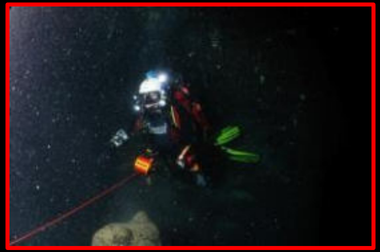

Marco Oliverio,

Marco with the speleo sampled at -48 m

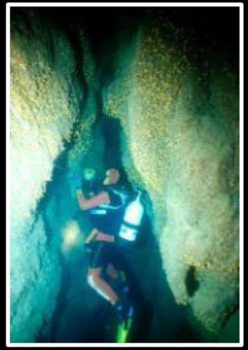

Gianfra Scicchitano

Argentarola Island
Argentario Promontory
Italy
Argentarola island
Rome
Adriatic Sea
Tyrrhenian Sea
Sardinia
Palinuro
Marettimo
Sicily

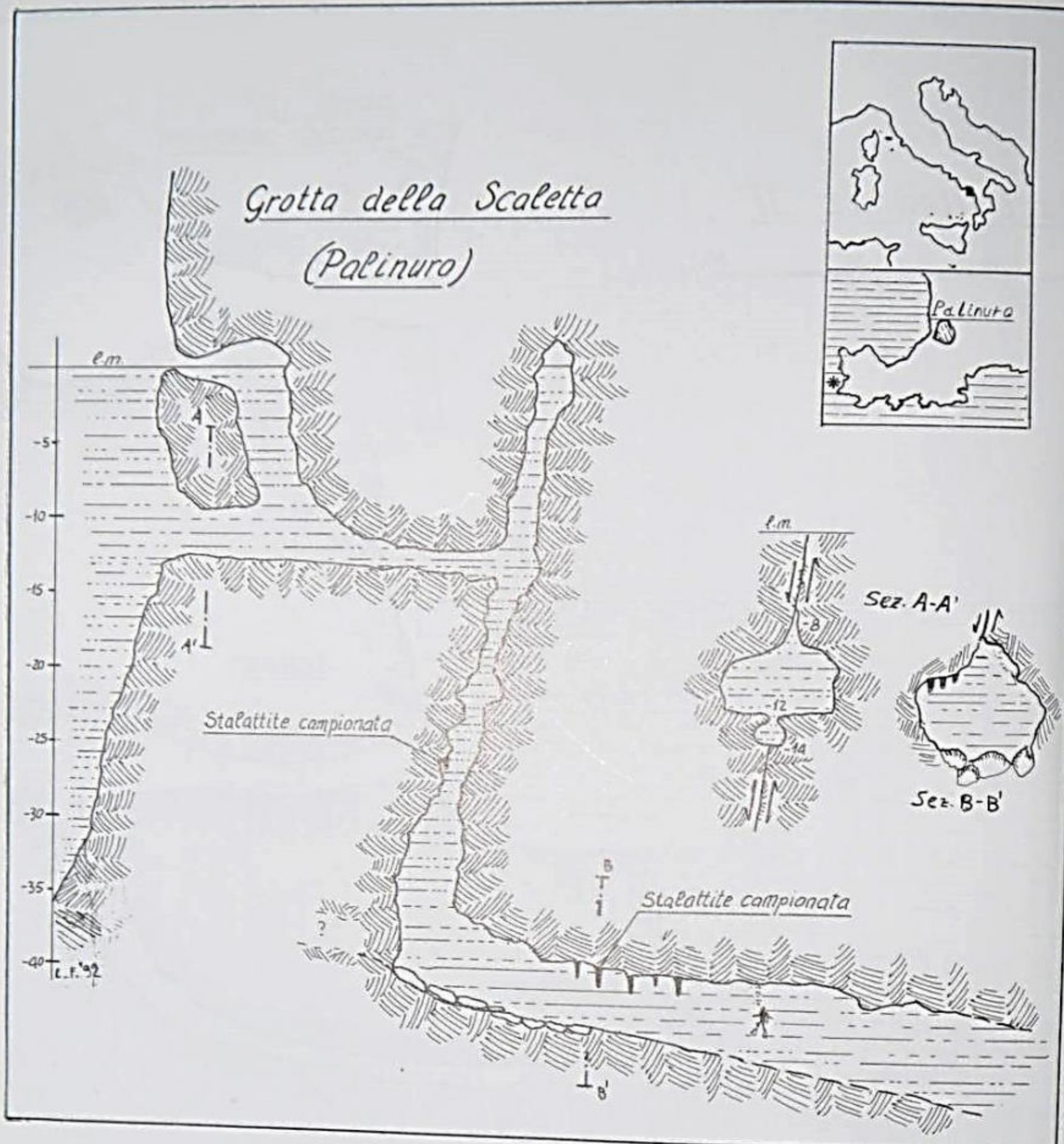

ne longitudinale della Grotta della Scaletta, Capo Palinuro.
itudinal section of Grotta della Scaletta at Cape Palinuro.



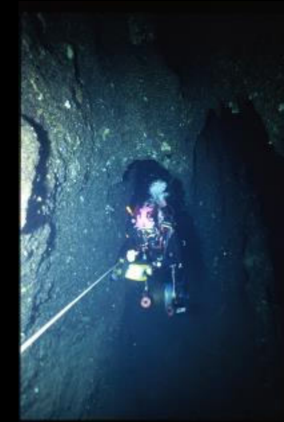

La stalattite can … **ta da Serpuldi**
e forata da Litho … **ga, ha fornito**
la data precisa d … **rio 1989**

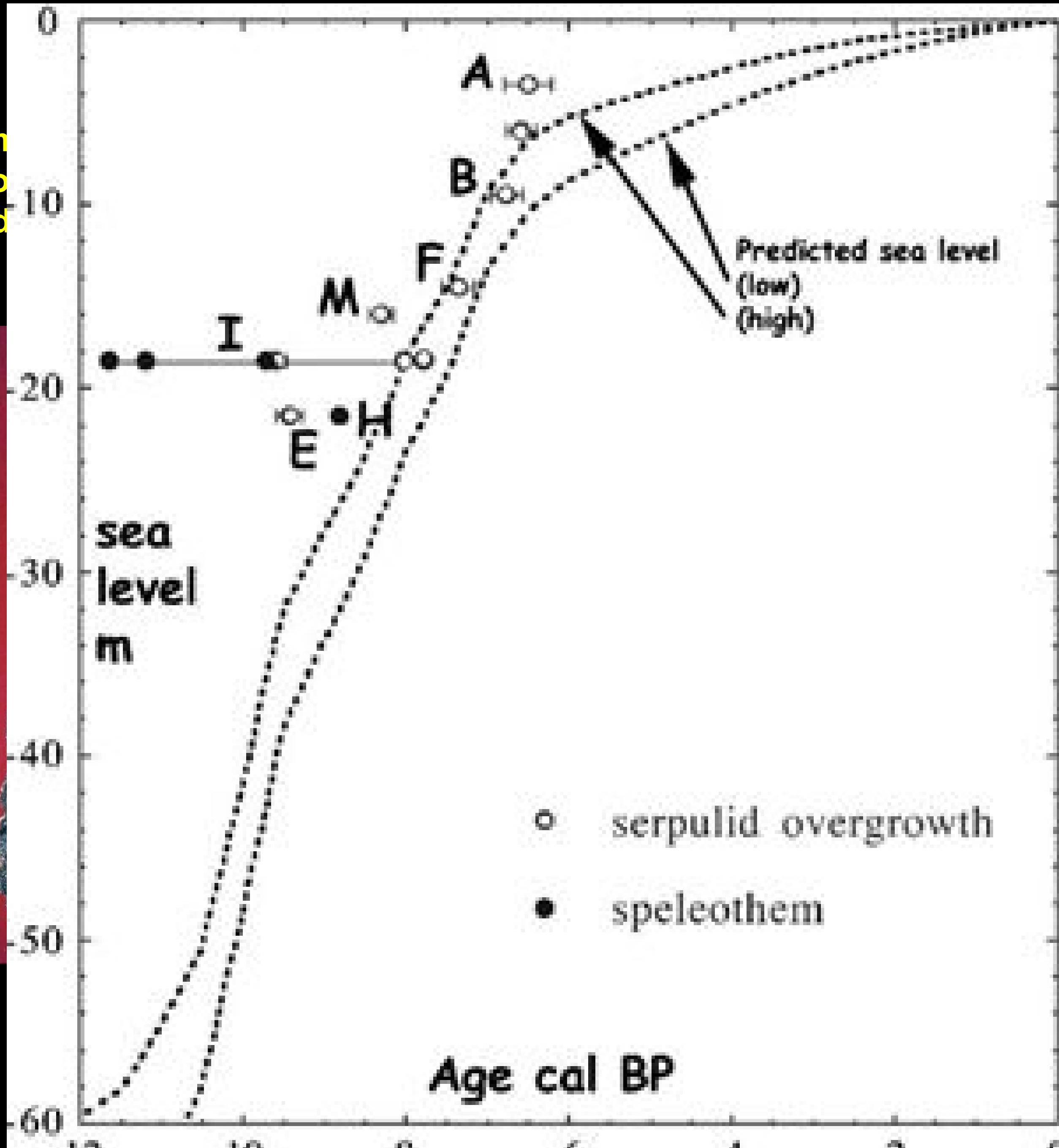

Cross Section of Argentarola Cave

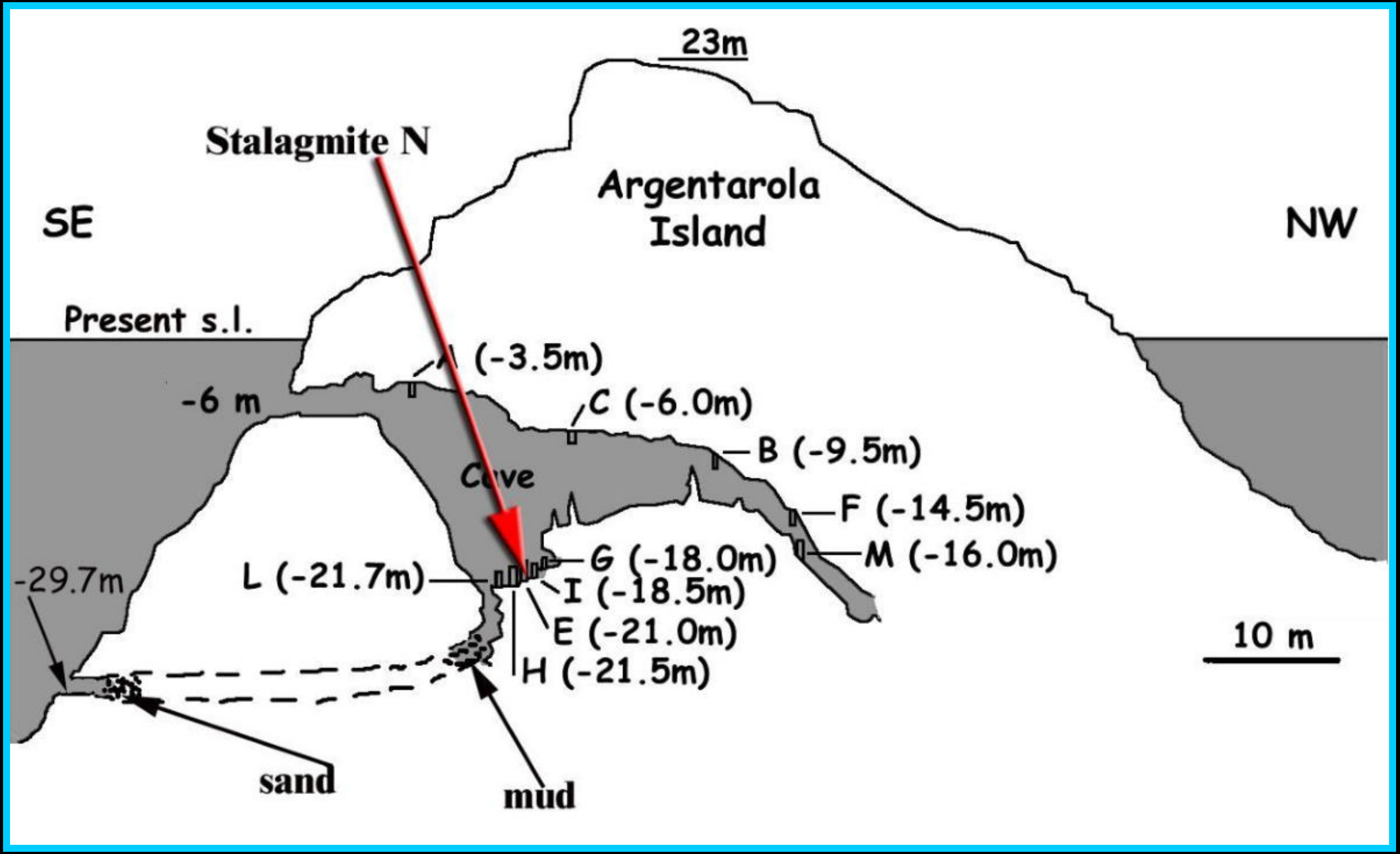

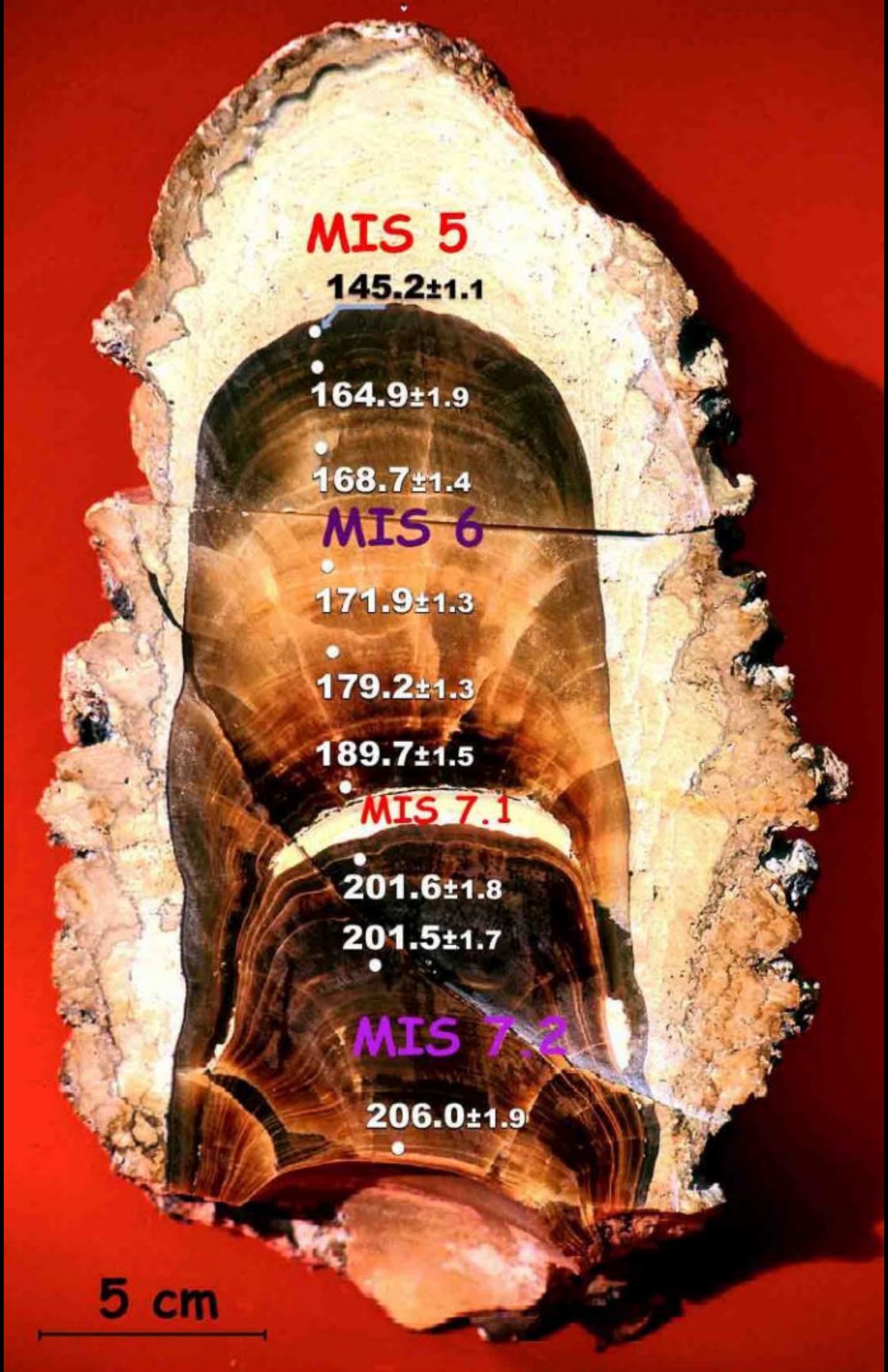
MIS 5
145.2±1.1
164.9±1.9
168.7±1.4
MIS 6
171.9±1.3
179.2±1.3
189.7±1.5
MIS 7.1
201.6±1.8
201.5±1.7
MIS 7.2
206.0±1.9
5 cm


This study
60
50
40
30
20
10

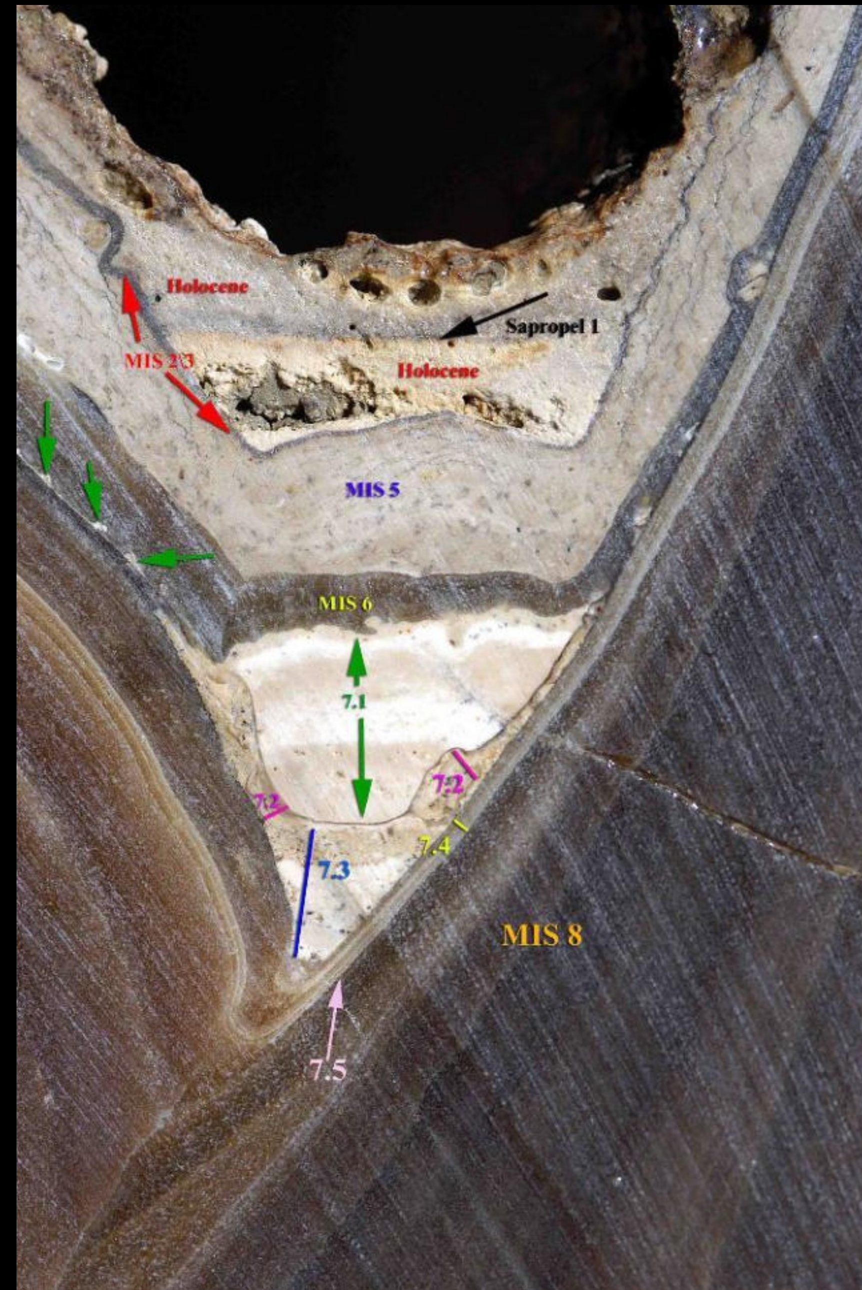
Holocene
Sapropel 1
MIS 2\3
Holocene
MIS 5
MIS 6
7.1
7.2
7.2
7.3
7.4
MIS 8
7.5

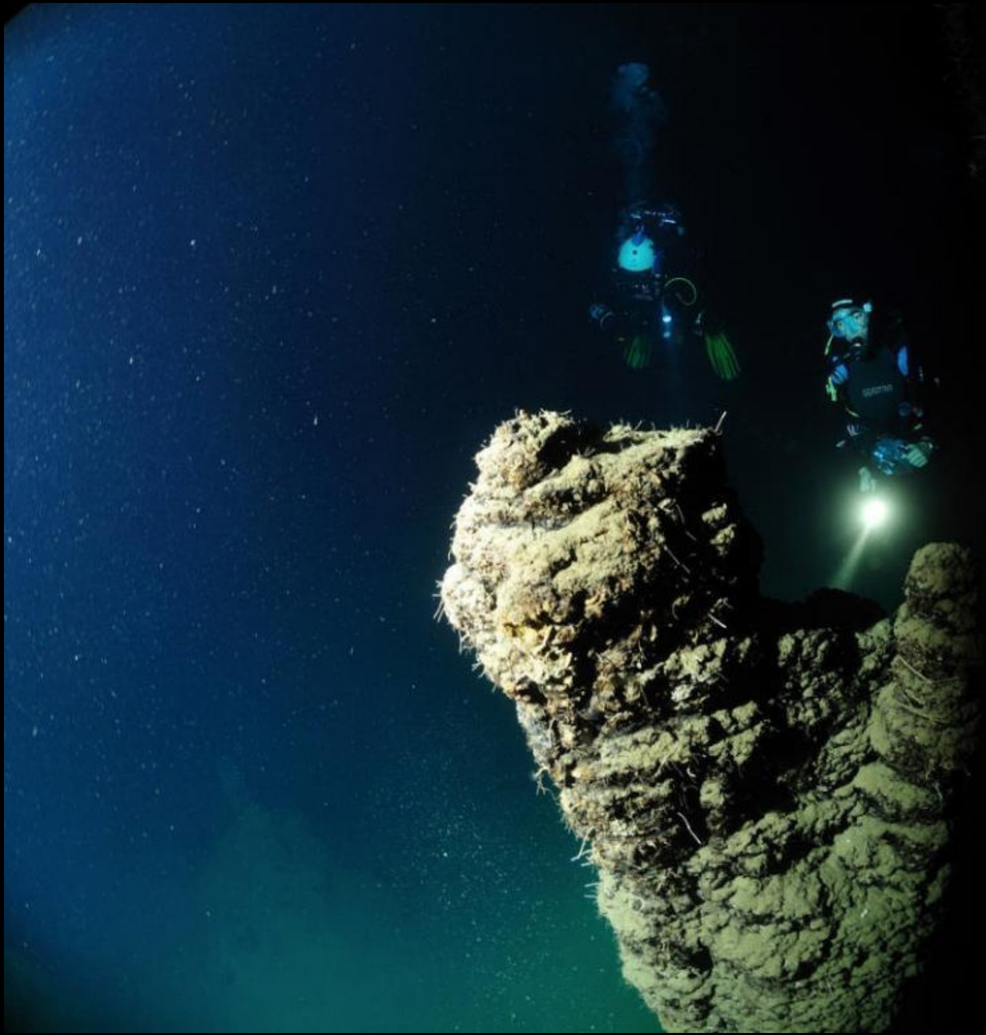
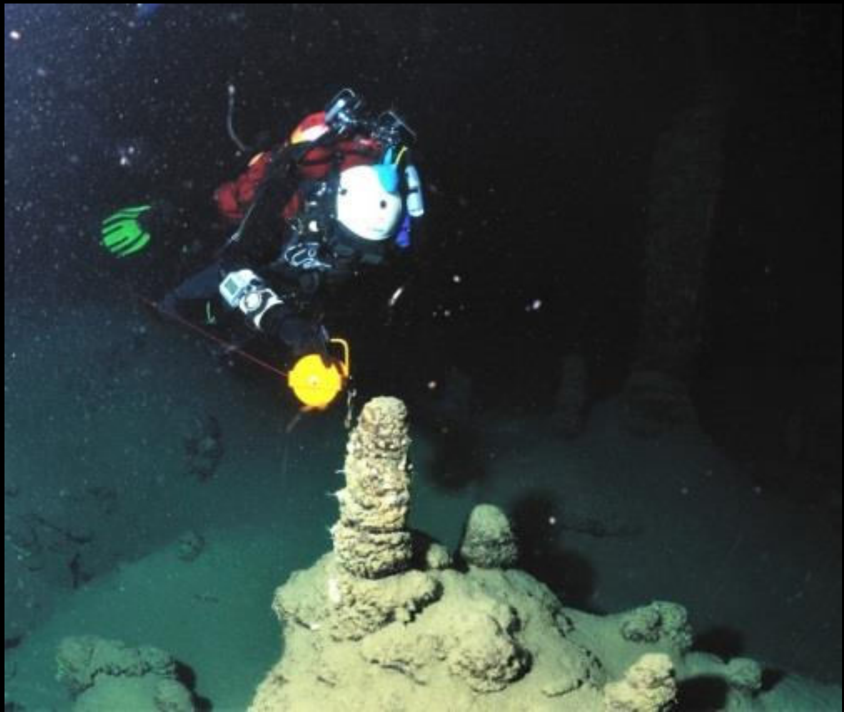

nature geoscience

LETTERS

PUBLISHED ONLINE: XX MONTH XXXX | DOI: 10.1038/NGEO470

Phasing and amplitude of sea-level and climate change during the penultimate interglacial

Andrea Dutton[1]*, Edouard Bard[2], Fabrizio Antonioli[3], Tezer M. Esat[1†], Kurt Lambeck[1] and Malcolm T. McCulloch[1]

Earth's present climate has evolved through oscillations between short-lived interglacial and extended glacial periods for the past million years. Direct markers of sea-level variations within these cycles that are absolutely dated are rare for periods older than the last interglacial; hence, our knowledge of sea-level change driven by the waxing and waning of continental ice sheets before that time is largely based on proxy records from deep-sea cores[1–3]. Here we present precise U–Th ages from a collection of submerged speleothems[4,5] from Italy, which record three sea-level highstands during the penultimate interglacial period, Marine Isotope Stage 7, from 245,000 to 190,000 years ago. We find that in the first and third highstands maximum sea levels of about −18 m (relative to modern sea level) were reached several thousand years before maximum northern hemisphere insolation, whereas in the second, Marine Isotope Stage 7.3, the highstand is essentially synchronous with the insolation maximum. Sea level during Stage 7.3 also peaked at about −18 m, even though the concurrent insolation forcing was the strongest of the three highstands. We attribute the different phasing and amplitude of this highstand to the extensive continental glaciation that preceded Marine Isotope Stage 7.3, and conclude that the response time of the cryosphere is an important component of the climate system.

Reconstructions of previous interglacial periods can help elucidate the phasing and causal mechanisms linking temperature, sea level and greenhouse gas concentrations that are critical to our understanding of climate dynamics during the present interglacial and into the future. Although the penultimate interglacial offers an important test for theories about the timing, duration, magnitude and driving mechanisms of sea-level highstands that have evolved out of studies of the last interglacial and the Holocene, fewer data are available for this period of time. Hence, the additional data presented herein provide an important test for several competing reconstructions of sea level during Marine Isotope Stage (MIS) 7 (refs 2,3,6–8) (Fig. 1).

A common approach to reconstruct past sea level is to measure the age and elevation of geologic archives that formed at a known position relative to the sea surface, such as corals[7] that grow in shallow water, or speleothems[9,10] that grow in caves and serve as an upper limit to sea level elevation. The strength of this method lies in the degree of confidence afforded by an accurate and precise chronology, such as provided by the U–Th dating technique, and in the ability to precisely measure the elevation relative to present sea level. We have applied this technique to submerged speleothems

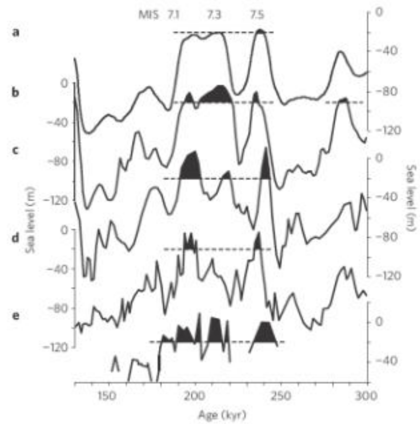

Figure 1 | Sea-level curves derived using five different methods. **a–e**, Reconstructions on the basis of model[6] driven by benthic oxygen isotope ($\delta^{18}O$) stack (**a**), benthic $\delta^{18}O$ data and ice-volume model[8] (**b**), seawater $\delta^{18}O$ calculated from paired Mg/Ca and $\delta^{18}O$ measurements on planktonic foraminifera[2] (**c**), reconstruction of Red Sea seawater $\delta^{18}O$ (ref. 3) (**d**) and open-system U–Th ages of corals[7] (**e**). Shading indicates periods of time for which sea level rises above −20 m (dashed lines), the approximate depth of Argentarola Cave speleothems. Note differences in the number of MIS 7 highstands predicted to exceed −20 m and the difference in elevation predicted for MIS 7.3 in particular.

recovered from Argentarola Cave, Italy, that preserve alternating layers of spelean calcite that grew when the caves were above sea level and biogenic calcite secreted by serpulid worms that colonized the speleothems during seawater submergence[4]. One of the advantages of the speleothem archive relative to corals is that dense spelean calcite is less susceptible to alteration, which allows for reconstructions farther back in time. Furthermore, by dating the timing of speleothem growth, the entire duration of time for a given sea-level highstand can be bracketed. In contrast, it is much more challenging to unambiguously determine the entire duration

[1]Research School of Earth Sciences, The Australian National University, 1 Mills Rd, Canberra, ACT, 0200, Australia, [2]CEREGE, UMR 6635 CNRS, Aix-Marseille University, IRD, College de France, Europole de l'Arbois BP 80, F-13545 Aix-en-Provence Cdx 4, France, [3]ENEA, cre Casaccia, via Anguillarese 301, 00123 Rome, Italy. [†]Present address: Australian Nuclear Science Technology Organisation, Institute for Environmental Research, Menai, NSW 2234, Australia. *e-mail: andrea.dutton@anu.edu.au.

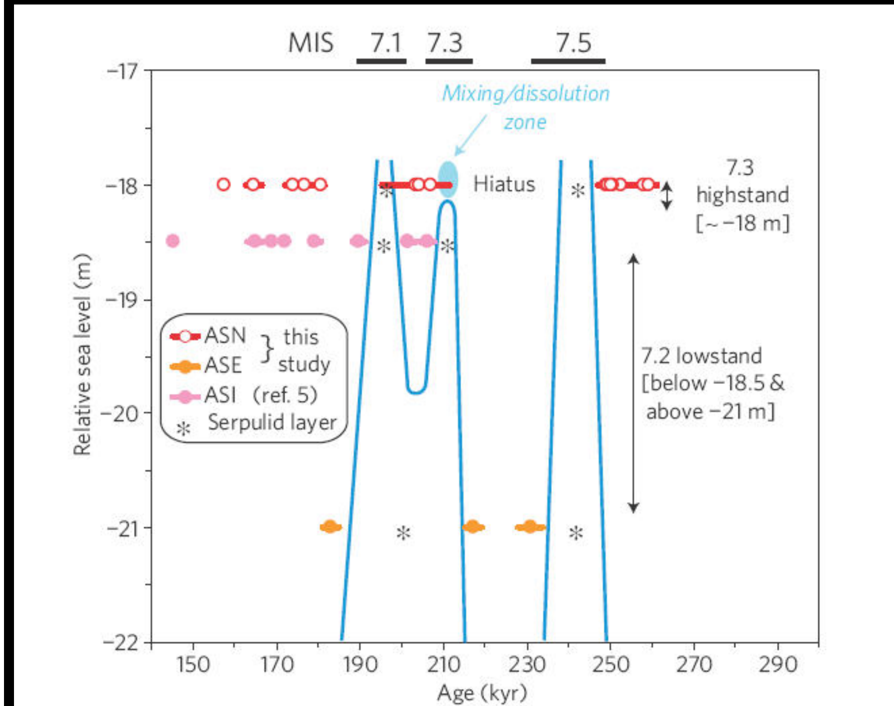

la sezione di una stalattite campionata a Custonaci (Tp, Sicilia). Lo speleotema è ricoperto da coralli e contiene 3 latus, corrispondenti a 4 trasgressioni marine nella grotta che ora si trova a 97 metri di quota. La datazione dei coralli è di 1.1 Milioni di anni. Le 4 tragressioni corrispondono agli stadi isotopici compresi tra 25,41 fino a 1.5 milioni di anni.Si tratta della più antico speleotema

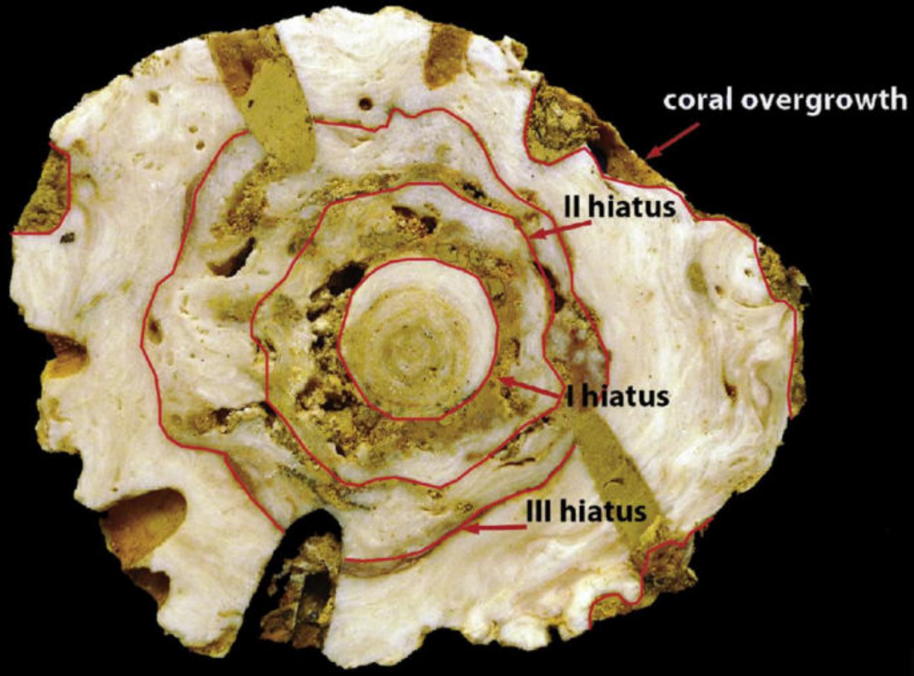


82.2
87.7
90.6

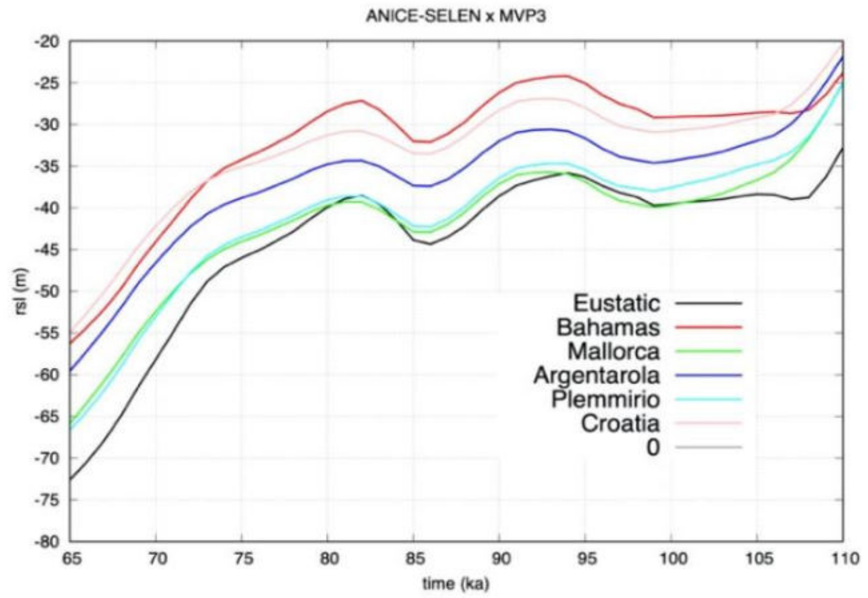

Figure 11. Predicted MIS 5.1–5.3 RSL curves for the Bahamas and at the relevant Mediterranean sites for ANICE-SELEN and the MVP 3 mantle viscosity profile. The black curve shows the eustatic.

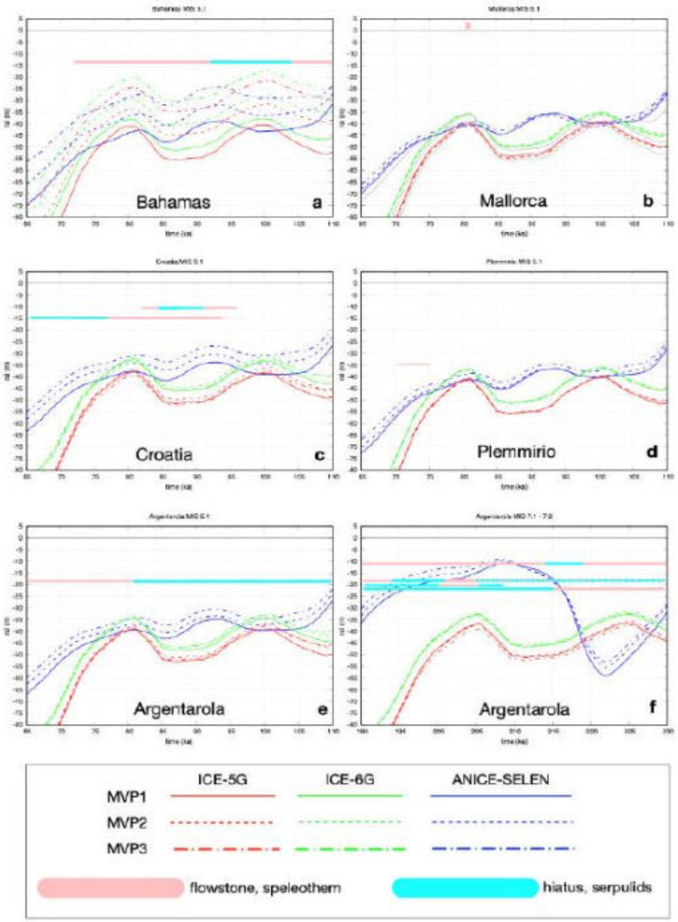

Figure 8. Predicted RSL curves for ICE-5G (red curves), ICE-6G (green curves), and ANICE-SELEN (blue curves) ice sheet models, in combination with mantle viscosity profiles (MVP) 1–3 (solid, dashed, and dotted, respectively) at each site and with respect to the measured elevations. (**a**) predicted RSL curves at MIS 5.1 in the Bahamas and with respect to the elevation of the flowstone. (**b**) predicted RSL curves at MIS 5.1 in Mallorca. (**c**) predicted RSL curves at MIS 5.1 in Croatia and elevation of the speleothems. (**d**) predicted RSL curves at MIS 5.1 at Plemmirio and elevation of the speleothem. (**e**) predicted RSL curves at MIS 5.1 at Argentarola and elevation of the speleothems. (**f**) predicted RSL curves at MIS 7.1–7.2 at Argentarola and elevation of the speleothems.

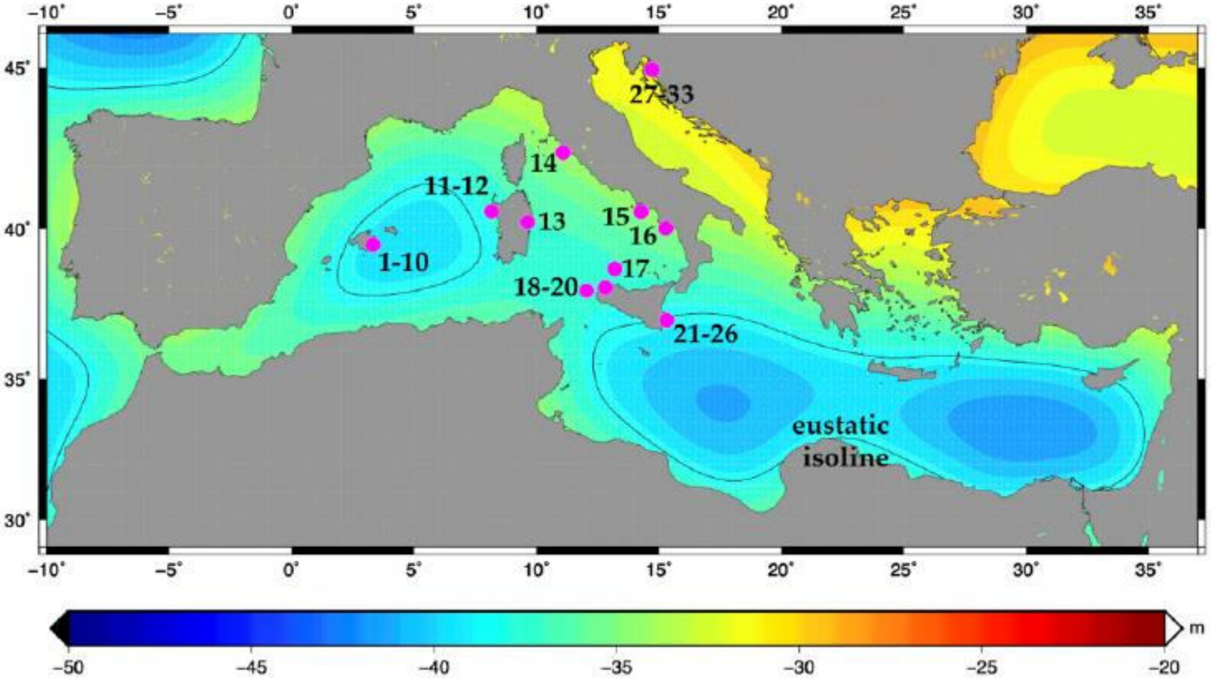

Figure 12. Predicted RSL elevation in the Mediterranean Sea during MIS 5.1 according to ANICE-SELEN and the MVP 3 mantle viscosity profile. The pink dots indicate the location of the sites. The black isoline corresponds to the eustatic value (−38.5 m).

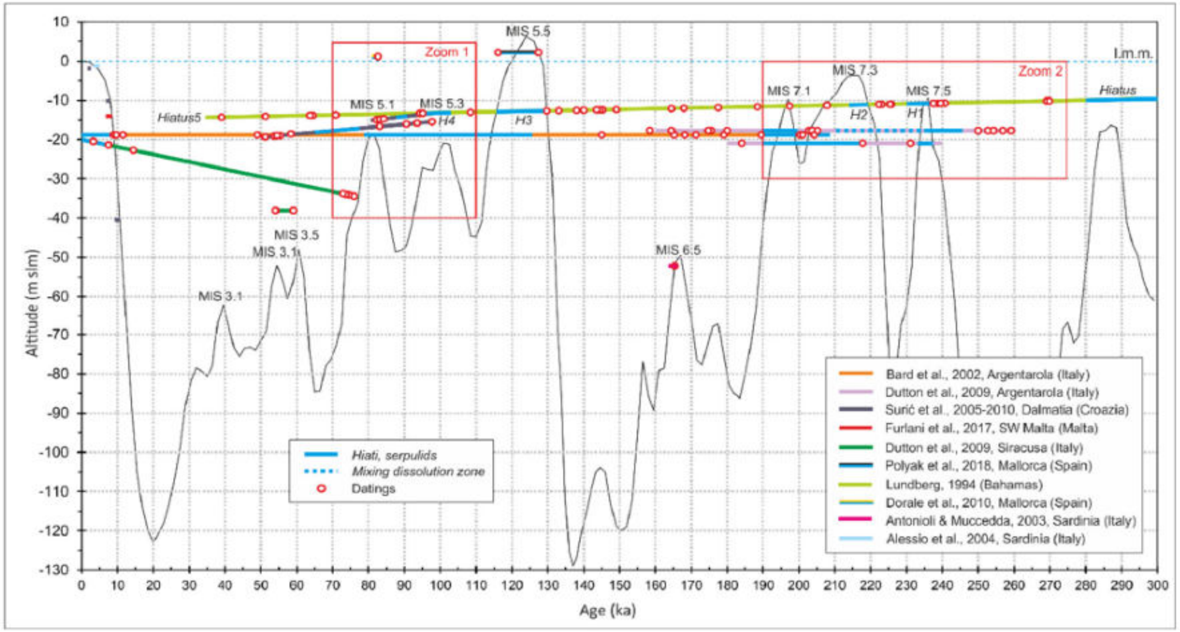

Figure 13. Elevations and radiometric ages ([14]C and U-Th) of the Mediterranean speleothems and marine overgrowths discussed in the present study and a comparison with the DWBAH flowstone Table A1. Argentarola (Italy), −18.5 m [2] and −18 and −21.7 m [22]; Plemmirio (Italy), −23 m [64]; Grotta di Nettuno (Italy), − 3 m [81]; U vode Pit (Krk Island, Croatia), Stalagmite K− 4 (−14.5 m) and K-18 (−18.8 m) [3]; POS from Mallorca (Spain), + 1.5 m [4,5]; Malta [65]; DWBAH Flowstone (Bahamas), −15 m [11]. Black line: global sea level curve reconstructed by [88].

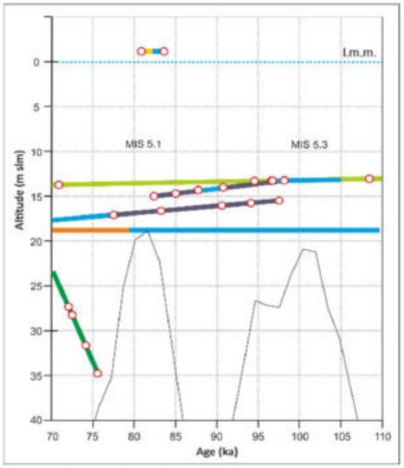

Figure 14. Zoom 1 of Figure 15. Light green line: DWBAH flowstone [11]; orange line: Stalagmite ASI (−18.5) from Argentarola cave, −18.5 m [2]; black line: Speleothems K14 and K18; yellow and blue line: Mallorca POS; green line: Plemmirio [64]; fine black line: global sea level curve reconstructed by [88].

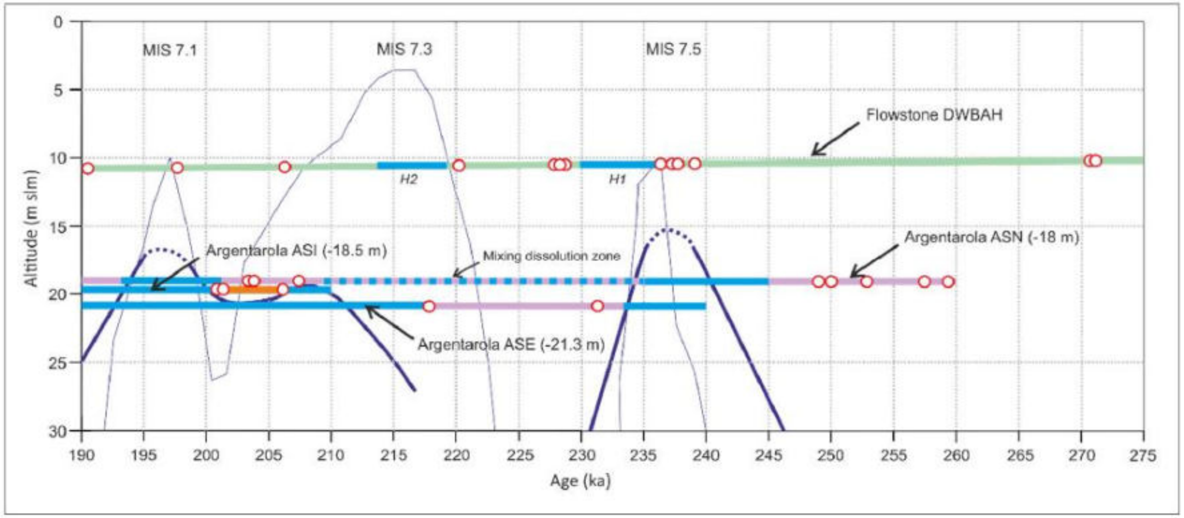

Figure 15. Zoom 2 of Figure 15. Green line: DWBAH flowstone [11]; orange line: Stalagmite ASN (−18 m) from Argentarola cave [22], and stalagmite ASI (−18.5) from Argentarola cave [2]; black line: global sea level curve reconstructed by [88]; dark blue line: sea level drown with observed data.

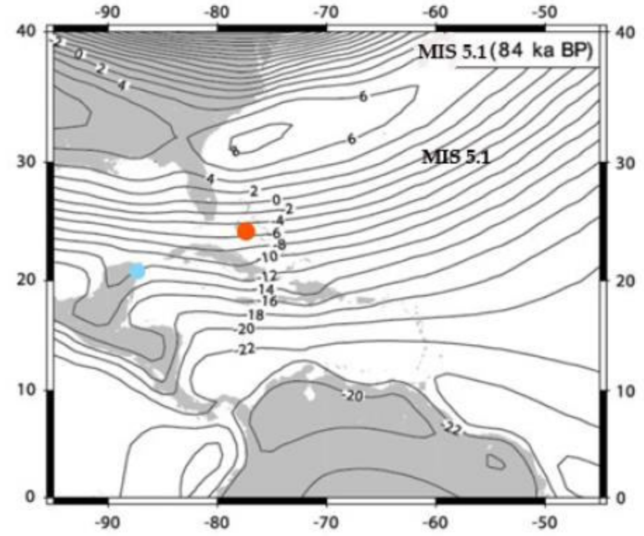

Figure A2. GIA for Caribbean Islands and Florida (redrawn from [39]).

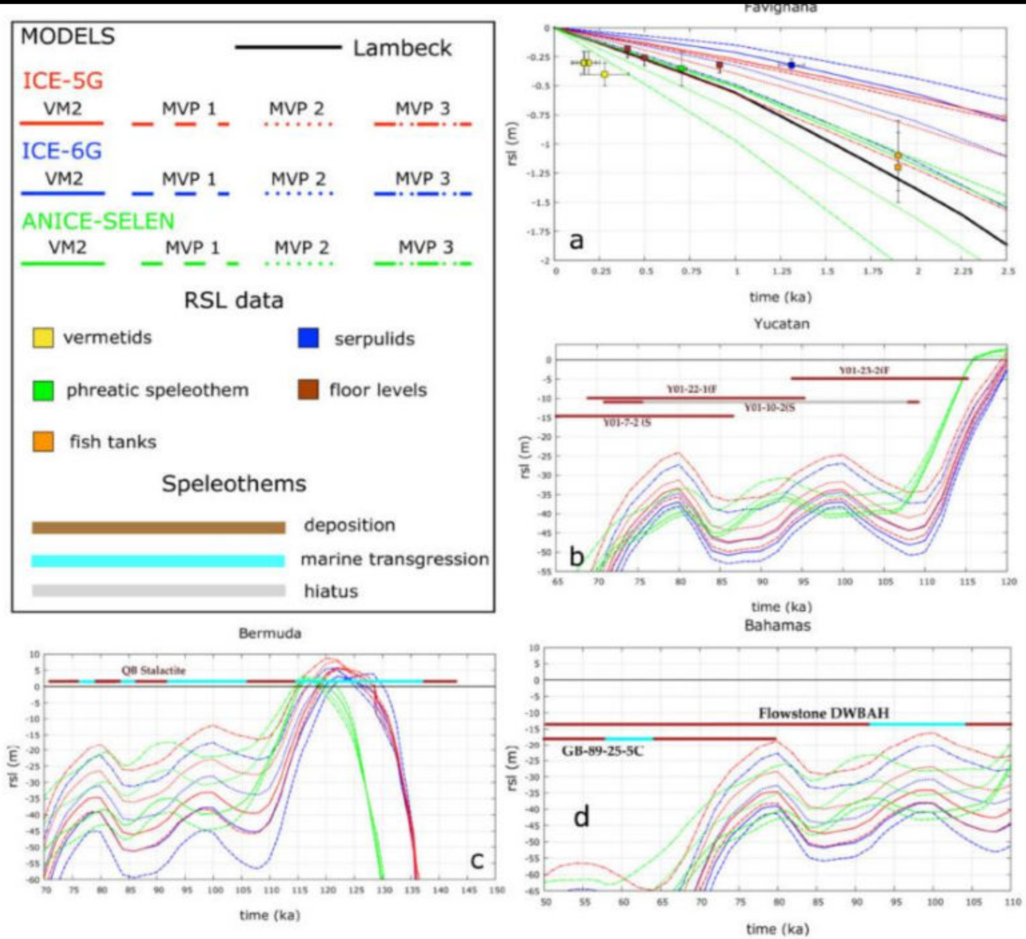

Figure 10. Predicted RSL curves for the ICE-5G (red curves), ICE-6G (green curves), and ANICE-SELEN (blue curves) ice-sheet models in combination with MVP 1–3 mantle viscosity profiles (solid, dashed and dotted lines, respectively) at each site and with respect to the measured elevations. (**a**) Favignana. (**b**) Yucatán. (**c**) Bermuda. (**d**) The Bahamas.

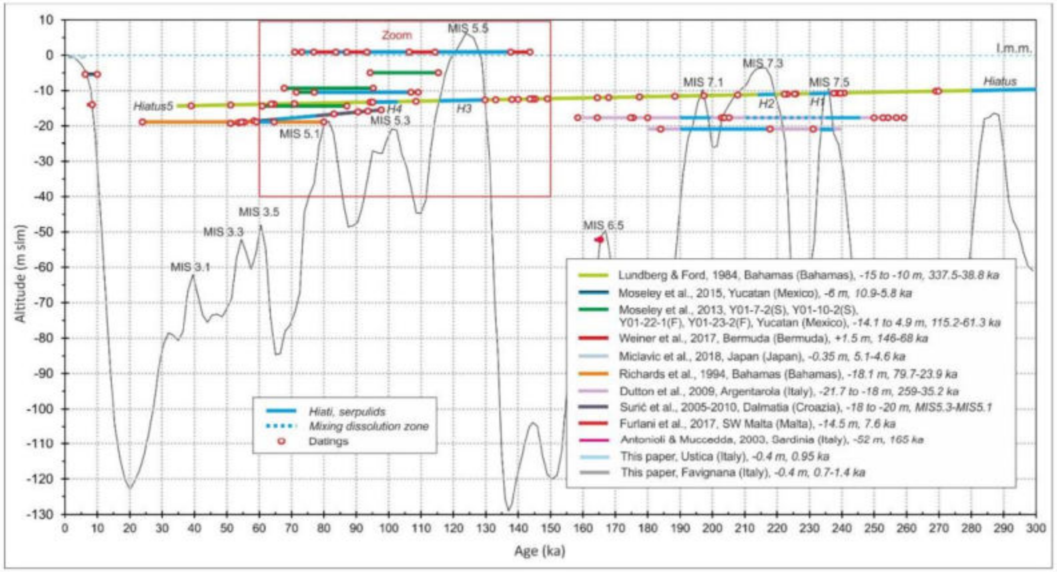

Figure 13. Elevations and radiometric ages (14C and U/Th) of the Caribbean, Japan, and some Mediterranean speleothems discussed in the present study and comparison with the: global sea level curve reconstructed by [79] Black line.

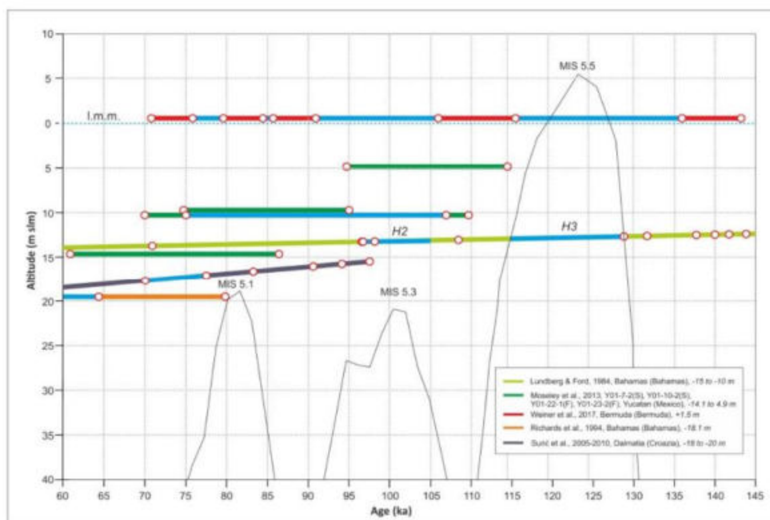

Figure 14. Zoomed in view of part of Figure 13. Fine black line is the global sea-level curve reconstructed by [79].

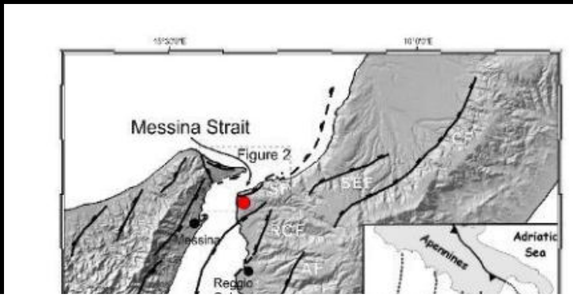
Messina Strait
Figure 2
Messina
Reggio
SEF
RCF
AF
Apennines
Adriatic
Sea


Cerasi
San Roberto
Calanna
Favazzina
Sambatello
Scilla
Cappuccini

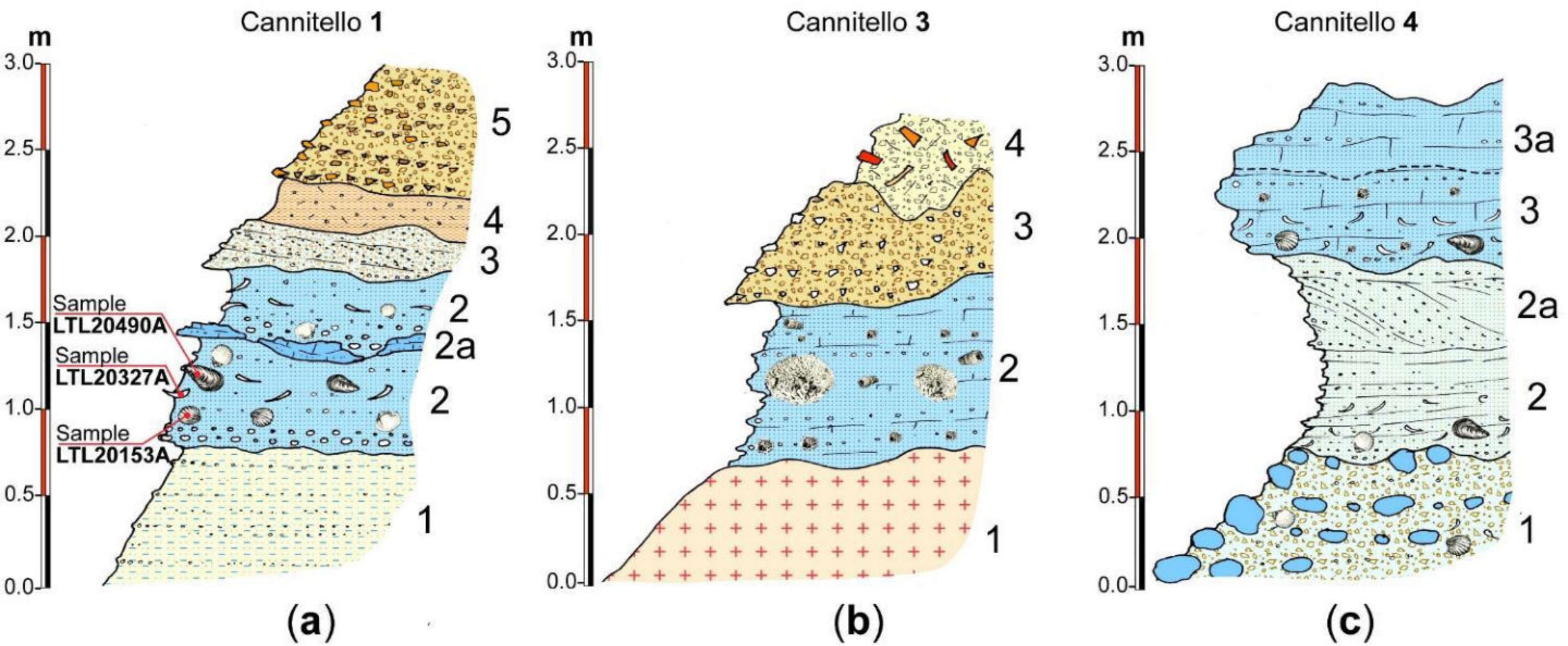
Cannitello 1
Cannitello 3
Cannitello 4
m
3.0
2.5
2.0
1.5
1.0
0.5
0.0
5
4
3
2
2a
2
1
Sample
LTL20490A
Sample
LTL20327A
Sample
LTL20153A
4
3
2
1
3a
3
2a
2
1
(a)
(b)
(c)

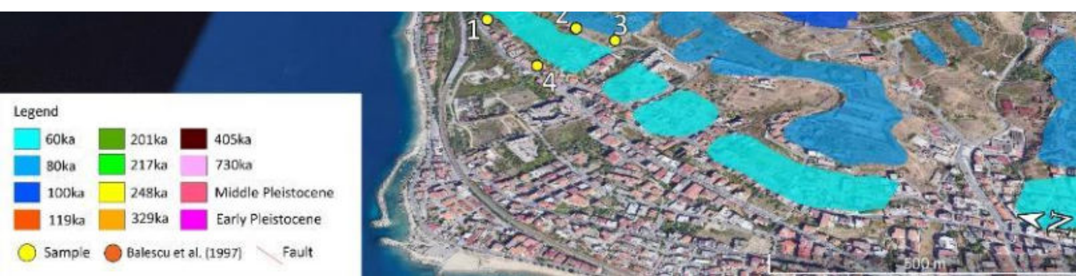
1
2
3
4
Legend
60ka
80ka
100ka
119ka
201ka
217ka
248ka
329ka
405ka
730ka
Middle Pleistocene
Early Pleistocene
Sample
Balescu et al. (1997)
Fault
500 m

water

Article

New Evidence of MIS 3 Relative Sea Level Changes from the Messina Strait, Calabria (Italy)

Fabrizio … naco [5,6,7],
Paolo O…
Paolo St…

Given the overall scarceness of MIS 3 marine outcrops that are explorable in coastal areas subject to important uplift, we consider the southern Calabrian site relevant for the assessment of past sea levels during this still poorly known interstadial.

The GIA results suggest that the δ^{18}O-based ice sheet models appear to significantly overestimate the ice sheet volumes during the MIS 3.1 and 3.3. Our data are in agreement with Gowan et al. [101], raising, by 40 metres, the eustatic contribution to sea level during interstadials MIS 3.1, 5.1, and 5.3 with respect to the current global sea level curve scenarios. Further, our reconstruction agrees well with the records proposing MIS 3 sea levels at depths between −18 and −40 m.

Our numerical results and observational data confirmed that the MIS 3 RSL changes at Cannitello are governed by glacio-eustasy, whereas GIA plays a secondary role. While the δ^{18}O dependent ice sheet models result in RSL curves that are always significantly lower than the observations, PaleoMIST 1.0 is the only model capable of returning a MIS 3.1 elevation that is in agreement with the observations. Indeed, we observe that there is a discrepancy (of at least 30–40 m) between the eustatic altitude of the MIS 3 of all global curves and those suggested by observations. Therefore, our results confirm previous evaluations by Pico et al. [63] and Gowan et al. [101] and support the contention that a reduction of global ice sheet volumes across the MIS 3, and specifically at the MIS 3.1 and 3.3, is needed.

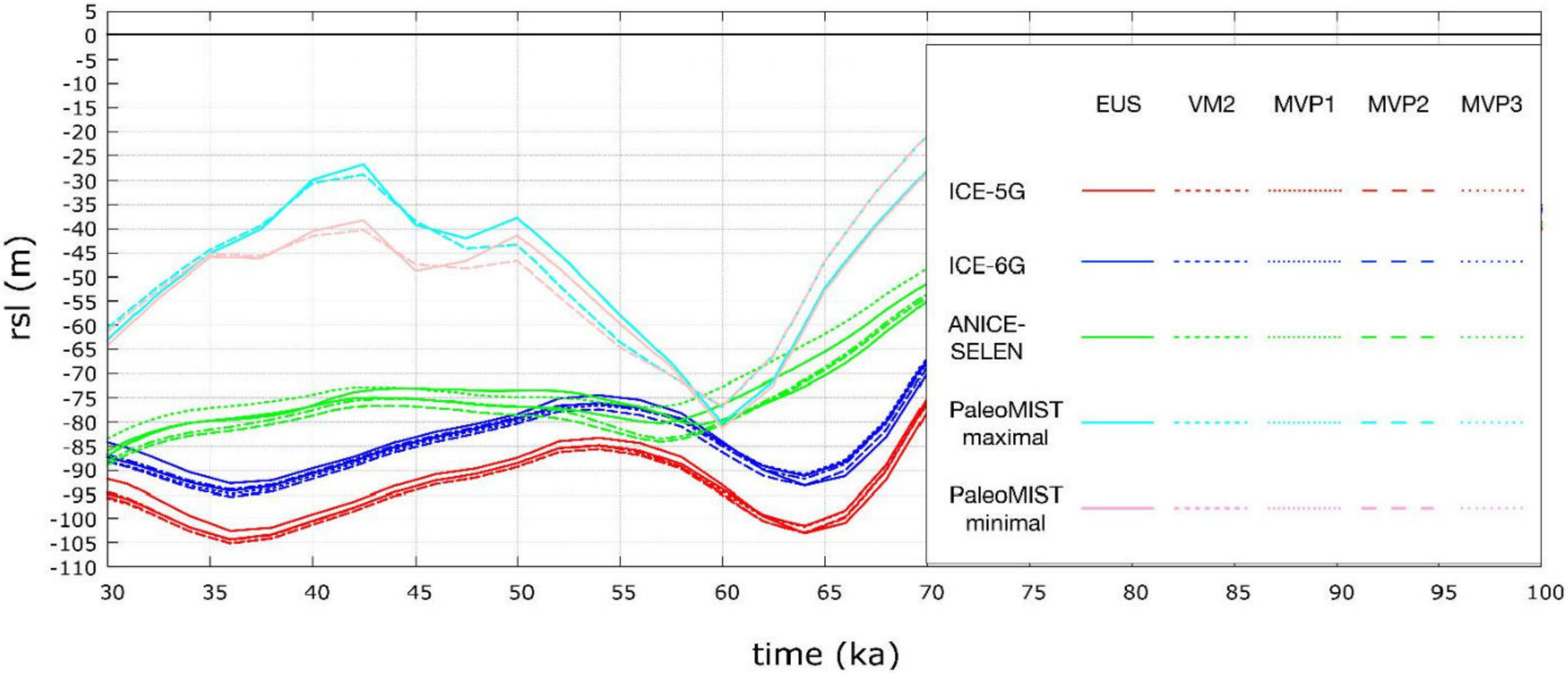

Figure 7. Predicted RSL curves for four ice sheet models: ICE-5G (red), ICE-6G (blue), ANICE-SELEN (cyan), and PaleoMIST 1.0 maximal and minimal (cyan and pink, respectively). The solid curves represent the eustatic. The dashed and dashed-dotted curves represent the GIA-modulated RSl predictions.

285 [2]	7.5	217.2 [5]	−17.5 [4]	1.1	
345 [2]	7.5	248.9 [5]	−13 [4]	1.2	
415 [2]	9	329 [6]	+4 [4]	1.3	
520 [3]	11	405 [6]	+5 [4]	1.2	
680 [3]	10	760 [6]	−5 [4]	0.9	0.9

Sicily, St Vito Lo Capo -56 m. Is this an archaeological marker for sea level change?

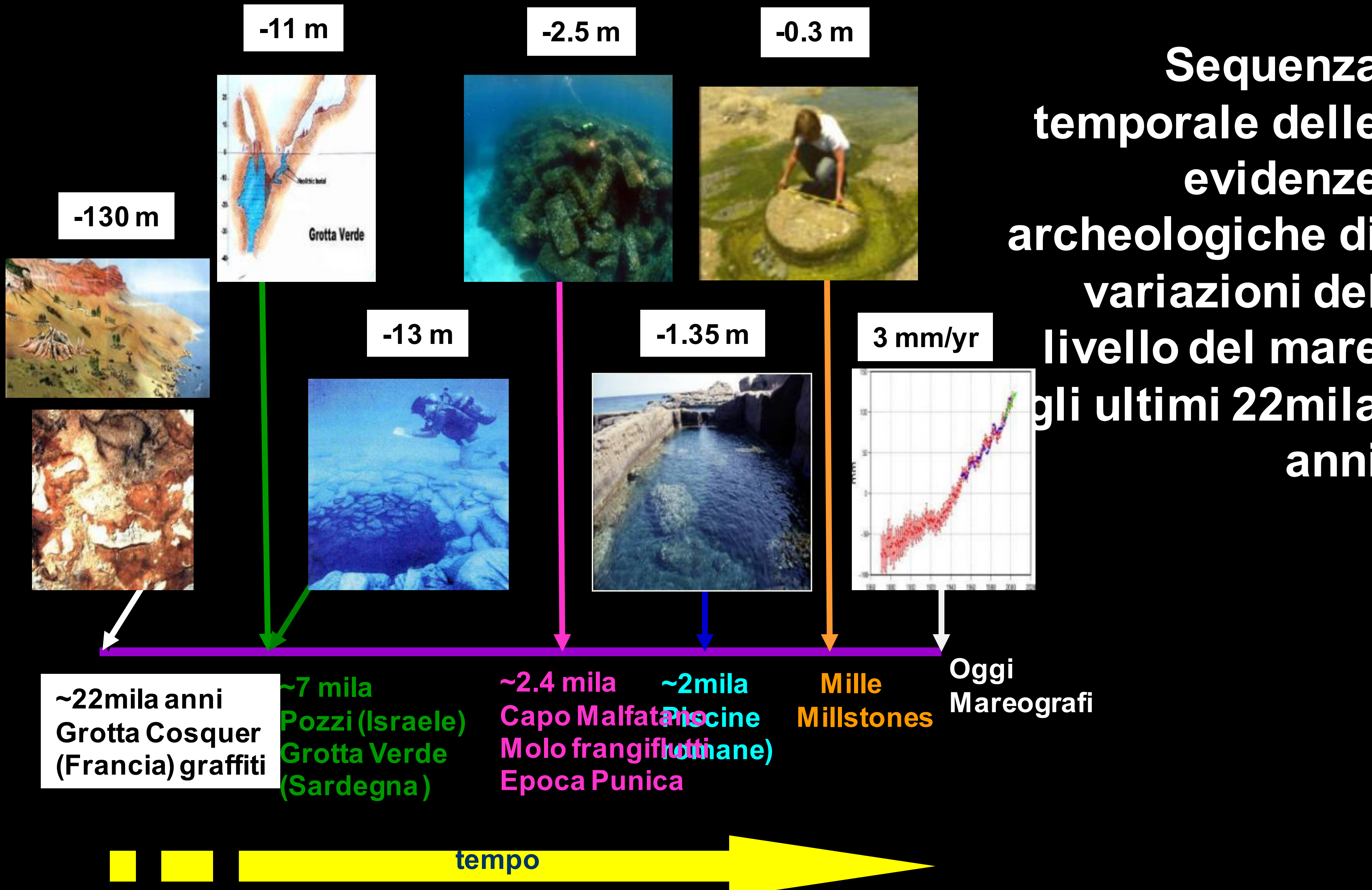

Sequenza temporale delle evidenze archeologiche di variazioni del livello del mare
gli ultimi 22mila anni
-130 m
-11 m
Grotta Verde
-13 m
-2.5 m
-1.35 m
-0.3 m
3 mm/yr
~22mila anni
Grotta Cosquer
(Francia) graffiti
~7 mila
Pozzi (Israele)
Grotta Verde
(Sardegna)
~2.4 mila
Capo Malfatano
Molo frangiflutti
Epoca Punica
~2mila
Piscine
(romane)
Mille
Millstones
Oggi
Mareografi
tempo

Cosquer cave - France

Today at -37 m

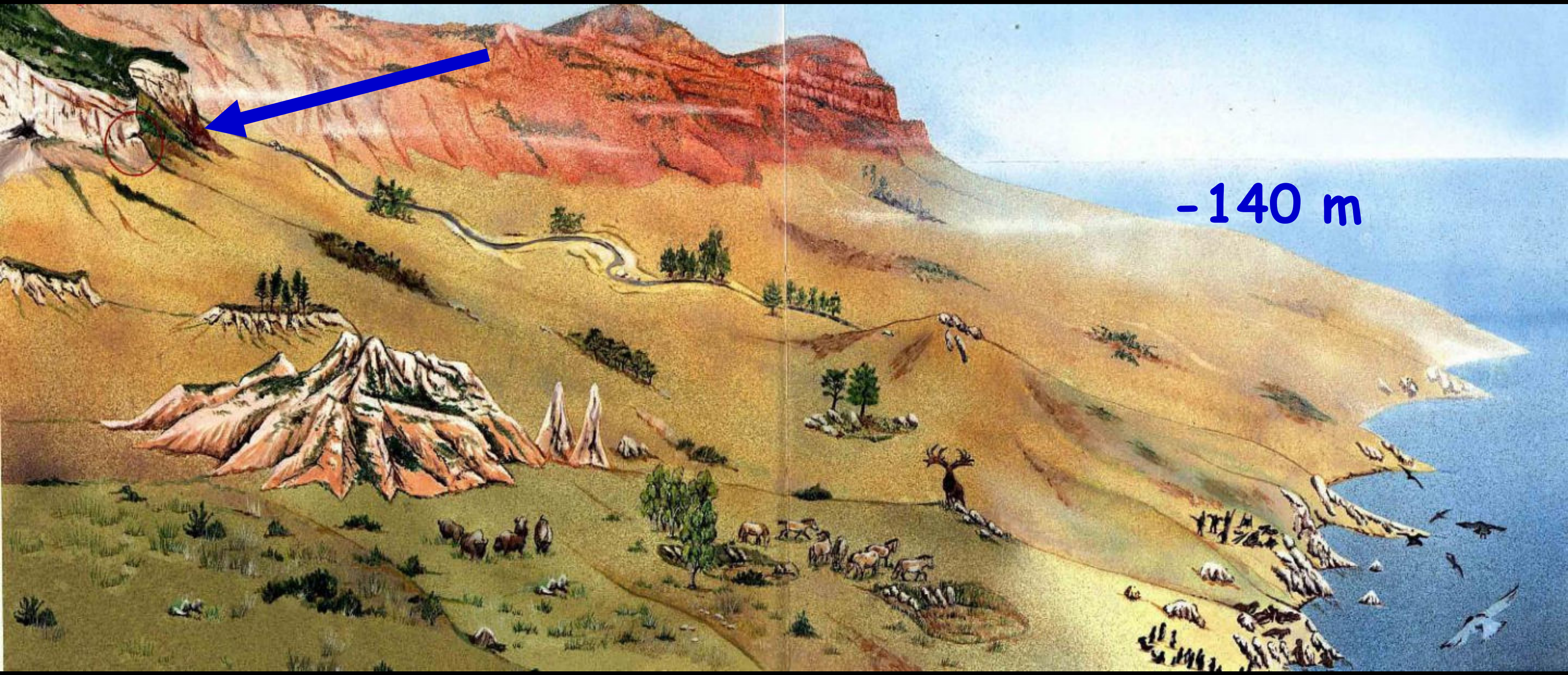

22 ka cal BP (dated from wall paintings, Clottes et al., 1992)

Sott'acqua puo essere facile prendere abbagli, quella che sembra una strada o un muro o un prosciutto, sono invece formazioni geologiche naturali.

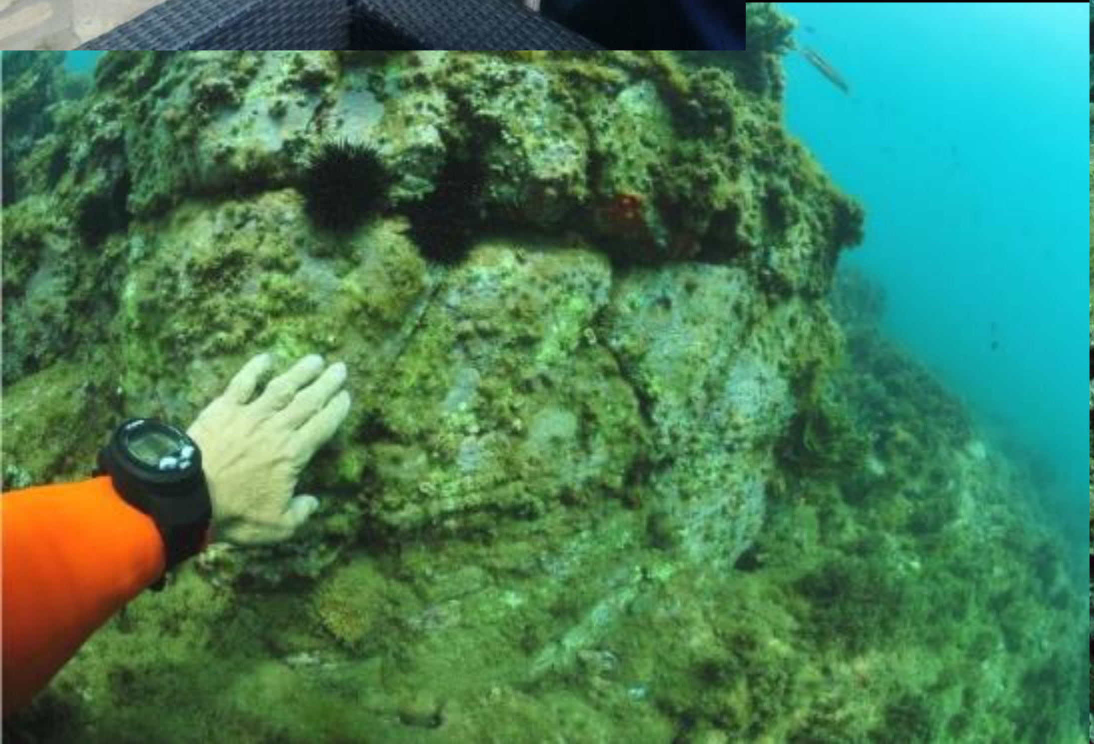

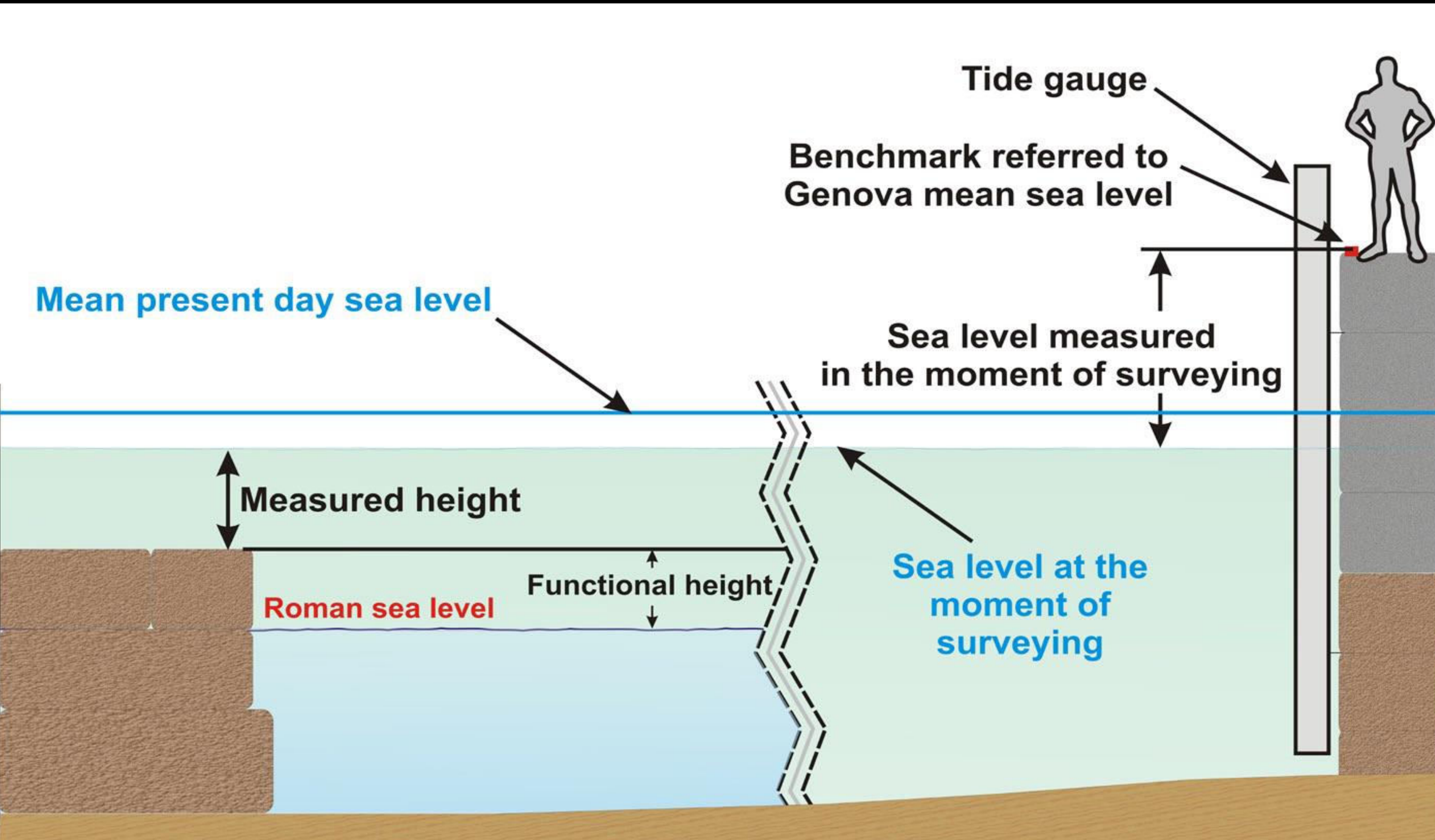
Tide gauge
Benchmark referred to
Genova mean sea level
Mean present day sea level
Sea level measured
in the moment of surveying
Measured height
Functional height
Roman sea level
Sea level at the
moment of
surveying

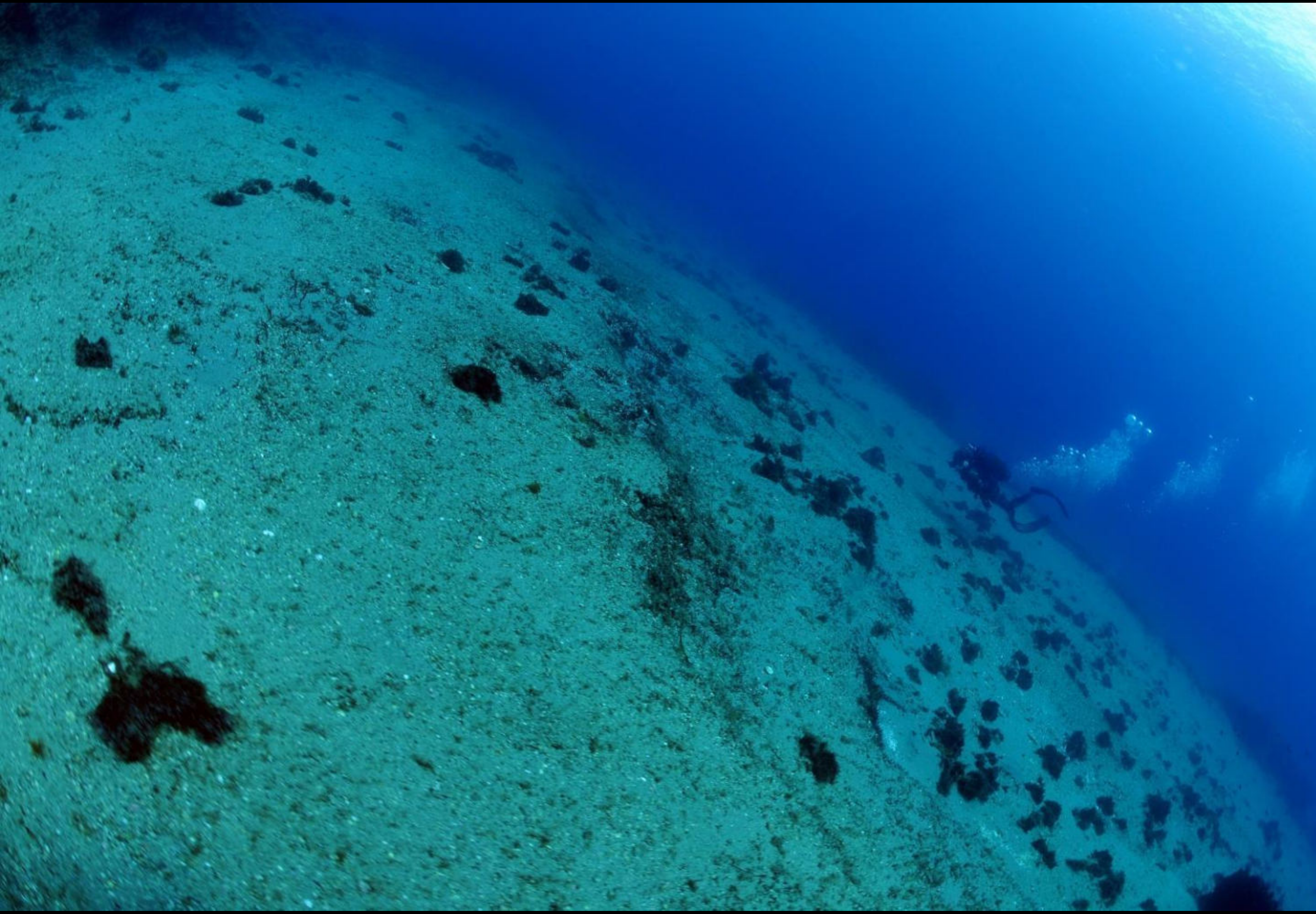

Conclusioni

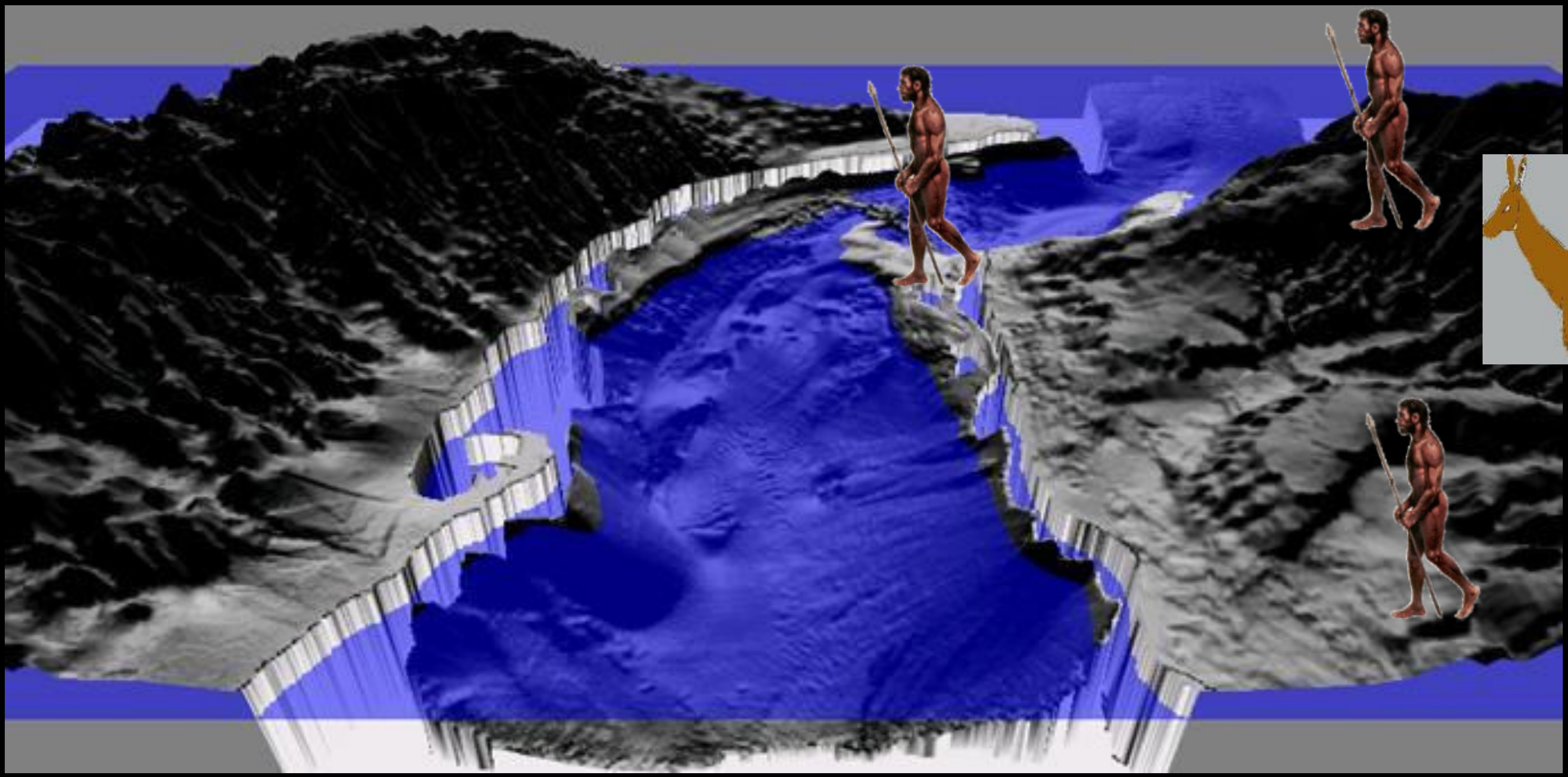

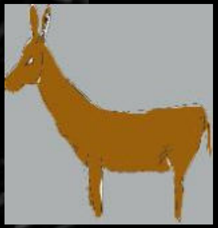

La litologia dei "pilastri" sommersi che compongono parte della Sella, corrisponde alla Formazione delle Ghiaie di Messina.

Il nostro schema di emersione del Ponte Continentale viene validato dagli studi antropologici per le presenze dell'Equus Hydruntinus e dell' Homo sapiens in Sicilia, rispettivamente datate a 18.8 e 17.5 ka cal BP.

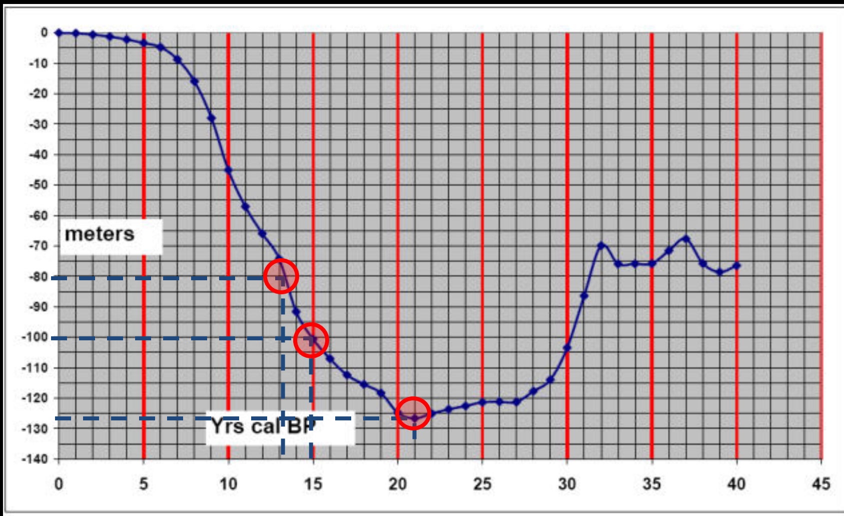
meters
Yrs cal BP
0
-10
-20
-30
-40
-50
-60
-70
-80
-90
-100
-110
-120
-130
-140
0
5
10
15
20
25
30
35
40
45

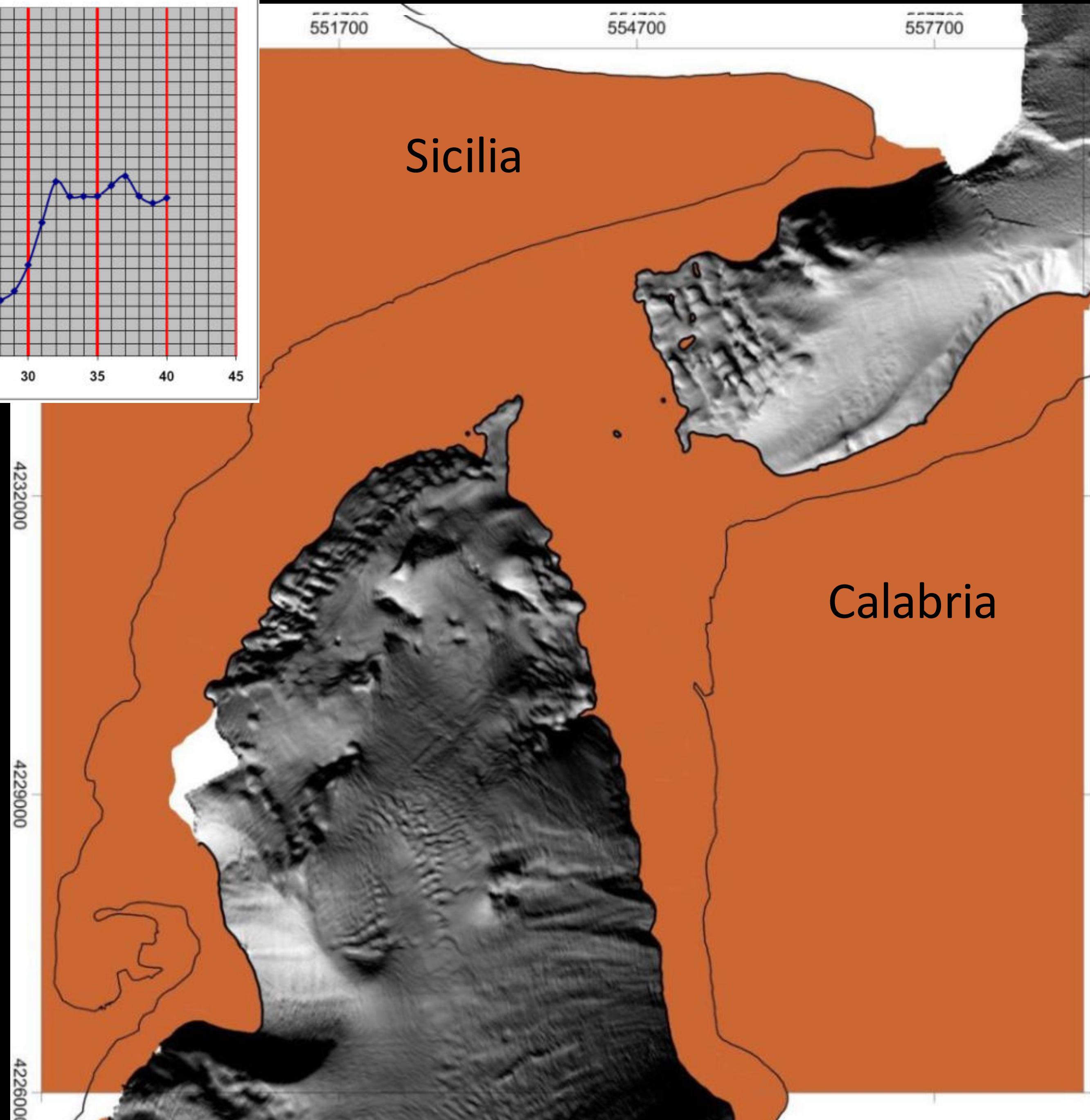
551700
554700
557700
Sicilia
Calabria
4232000
4229000
4226000

Esistono conferme a questo schema di evoluzione?

Homo sapiens in Italy about 30/43 ka

Homo sapiens in Sicily, about 17 ka

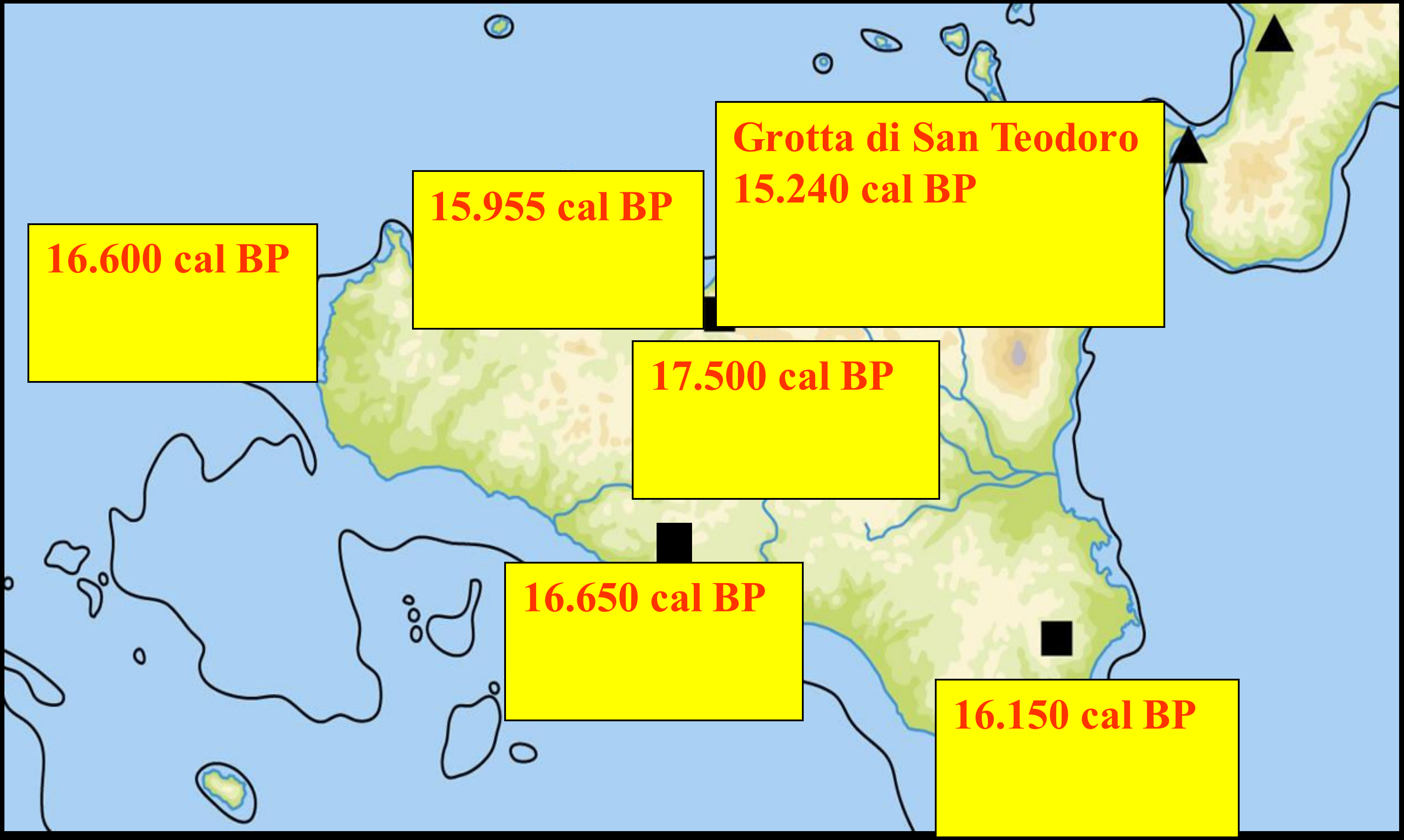

Intervallo di tempo minimo: 21.5-20 ka;
Intervallo di tempo massimo: 18-29 ka;

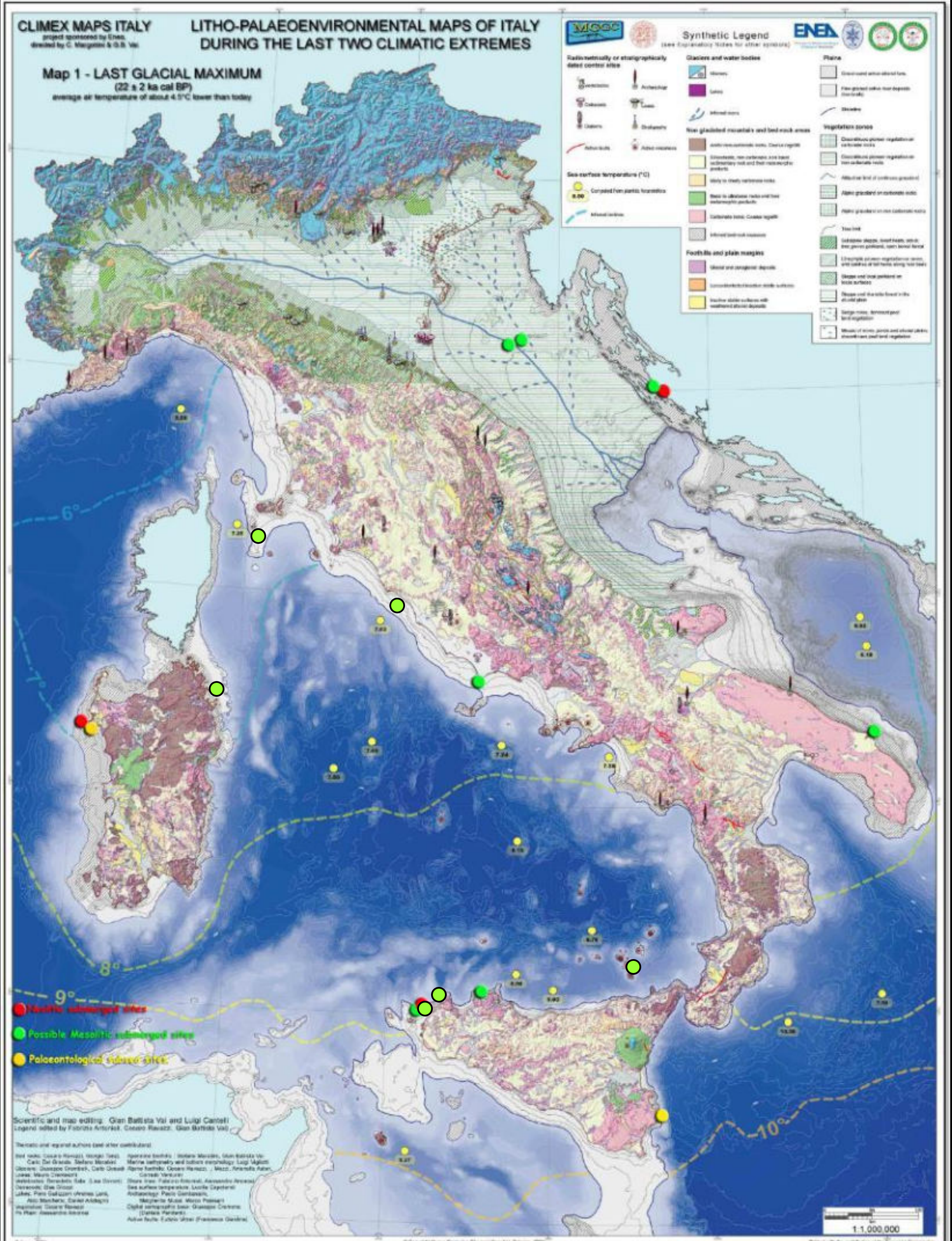

Map showing Mesolithic and Neolithic archaeological sites which are potentially correlated with submerged archaeological landscape

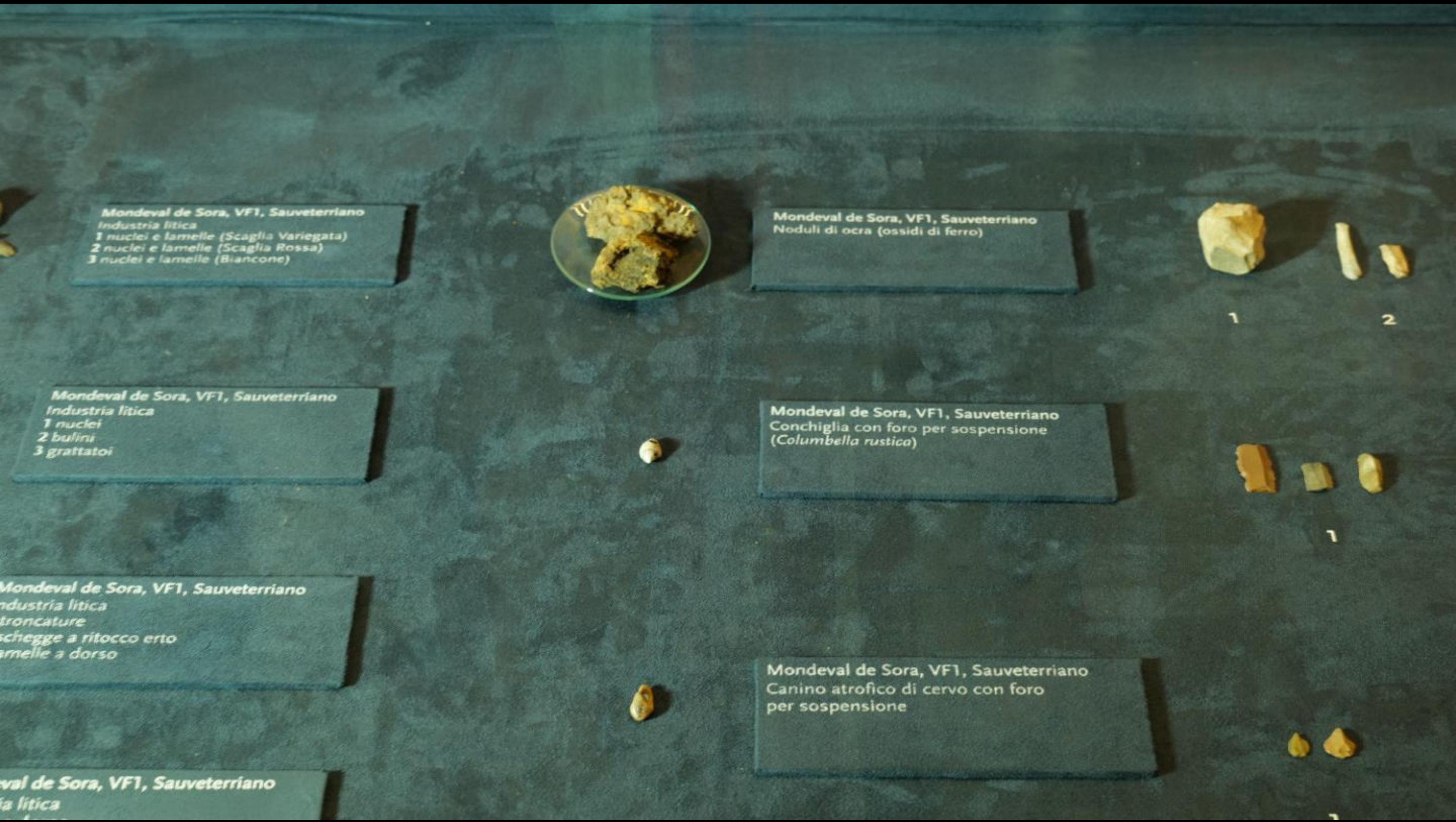

Mondeval de Sora, VF1, Sauveterriano
Industria litica
1 nuclei e lamelle (Scaglia Variegata)
2 nuclei e lamelle (Scaglia Rossa)
3 nuclei e lamelle (Biancone)
Mondeval de Sora, VF1, Sauveterriano
Noduli di ocra (ossidi di ferro)
1
2
Mondeval de Sora, VF1, Sauveterriano
Industria litica
1 nuclei
2 bulini
3 grattatoi
Mondeval de Sora, VF1, Sauveterriano
Conchiglia con foro per sospensione
(Columbella rustica)
1
Mondeval de Sora, VF1, Sauveterriano
ndustria litica
troncature
schegge a ritocco erto
amelle a dorso
Mondeval de Sora, VF1, Sauveterriano
Canino atrofico di cervo con foro
per sospensione
val de Sora, VF1, Sauveterriano
ia litica

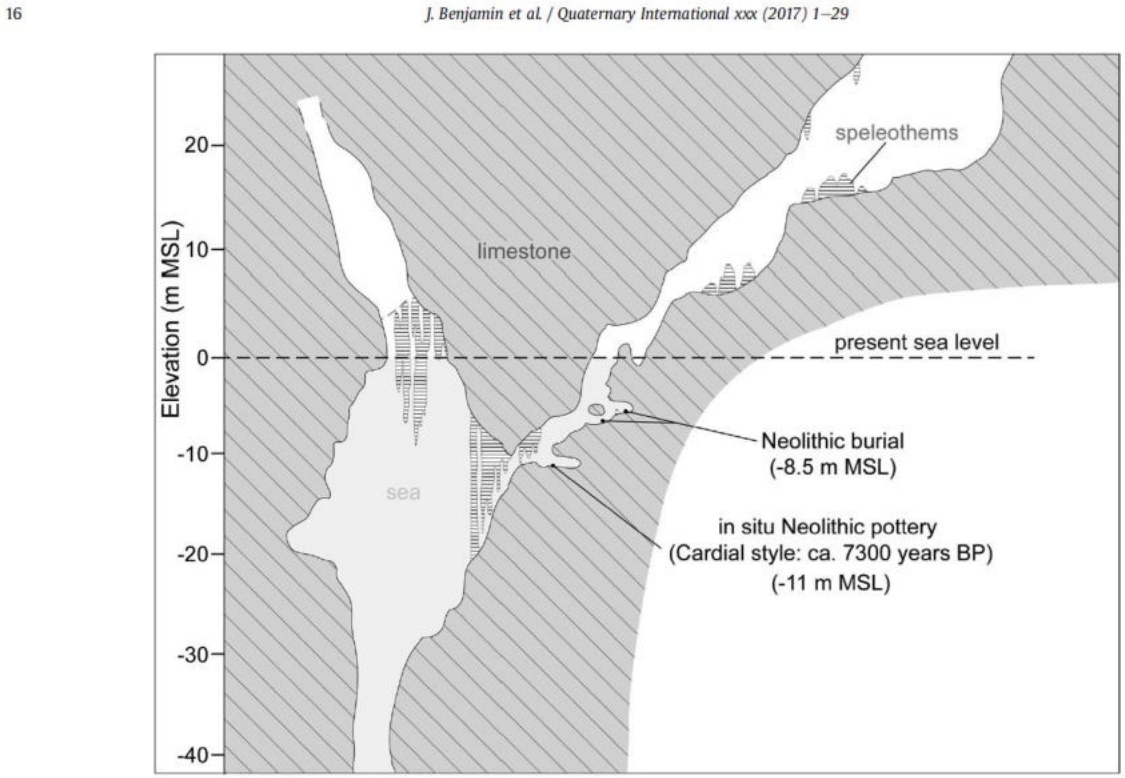

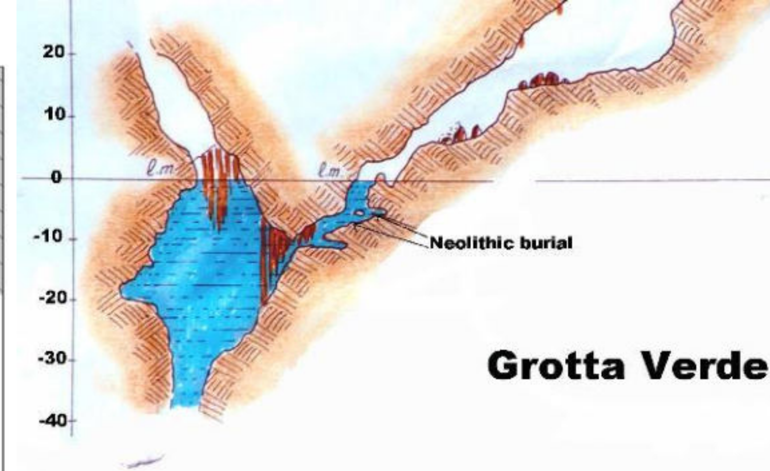

Capo Caccia, Sassari, Sardegna, si tratta dell'affioramento più antico e piu interessante mai studiato in Italia, scoperto negli anni '70, fu studiato dalla locale Sprintendenza con notevoli difficoltà tecniche, buio, sospensioni fangose, ecc. Ma vennero ritrovate inumazioni in situ, nelle tombe scavate nella roccia a circa 8 metri di profondità, le ceramiche cardiali tipiche del Neolitico Antico Sardo dettero la possibilità di una datazione precisa: 7300 anni fa (Antonioli et al., 1996, Benjamin et al 2017. Alcuni vasi trovati in situ, sull'orlo di una profonda cavità sulla quale, ai tempi delle inumazioni l'acqua dolce galleggiava su quella salata, dettero la possibilità di attribuire al livello del mare di 7.3 mila anni fa una quota inferiore a -11 metri. Tutto ciò in perfetto accordo con quanto predetto dal Modello di Lambeck et al., 2011.


Data SIO, NOAA, U.S. Navy, NGA, GEBCO
Image © 2009 TerraMetrics
Image © 2009 DigitalGlobe
© 2009 Cnes/Spot Image
1129 mi

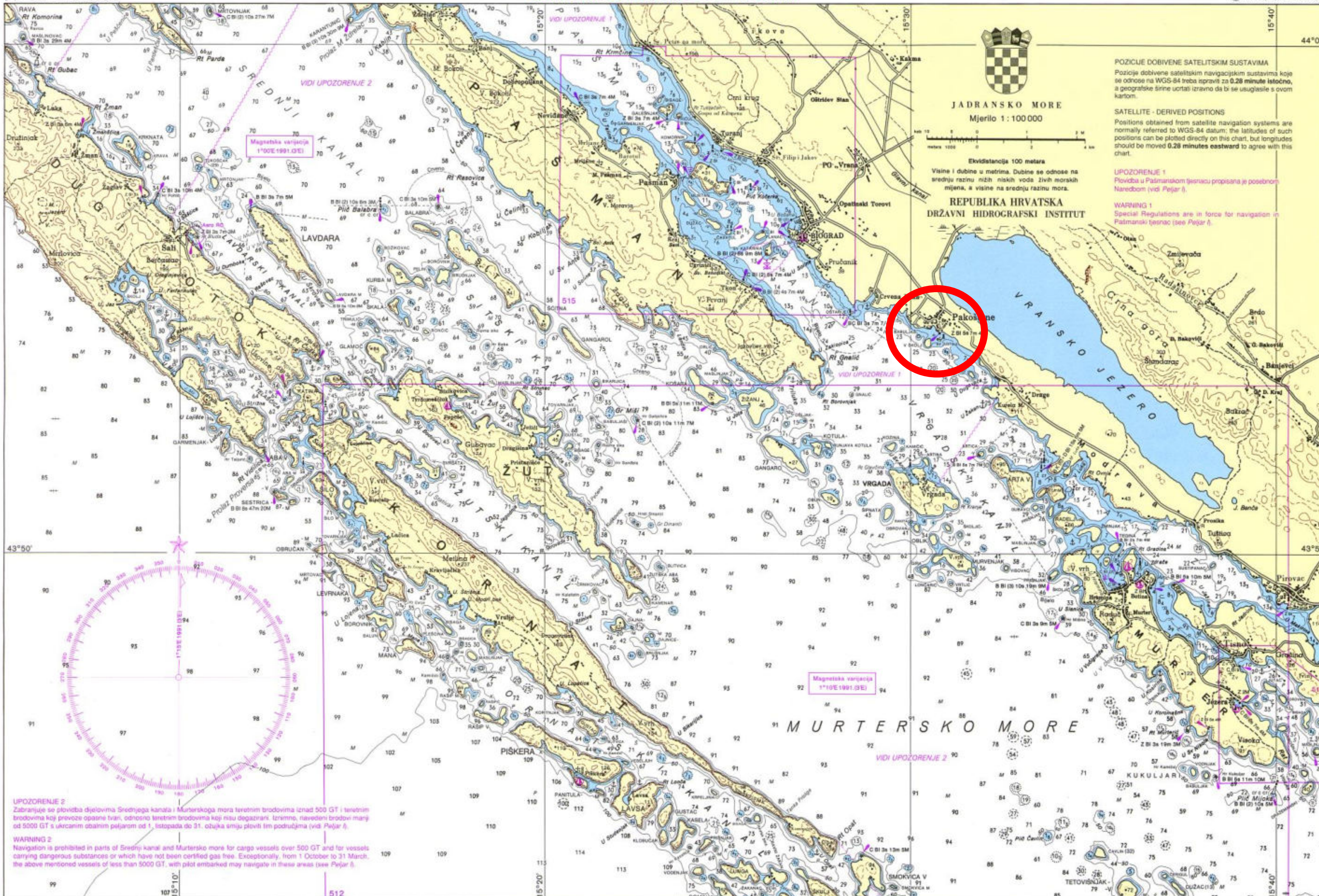
JADRANSKO MORE
Mjerilo 1 : 100 000
Ekvidistancija 100 metara
Visine i dubine u metrima. Dubine se odnose na srednju razinu nižih niskih voda živih morskih mijena, a visine na srednju razinu mora.
REPUBLIKA HRVATSKA
DRŽAVNI HIDROGRAFSKI INSTITUT
POZICIJE DOBIVENE SATELITSKIM SUSTAVIMA
Pozicije dobivene satelitskim navigacijskim sustavima koje se odnose na WGS-84 datum treba ispraviti za 0.28 minute istočno, a geografske širine uortati izravno da bi se usuglasile s ovom kartom.
SATELLITE - DERIVED POSITIONS
Positions obtained from satellite navigation systems are normally referred to WGS-84 datum; the latitudes of such positions can be plotted directly on this chart, but longitudes should be moved 0.28 minutes eastward to agree with this chart.
UPOZORENJE 1
Plovidba u Pašmanskom tjesnacu propisana je posebnom Naredbom (vidi Peljar I).
WARNING 1
Special Regulations are in force for navigation in Pašmanski tjesnac (see Peljar I).
UPOZORENJE 2
Zabranjuje se plovidba dijelovima Srednjega kanala i Murterskoga mora teretnim brodovima iznad 500 GT i teretnim brodovima koji prevoze opasne tvari, odnosno teretnim brodovima koji nisu degazirani. Iznimno, navedeni brodovi manji od 5000 GT s ukrcanim obalnim peljarom od 1. listopada do 31. ožujka smiju ploviti tim područjima (vidi Peljar I).
WARNING 2
Navigation is prohibited in parts of Srednji kanal and Murtersko more for cargo vessels over 500 GT and for vessels carrying dangerous substances or which have not been certified gas free. Exceptionally, from 1 October to 31 March, the above mentioned vessels of less than 5000 GT, with pilot embarked may navigate in these areas (see Peljar I).
Magnetska varijacija 1°00'E 1991.(3'E)
Magnetska varijacija 1°10'E 1991.(3'E)
VIDI UPOZORENJE 1
VIDI UPOZORENJE 2
SREDNJI KANAL
PAŠMAN
PAŠMANSKI KANAL
DUGI OTOK
LAVDARA
LAVDARSKI KANAL
SITSKI KANAL
ŽUT
ŽUTSKI KANAL
KORNAT
KORNATSKI KANAL
VRGADA
VRGADSKI KANAL
MURTERSKO MORE
MURTER
VRANSKO JEZERO
BIOGRAD
Pakoštane
Pašman
Turanj
Sv. Filip i Jakov
Pirovac
Tisno
Jezera
Sali
PIŠKERA
LAVSA
KUKULJARI
Modrava
Crna gora
Drage
44°00'
43°50'
15°10'
15°20'
15°30'
15°40'
515
512

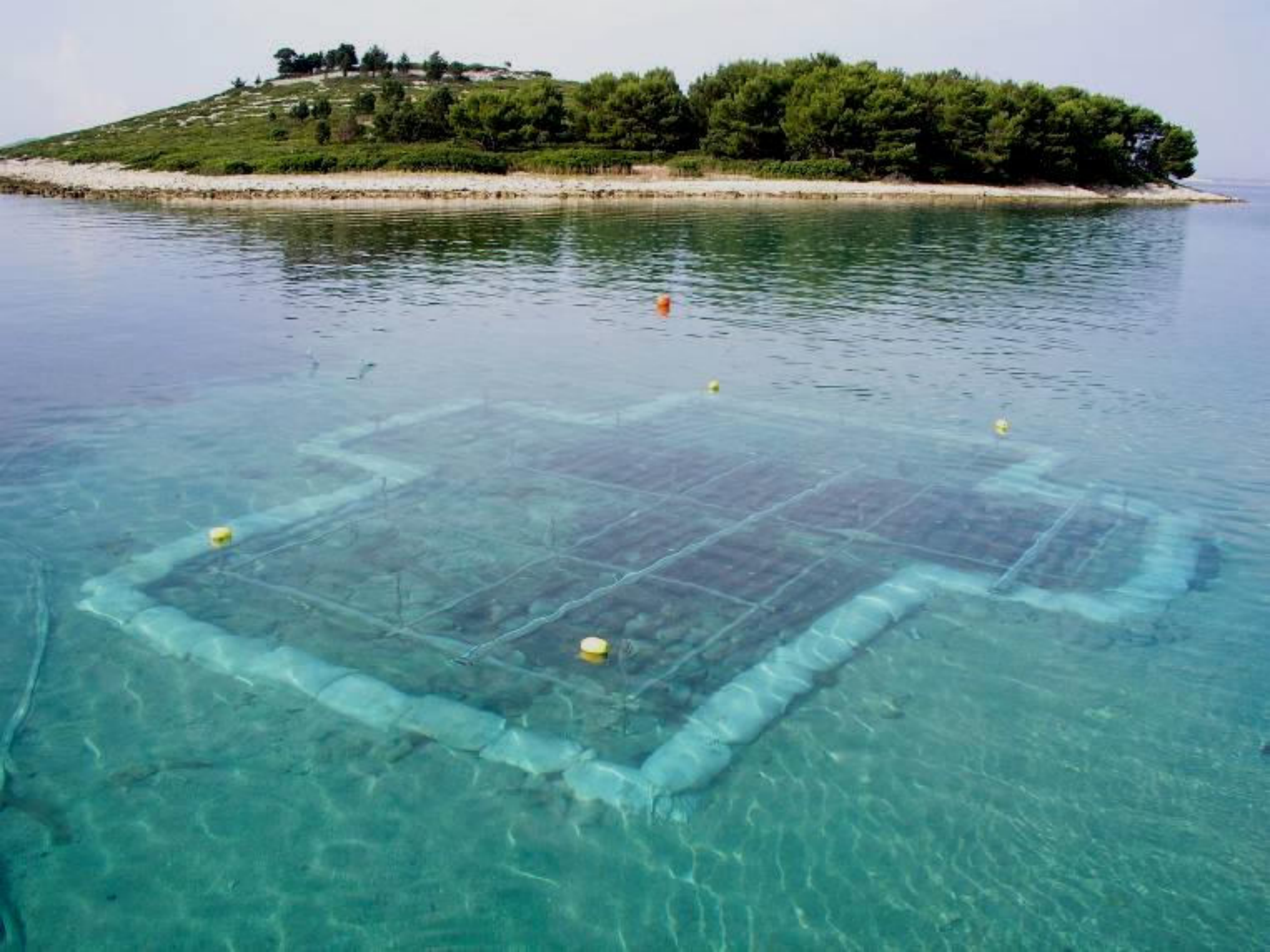

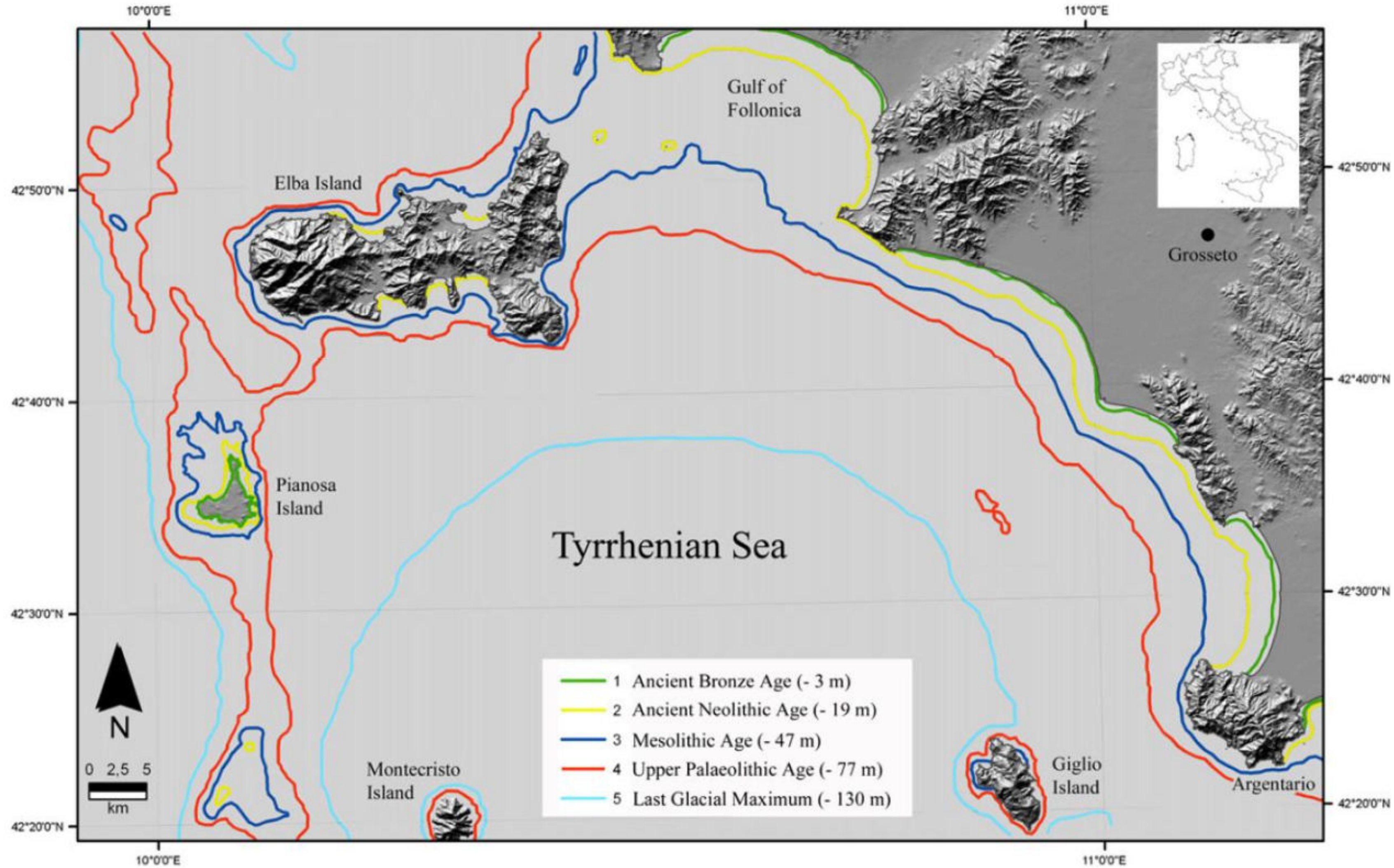

Fig. 11. Palaeocoastline variations since 20 ka cal BP on central Italy coast. See Fig. 10 for timing and sea level change curves.

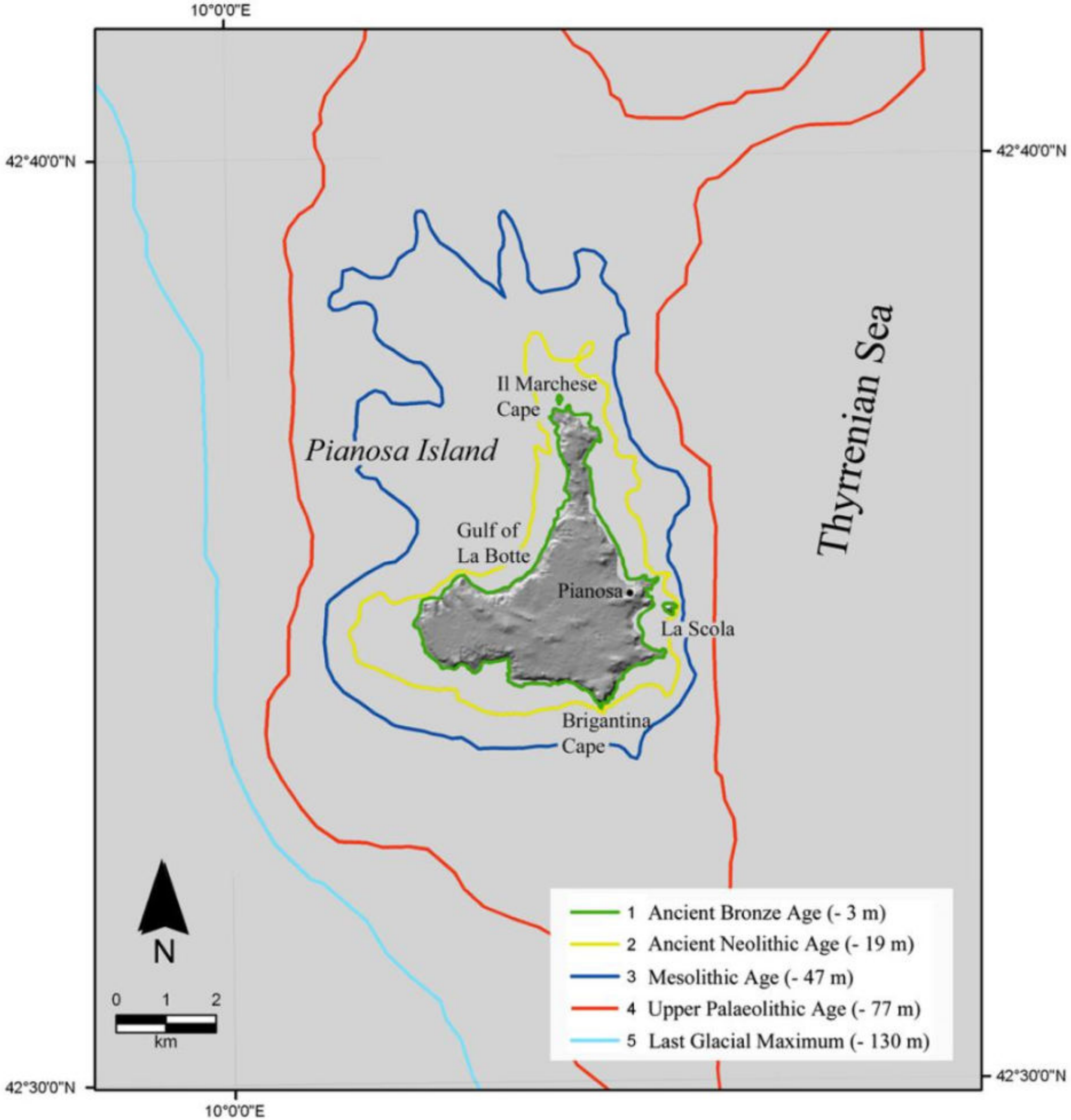

ig. 12. Palaeocoastline variations since 20 ka cal BP at Pianosa. See Figs. 10 and 11 for timing and sea level change curves.

Prof. Rita Auriemma molo romano di Punta Sottile, Trieste

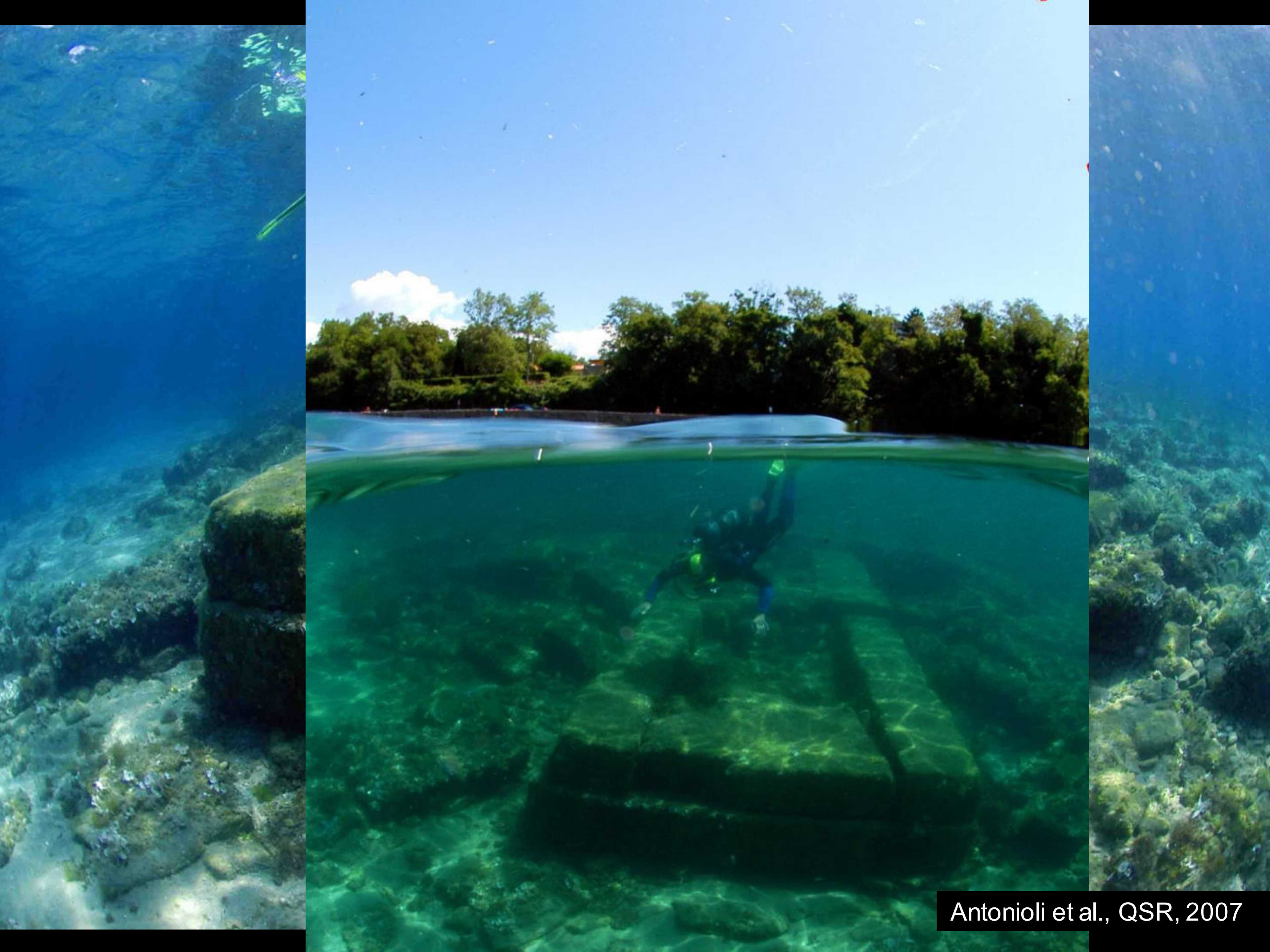

Antonioli et al., QSR, 2007


Ponza fishtanks

La piscina di allevamento per pesci di Punta della Vipera, Civitavecchia, uno dei migliori esempi di realizzazione ingegneristica di 2000 anni fa, in questo caso i canali di entrata ed uscita dell’acqua si trovano a -1,28 metri. Nel passato, misure errate effettuate sui muretti e non dei canali avevano fornito la quota di -50 cm.

Sluice gates: the precise ~2ka benchmarks

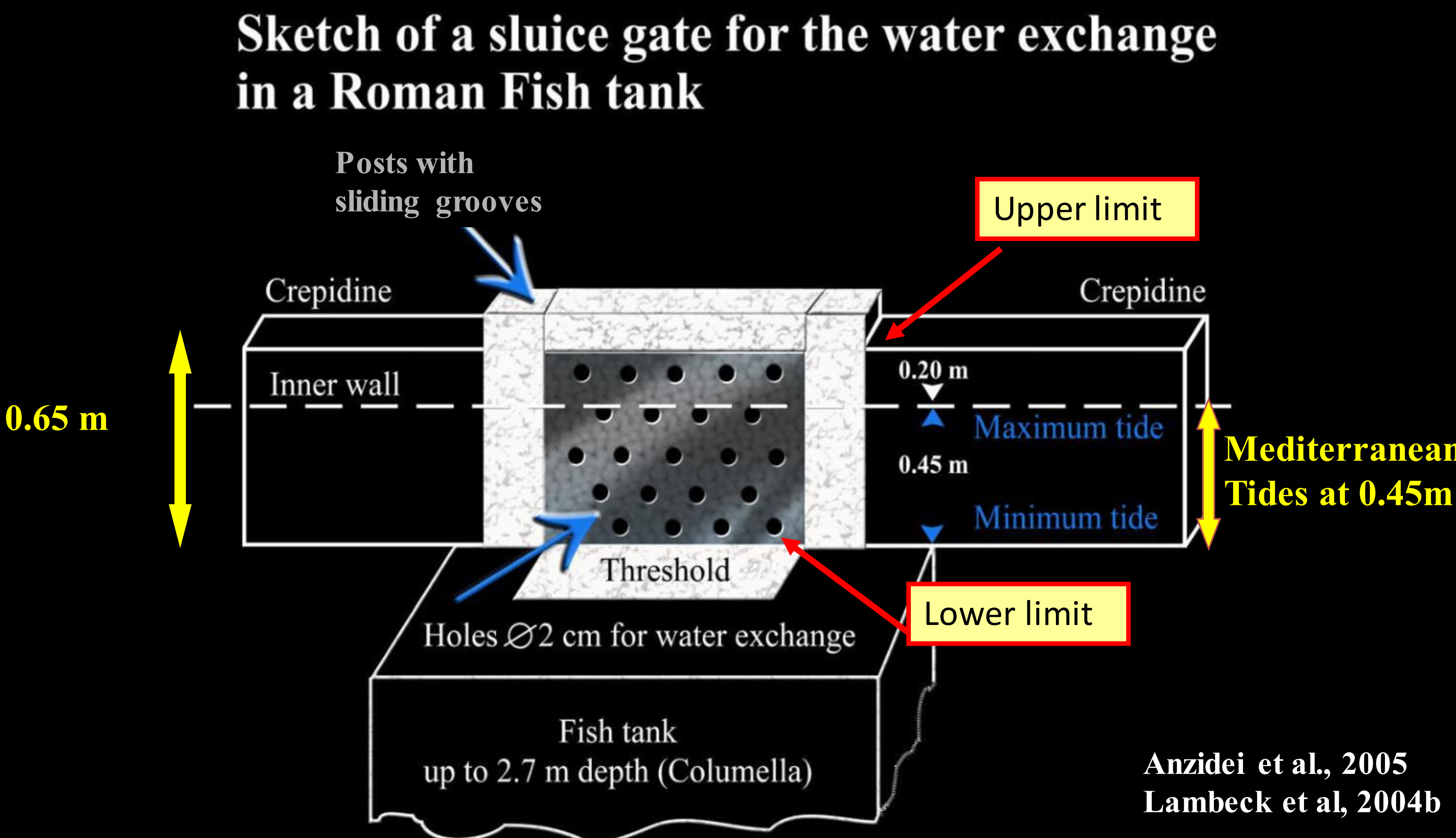

The top of the sluice gate coincides with the elevation of the lowest level foot-walk (crepidine), to a position above the highest tide level.

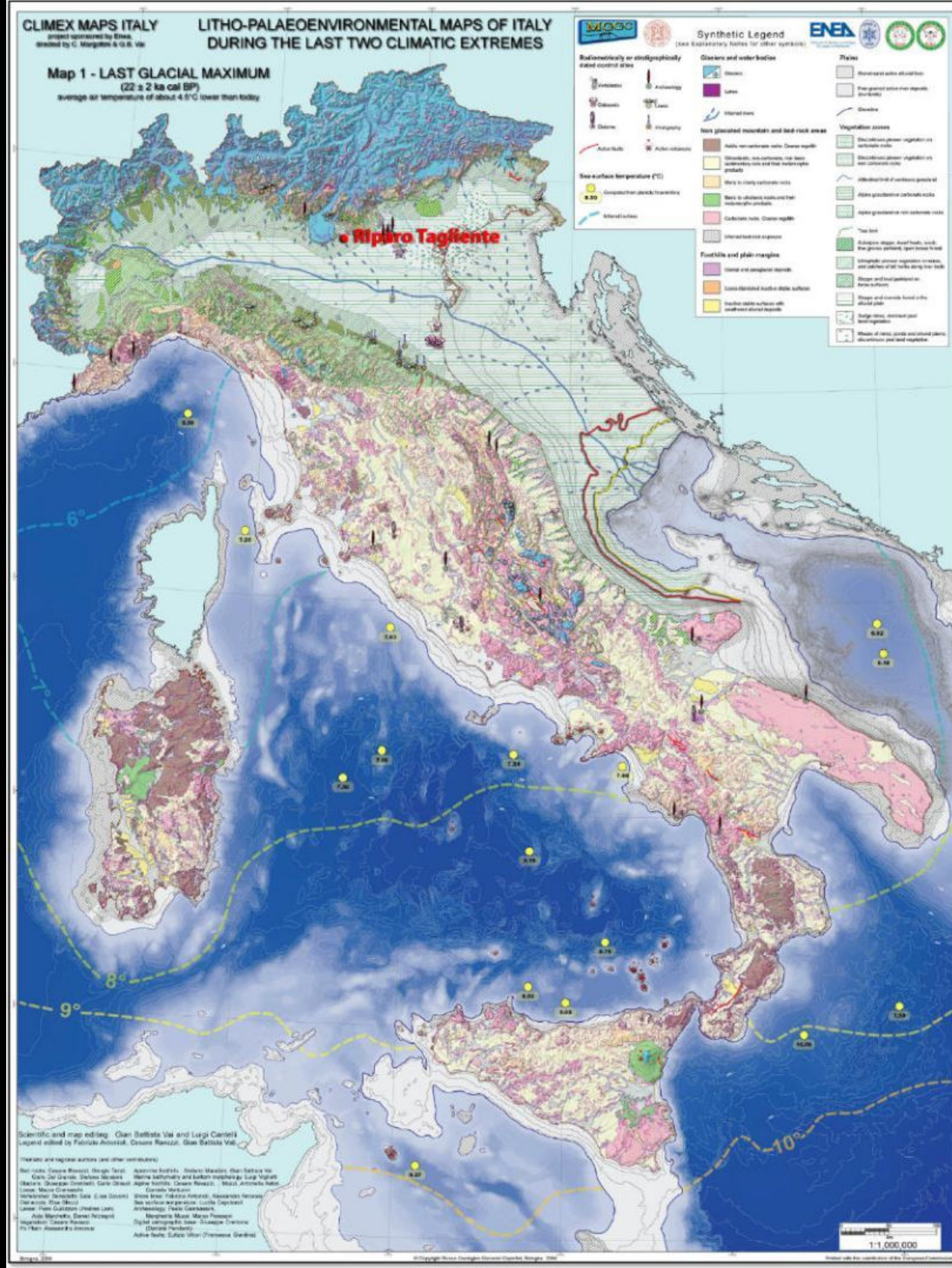

CLIMEX MAPS ITALY
LITHO-PALAEOENVIRONMENTAL MAPS OF ITALY
DURING THE LAST TWO CLIMATIC EXTREMES
Map 1 - LAST GLACIAL MAXIMUM
(22 ± 2 ka cal BP)
Synthetic Legend
Riparo Tagliente
6°
7°
8°
9°
10°
1:1,000,000

Quaternary International xxx (2014) 1–17

Contents lists available at ScienceDirect

Quaternary International

journal homepage: www.elsevier.com/locate/quaint

Millstone coastal quarries of the Mediterranean: A new class of sea level indicator

V. Lo Presti [a,*], F. Antonioli [b], R. Auriemma [c], A. Ronchitelli [d], G. Scicchitano [e,f], C.R. Spampinato [e,g], M. Anzidei [h], S. Agizza [i], A. Benini [j], L. Ferranti [k], M. Gasparo Morticelli [a], C. Giarrusso [l], G. Mastronuzzi [m], C. Monaco [e], A. Porqueddu [n]

Geoswim a Paros, Grecia, 2017

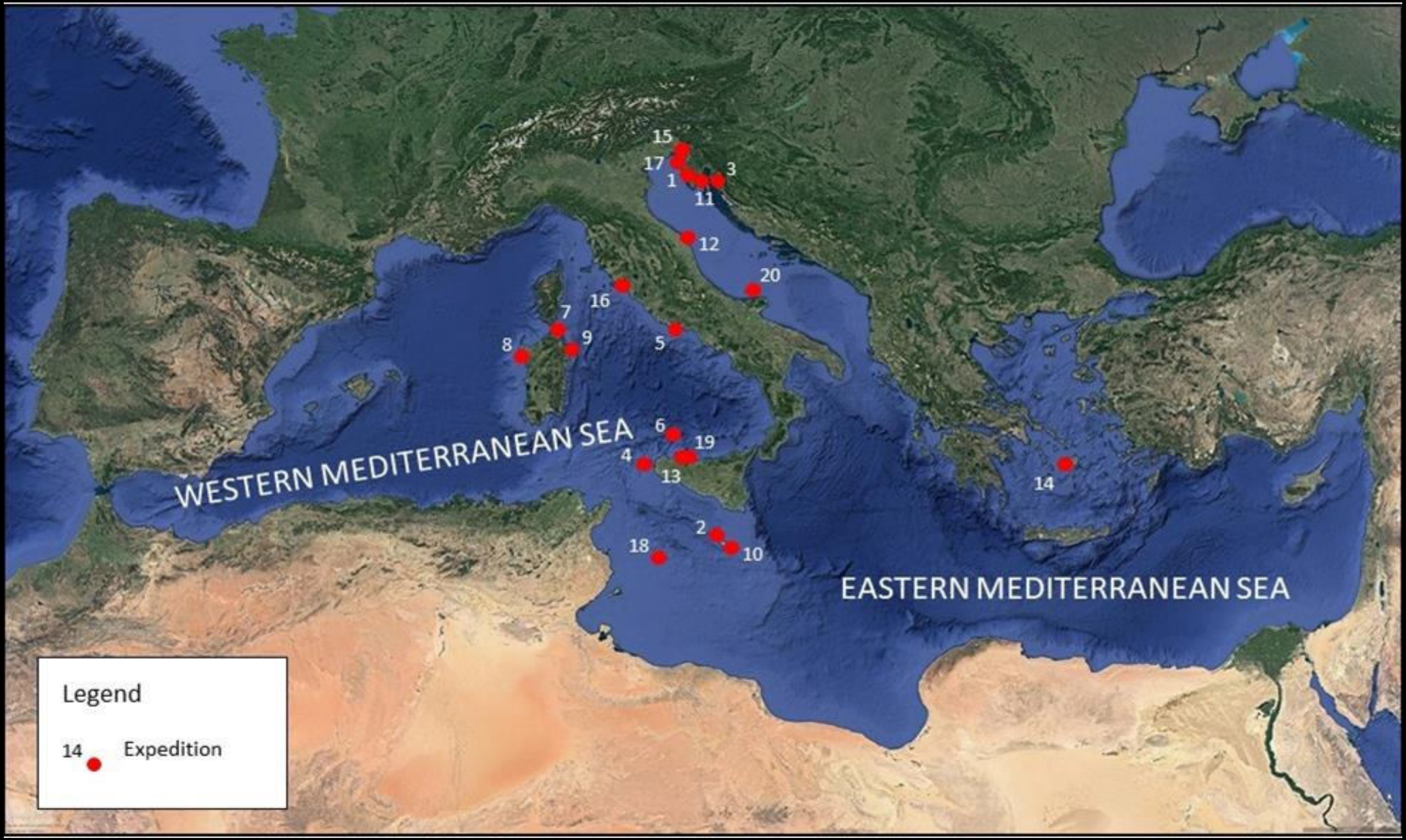

15
17
1
3
11
12
20
16
7
9
8
5
6
19
4
13
WESTERN MEDITERRANEAN SEA
14
2
18
10
EASTERN MEDITERRANEAN SEA
Legend
14
Expedition

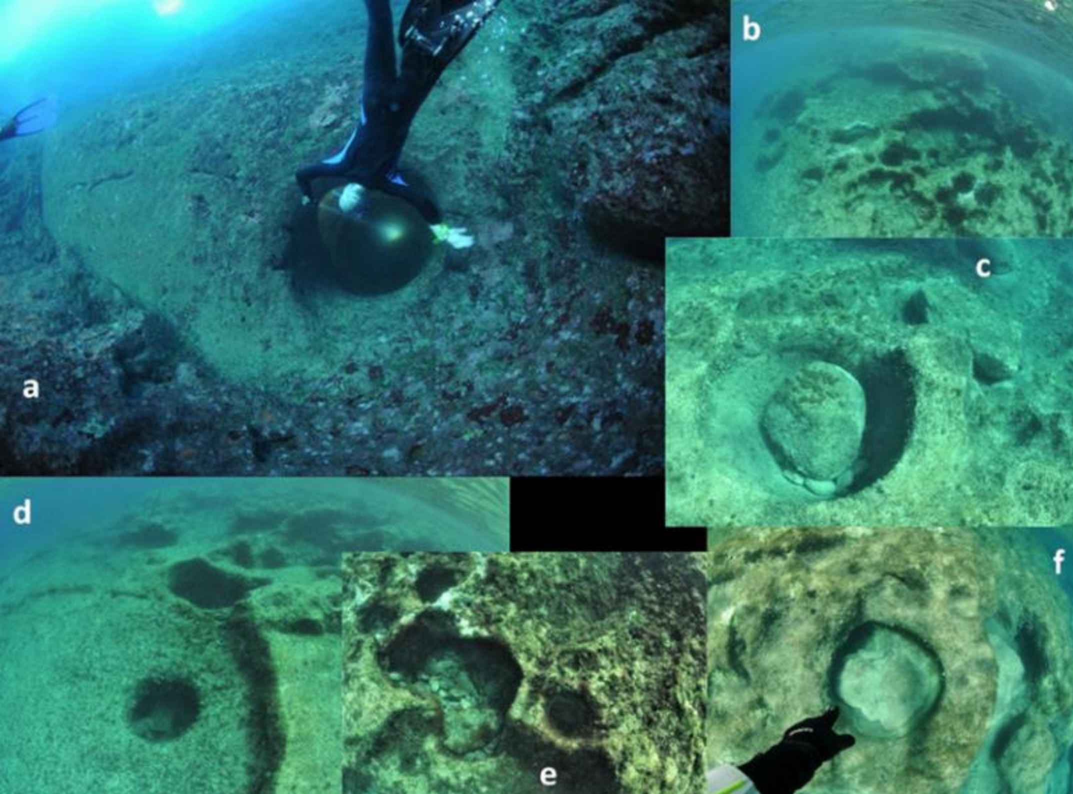
a
b
c
d
e
f

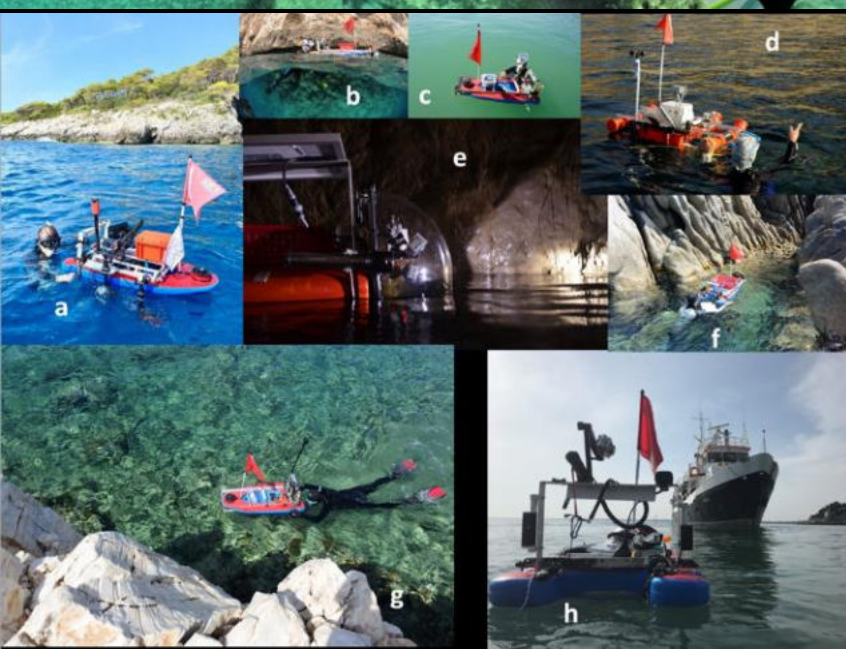
a
b
c
d
e
f
g
h

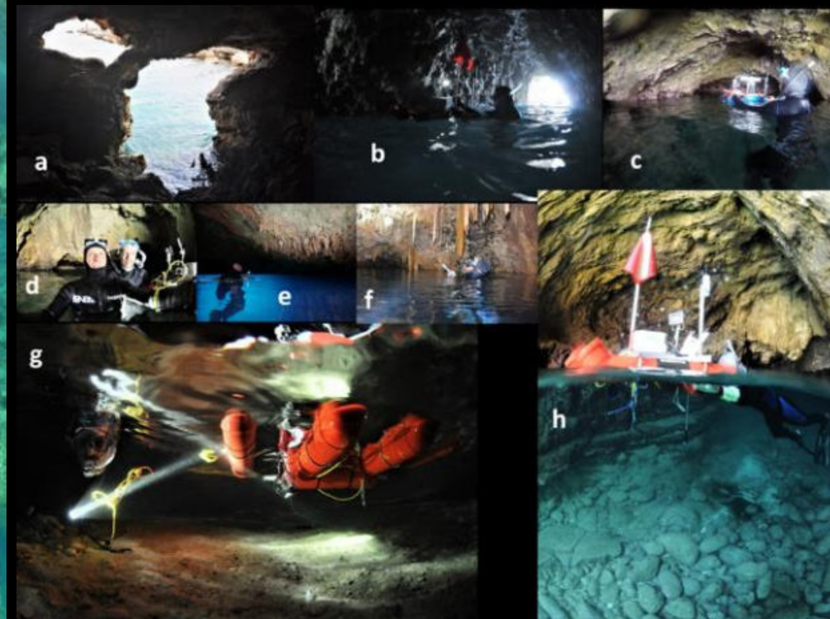
a
b
c
d
e
f
g
h

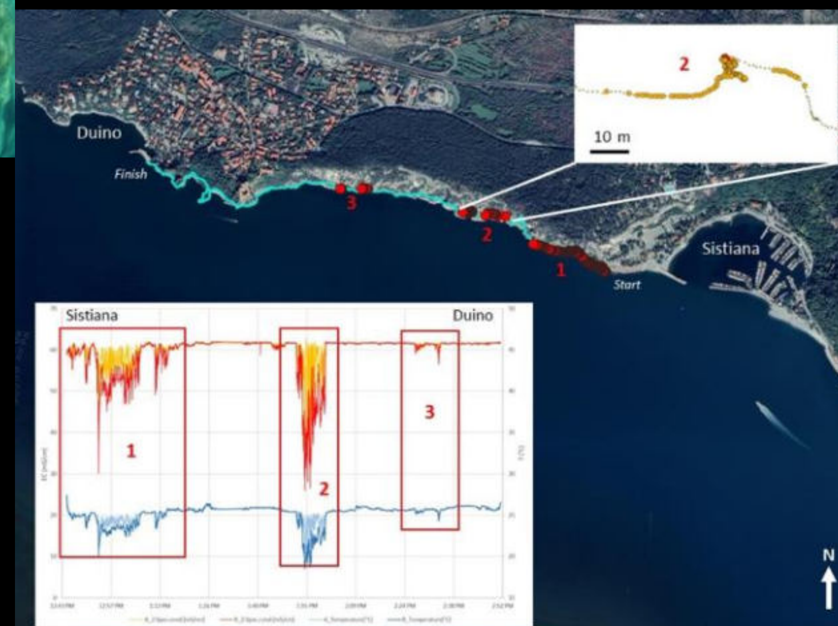
Duino
Finish
Sistiana
Start
10 m
N
1
2
3
Sistiana
Duino

A ID	B Year	C Location	D Videos (Y/N, a/b/w, duration (hours))	E Time-lapse images (Y/N, a/b/w)	F Outline images (Y/N, a/b)	G Total lenght (km)	H Days of survey	I Literature
1	2012	W Istrian Peninsula (Croatia, Slovenia, Italy)	(Y, a/b)	(N)	(Y, a/b)	253,2	27	Furlani, 2012; Furlani et al. 2014a
2	2013	Gozo and Comino (Malta)	(Y, a/b)	(N)	(Y, a/b)	57	7	Furlani et al., 2017a
3	2013	Stara Baska (Krk, Croatia)	(Y, a/b)	(N)	(Y, a/b)	2,2	1	/
4	2014	Egadi Islands (Italy)	(Y, w)	(N)	(Y, a/b)	67	7	Busetti et al., 2015 Furlani et al., 2021 Antonioli et al 2021
5	2015	Gaeta Promontory (Latium, Italy)	(Y, w)	(N)	(Y, a/b)	2,5	1	Furlani et al., 2021a
6	2015	Ustica (Sicily, Italy)		(N)	(Y, a/b)	14	2	Furlani et al., 2017b
7	2015	Razzoli, Budelli, Santa Maria (Sardinia, Italy)	(N)	(Y, w)	(Y, a/b)	22,5	3	Furlani et al., 2021a
8	2015	Capo Caccia (Sardinia, Italy)	(N)	(Y, w)	(Y, a/b)	26	2	Furlani et al., 2021a
9	2015	Tavolara (Sardinia, Italy)	(N)	(Y, w)	(Y, a/b)	14,9	2	Furlani et al., 2021a
10	2015	Malta (Malta)	(N)	(Y, w)	(Y, a/b)	19,2	3	Furlani et al., 2021a
11	2015	SE Istria (Croatia)	(N)	(Y, w)	(N)	7	1	Vaccher, unpublished thesis
12	2016	Monte Conero (W Adriatic Sea, Italy)	(N)	(Y, w)	(Y, a/b)	2,9	1	Furlani et al., 2018
13	2016	Addaura (Palermo, Sicily, Italy)	(N)	(N)	(Y, a/b)	7	1	Caldareri et al., 2018
14	2017	Paros (Greece)	(Y, w)	(Y, w)	(Y, a/b)	24	8	Furlani et al., 2021b
15	2017	Sistiana-Duino (Gulf of Trieste, Italy)	(N)	(Y, a/b)	(N)	2	1	Furlani and Biolchi, 2018
16	2018	Ansedonia and Argentario (Tuscany, Italy)	(Y, w)	(Y, a/b)	(Y, a/b)	10	2	Furlani et al., 2021
17	2019	Savudrija (Croatia)	(N)	(Y, a/b)	(N)	1.1	1	Furlani et al., 2021
18	2020	Isole Pelagie (Sicily, Italy)	(Y, a)	(Y, a/b)	(Y, a/b)	43.9	9	/
19	2020	Arenella (Sicily Italy)	(N)	(n, a/b)	(Y, a/b)	0.6	1	Furlani et al., 2021 Antonioli et al. 2021
20	2021	Isole Tremiti (Puglia, Italy)	(Y, a/b)	(Y, a/b)	(Y, a)	5.7	1	/
	TOTAL					**532**	**81**	

Article

Preserv
Biologi

Stefano Furl
Alice Busetti
Elisa Dal Bo
Thalassia Gi
Alessandro F
Matteo Vacc

Citation: Furlani,
Antonioli, F.; Agat
Boccali, C.; Busetti
Canziani, F.; Chem
Preservation of Mo
Erosional Landfor
Structures as Sea L
Matter of Luck? W
https://doi.org/1

40 coastal area that could be flooded by the sea for 2100

completed maps

maps to finish

FLOODING SCENARIO AT FOUR ITALIAN COASTAL PLAINS USING THREE RELATIVE SEA LEVEL RISE MODELS: THE NORTH ADRIATIC AREA

A. Marsico[1], S. Lisco[1], V. Lo Presti[2], F. Antonioli[2], A. Amorosi[3], M. Anzidei[4], G. Deiana[5], G. De Falco[6], A. Fontana[7], G. Fontolan[8], M. Moretti[1], P. Orru[5], G. Sannino[2], E. Serpelloni[4], A. Vecchio[9], G. Mastronuzzi[1]

[1]Dipartimento di Scienze della Terra e Geoambientali, University "Aldo Moro", CONISMA Italy; [2]ENEA, SSPT, Roma, Italy; [3]Dipartimento di Scienze Biologiche, Geologiche e Ambientali, University of Bologna, Italy; [4]Istituto Nazionale di Geofisica e Vulcanologia, Italy; [5]Dipartimento di Scienze Chimiche e Geologiche, University of Cagliari, CONISMA Italy; [6]CNR Oristano; [7]Dipartimento di Geoscienze, University of Padova, CONISMA Italy; [8]Dipartimento di Matematica e Geoscienze, University of Trieste, CONISMA Italy; [9]Lesia Observatoire de Paris, Section de Meudon 5, France

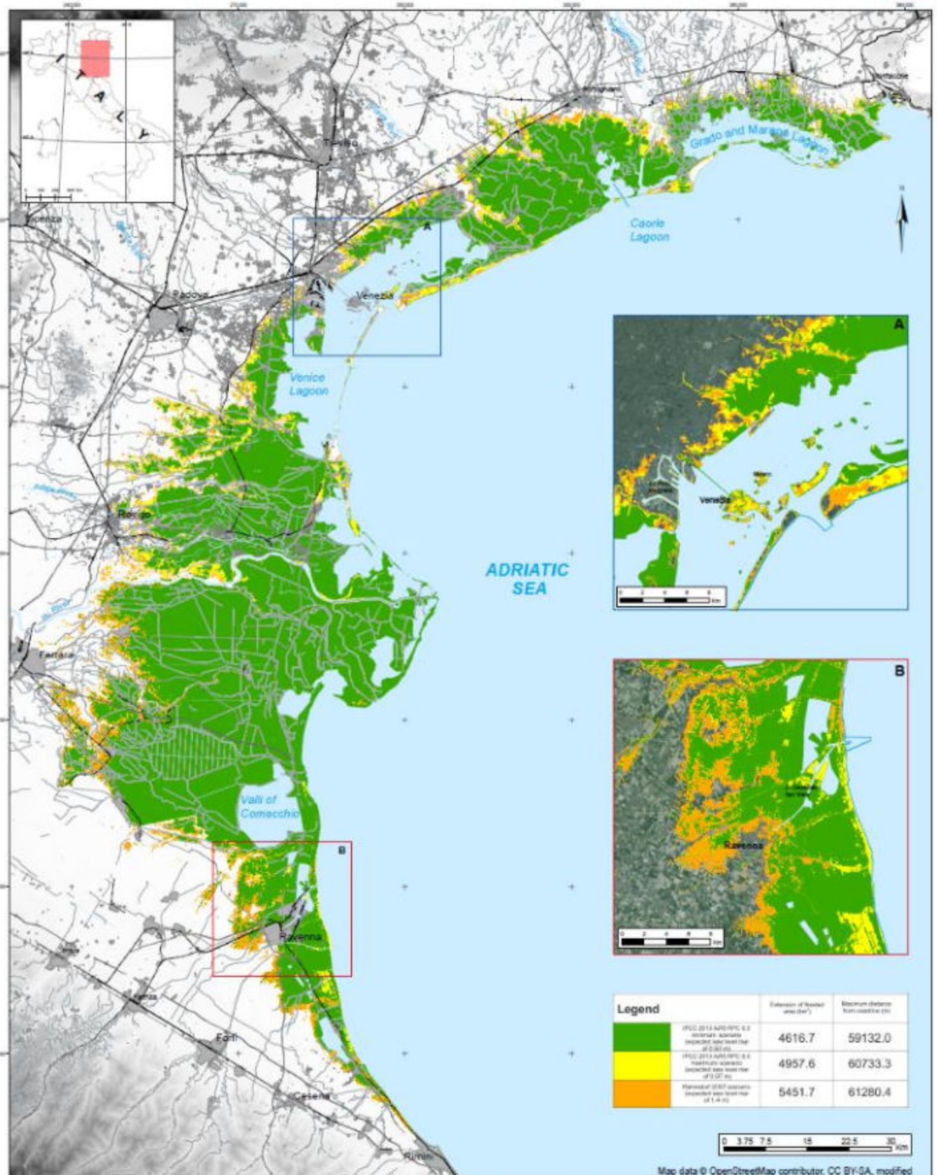

DATUM: WGS 1984 - Projection: Transverse Mercator ZONE 33, Northern Hemisphere - EPSG: 32633

ALTIMETRIC MAP OF THE COASTAL POTENTIAL SUBMERSION IN 2100
STAGNONE E SALINE DI MARSALA

Dr Valeria Lo Presti PhD - Geologo marino/costiero.
Prof. Giovanni Randazzo - Università degli Studi di Messina, Dipartimento di Scienze Matematiche e Informatiche, Scienze Fisiche e Scienze della Terra (MIFT).
Dr. Fabrizio Antonioli - Enea Casaccia, Laboratorio di Modellistica e Impatti.

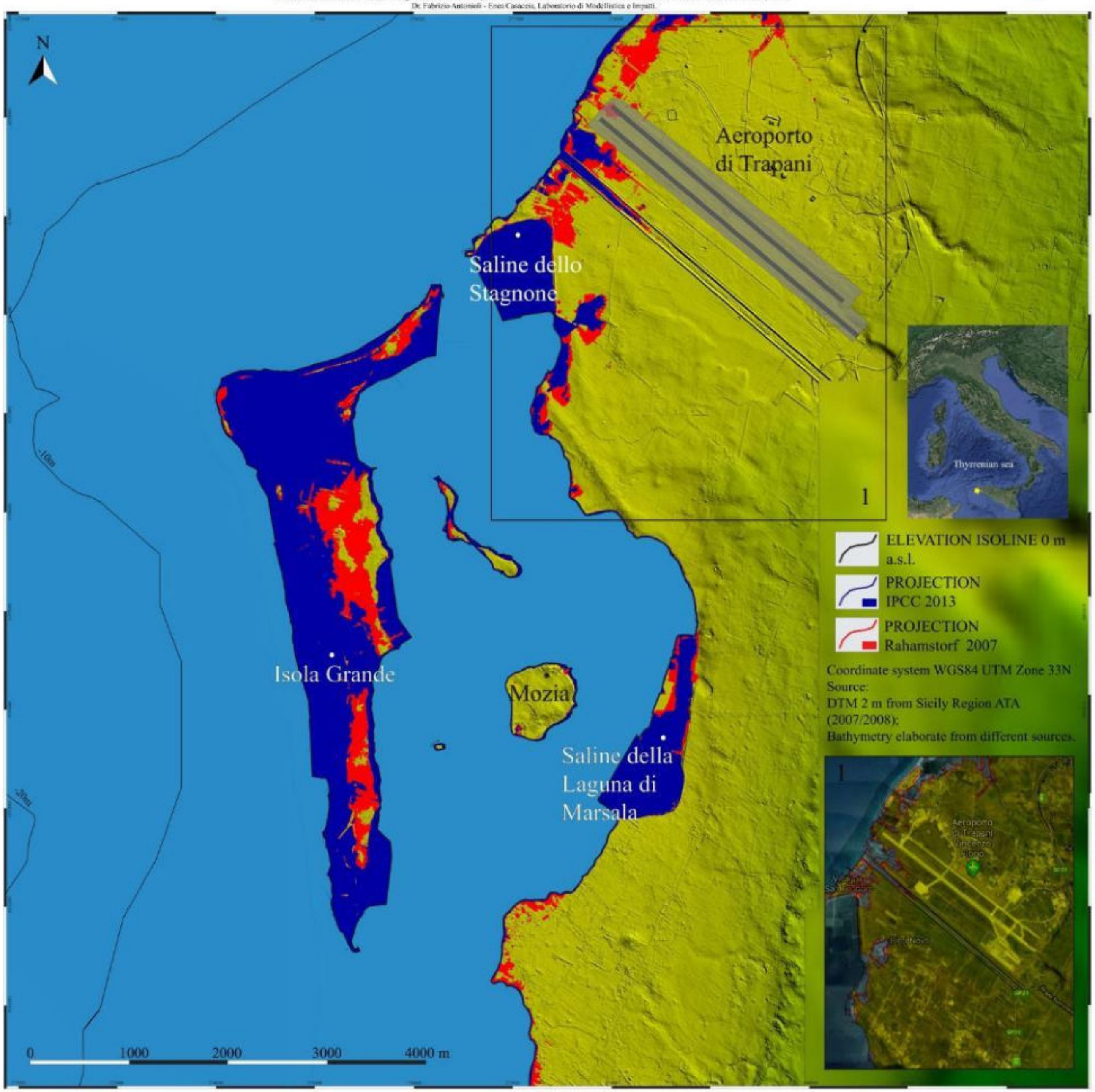

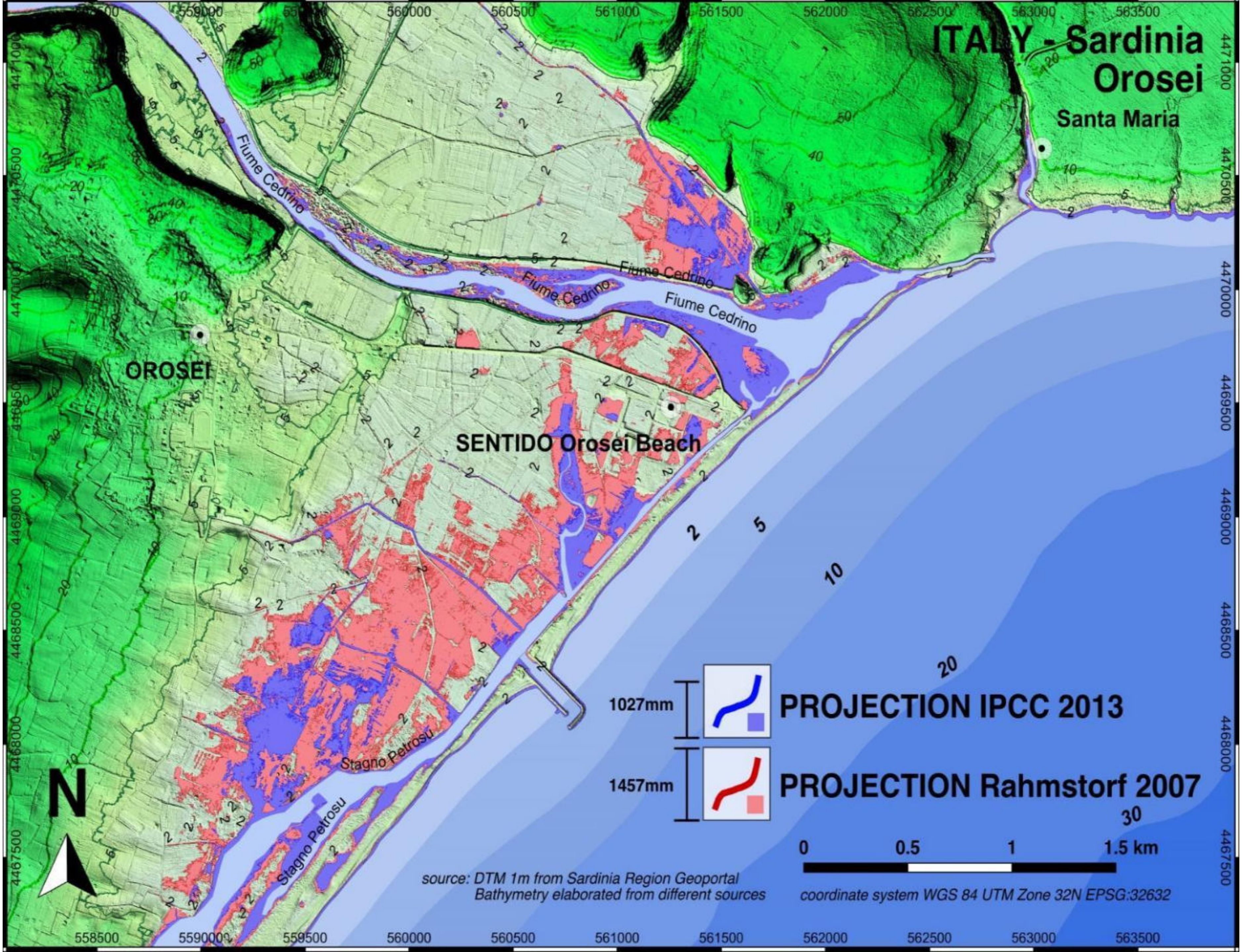

ITALY - Sardinia
Orosei
Santa Maria
OROSEI
SENTIDO Orosei Beach
Fiume Cedrino
Stagno Petrosu
1027mm
PROJECTION IPCC 2013
1457mm
PROJECTION Rahmstorf 2007
0
0.5
1
1.5 km
N
source: DTM 1m from Sardinia Region Geoportal
Bathymetry elaborated from different sources
coordinate system WGS 84 UTM Zone 32N EPSG:32632

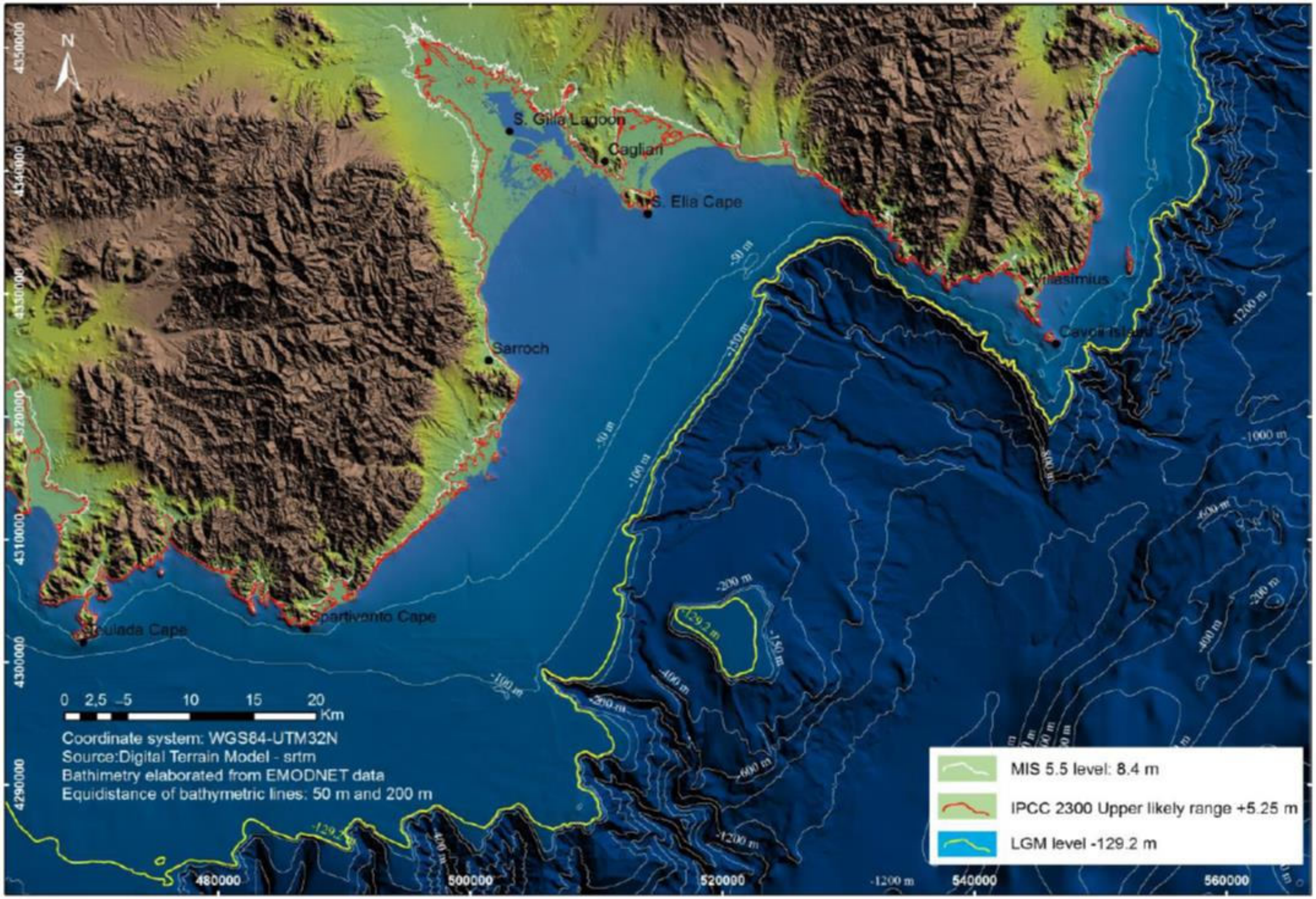

Figure 16 The Cagliari plane map showing the potential submersion area using IPCC AR5 RCP 8.5 for 2100 and 2300: The MIS 5.5 extension occurred 119 ka BP.

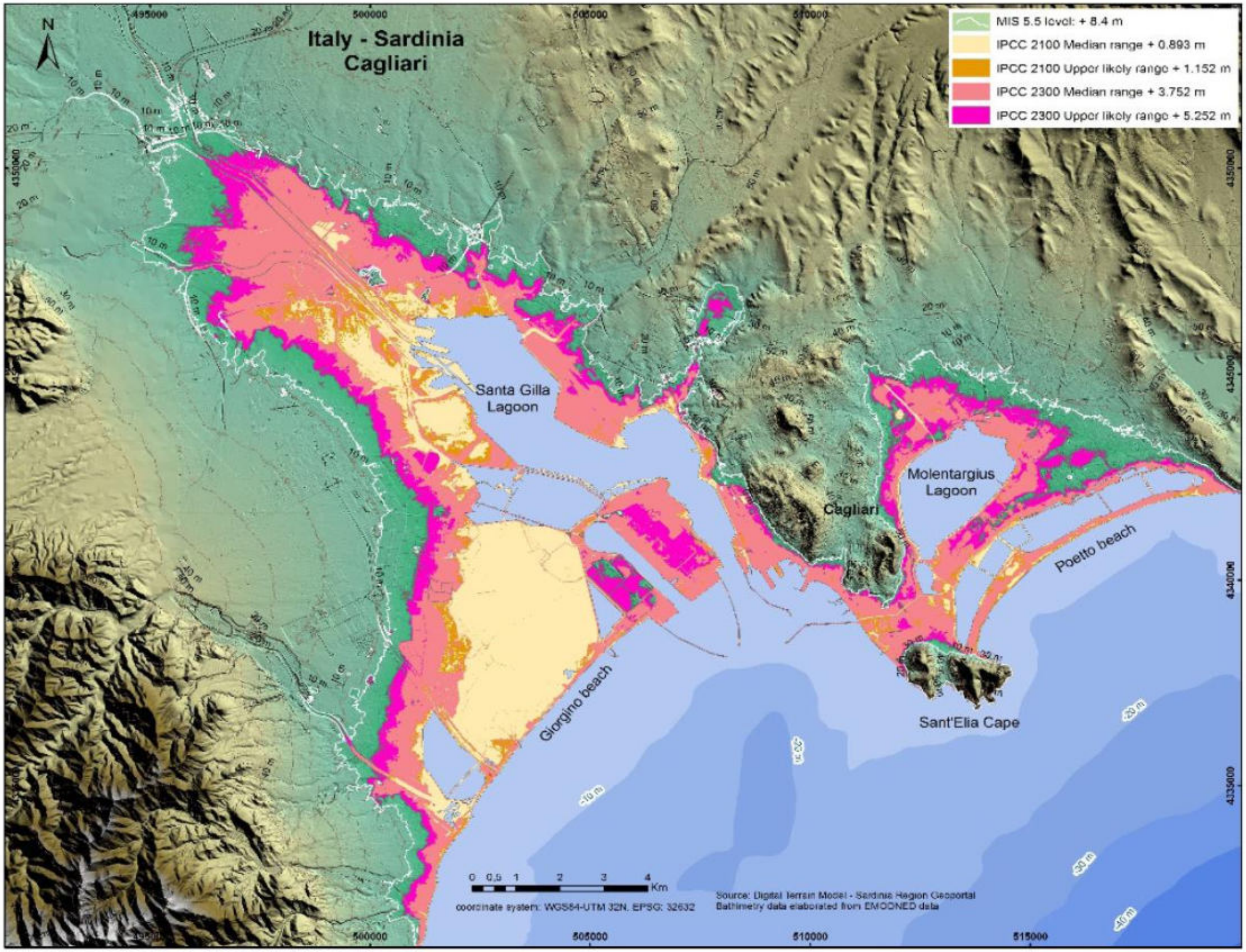

Figure 17. Map of Cagliari plane, (see also Figure 2 for location). The potential submersion area, using IPCC AR5 RCP 8.5 projections at 2100 and 2300.

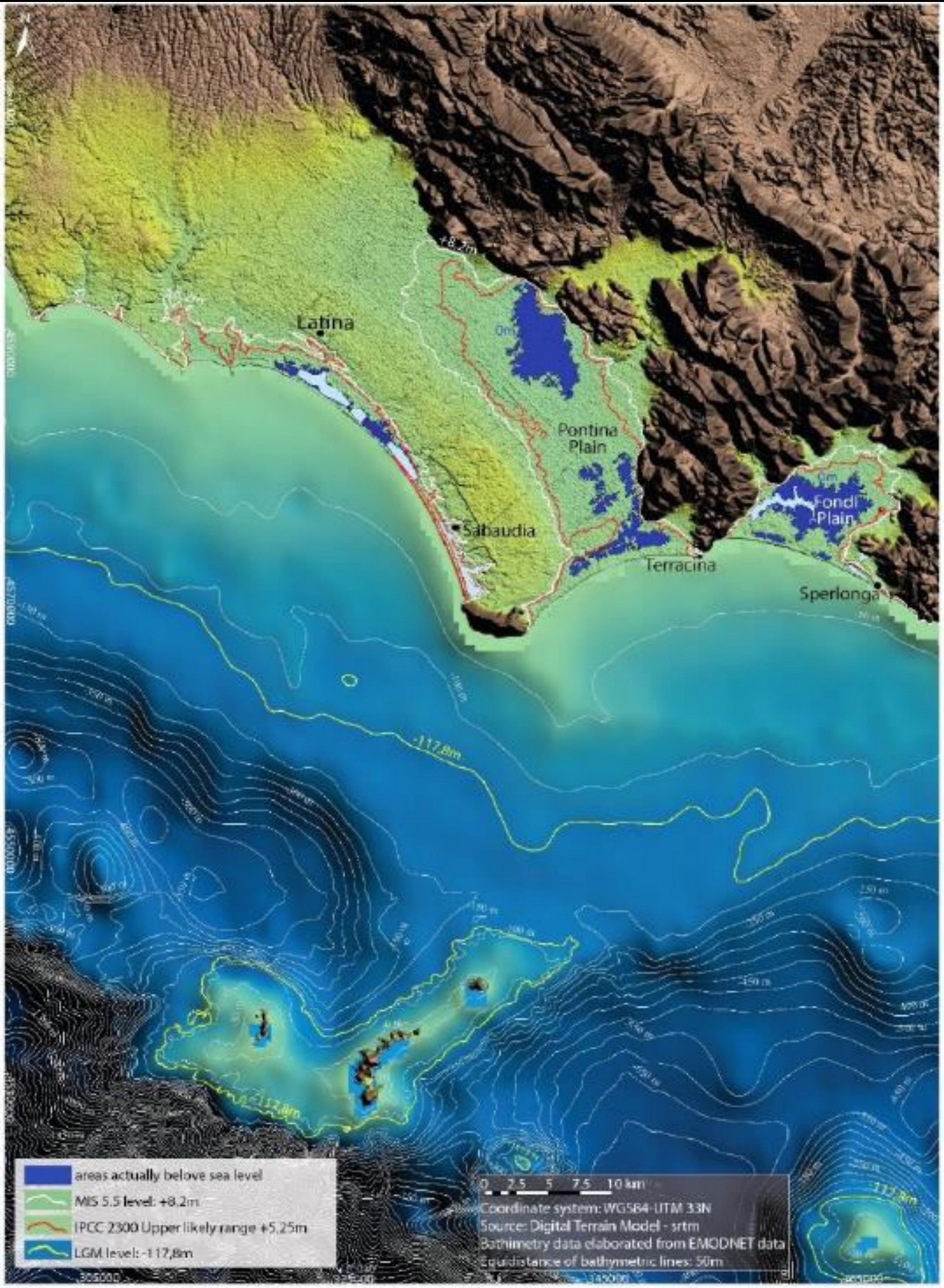

Figure 15. The Pontina and Fondi Plains maps showing the potential submersion area using IPCC AR5 RCP 8.5 for 2100 and 2300: the MIS 5.5 extension occurred 119 ka BP.


Chloe Sladden
Farrell e Mortensen interpretano due dei soccorritori intervenuti per salvarli.
00:51 / 01:25
"TREDICI VITE", IL FILM CHE HA SCATENATO IL PANICO DI COLIN FARRELL


RICHARD STANTON


2100
ADRIATICO
VELE, SQUALI, PILOTI
mare nordest

Thalassia Giaccone


A film by Fabrizio Antonioli and Thalassia Giaccone
Rome International Movie Awards 2022
OFFICIAL SELECTION Madonie Film Festival, Region of Sicily 2023
OFFICIAL SELECTION Ecocine - Festival Internacional de Cinema Ambiental e Direitos Humanos 2022
OFFICIAL SELECTION Vesuvius International Film Fest 2021
BEST EDITING Rome International Movie Awards 2022
HONORABLE MENTION Madonie Film Festival, Region of Sicily 2023
OFFICIAL SELECTION Blue Water Film Festival 2022
2100
There's no time to waste.
OFFICIAL SELECTION Seaside Sustainability Film Festival 2022
IGAG
Consiglio Nazionale delle Ricerche
written by MARTINA CAMATTA edited by VERONICA ARGANESE
camera FABRIZIO ANTONIOLI drone VALERIA LO PRESTI
visual effects EMANUELE DRAGONE sound LEONARDO SAVINI
project management FLAVIO LENOCI
produced by FABRIZIO ANTONIOLI and THALASSIA GIACCONE
in collaboration with SUPERINTENDENCY OF THE SEA, DEPARTMENT OF CULTURAL HERITAGE AND OF THE SICILIAN IDENTITY
CAORLE FILM FESTIVAL 2022 5th Edition OFFICIAL SELECTION
OFFICIAL SELECTION Procida International Film Festival 2022
Quarter Finalist
HOLLYWOOD in ITALIA